

ลักษณะเฉพาะทางวิทยาแร่และธรณีเคมีของหินทิ้งและกากแร่จากเหมืองทอง  
ในภาคตะวันออกเฉียงเหนือของประเทศไทย การประยุกต์สำหรับการป้องกันผลกระทบสิ่งแวดล้อม



บทคัดย่อและแฟ้มข้อมูลฉบับเต็มของวิทยานิพนธ์ตั้งแต่ปีการศึกษา 2554 ที่ให้บริการในคลังปัญญาจุฬาฯ (CUIR)  
เป็นแฟ้มข้อมูลของนิสิตเจ้าของวิทยานิพนธ์ ที่ส่งผ่านทางบัณฑิตวิทยาลัย

The abstract and full text of theses from the academic year 2011 in Chulalongkorn University Intellectual Repository (CUIR)  
are the thesis authors' files submitted through the University Graduate School.

วิทยานิพนธ์นี้เป็นส่วนหนึ่งของการศึกษาตามหลักสูตรปริญญาวิทยาศาสตรดุษฎีบัณฑิต  
สาขาวิชาธรณีวิทยา ภาควิชาธรณีวิทยา  
คณะวิทยาศาสตร์ จุฬาลงกรณ์มหาวิทยาลัย  
ปีการศึกษา 2559  
ลิขสิทธิ์ของจุฬาลงกรณ์มหาวิทยาลัย

MINERALOGICAL AND GEOCHEMICAL CHARACTERISTICS OF WASTE ROCKS AND  
TAILINGS FROM A GOLD MINE IN NORTHEASTERN THAILAND: APPLICATION FOR  
ENVIRONMENTAL IMPACT PROTECTION

Miss Thitiphon Assawincharoenkij



A Dissertation Submitted in Partial Fulfillment of the Requirements  
for the Degree of Doctor of Philosophy Program in Geology

Department of Geology

Faculty of Science

Chulalongkorn University

Academic Year 2016

Copyright of Chulalongkorn University

Thesis Title MINERALOGICAL AND GEOCHEMICAL CHARACTERISTICS  
OF WASTE ROCKS AND TAILINGS FROM A GOLD  
MINE IN NORTHEASTERN THAILAND: APPLICATION FOR  
ENVIRONMENTAL IMPACT PROTECTION

By Miss Thitiphan Assawincharoenkij

Field of Study Geology

Thesis Advisor Associate Professor Chakkaphan Sutthirat, Ph.D.

Thesis Co-Advisor Associate Professor Christoph A. Hauzenberger, Ph.D.

---

Accepted by the Faculty of Science, Chulalongkorn University in Partial Fulfillment of  
the Requirements for the Doctoral Degree

.....Dean of the Faculty of Science  
(Associate Professor Polkit Sangvanich, Ph.D.)

THESIS COMMITTEE

.....Chairman  
(Professor Montri Choowong, Ph.D.)

.....Thesis Advisor  
(Associate Professor Chakkaphan Sutthirat, Ph.D.)

.....Thesis Co-Advisor  
(Associate Professor Christoph A. Hauzenberger, Ph.D.)

.....Examiner  
(Associate Professor Punya Charusiri, Ph.D.)

.....Examiner  
(Associate Professor Srilert Chotpantarat, Ph.D.)

.....External Examiner  
(Associate Professor Wasant Pongsapich, Ph.D.)

.....External Examiner  
(Chulalak Changul, Ph.D.)

ฐิติพรรณ อัครวินเจริญกิจ : ลักษณะเฉพาะทางวิทยาแร่และธรณีเคมีของหินทิ้งและกากแร่จากเหมืองทอง  
ในภาคตะวันออกเฉียงเหนือของประเทศไทย การประยุกต์สำหรับการป้องกันผลกระทบสิ่งแวดล้อม  
(MINERALOGICAL AND GEOCHEMICAL CHARACTERISTICS OF WASTE ROCKS AND  
TAILINGS FROM A GOLD MINE IN NORTHEASTERN THAILAND: APPLICATION FOR  
ENVIRONMENTAL IMPACT PROTECTION) อ.ที่ปริกษานิพนธ์หลัก: รศ. ดร. จักรพันธ์ สุทธิ  
รัตน์, อ.ที่ปริกษานิพนธ์ร่วม: รศ. ดร. คริสทอปท์ ฮิวเซนเบอร์เจอร์, 110 หน้า.

ปัจจุบันผลกระทบจากการทำเหมืองแร่ทองคำได้รับความสนใจเพิ่มมากขึ้น โดยเฉพาะด้าน  
สภาพแวดล้อมและสุขภาพอนามัยของประชาชนในท้องถิ่นโดยเฉพาะอย่างยิ่งในพื้นที่บริเวณภาค  
ตะวันออกเฉียงเหนือ แม้ว่าจะมีการทำเหมืองแร่ทองคำในประเทศไทยมาเป็นเวลานานกว่าสิบปี แต่การศึกษา  
ศักยภาพในการทำให้เกิดน้ำเหมืองเป็นกรด และการปนเปื้อนของสารอันตรายยังไม่ได้ดำเนินการอย่างจริงจัง ของ  
เสียที่เกิดจากการทำเหมืองอาจมีธาตุหรือองค์ประกอบที่เป็นอันตราย เช่น สารหนู ตะกั่ว สังกะสี แคดเมียมและ  
ไซยาไนด์ ซึ่งองค์ประกอบเหล่านี้อาจถูกปลดปล่อยออกมาโดยน้ำเหมืองที่เป็นกรด โดยมักจะพบในการทำเหมืองแร่  
โลหะซัลไฟด์รวมทั้งการทำเหมืองทองคำด้วย ของเสียที่เกิดจากการทำเหมืองในพื้นที่ศึกษานี้ ได้แก่ กากแร่และหินทิ้ง  
ซึ่งได้ถูกนำมาศึกษาองค์ประกอบทางแร่โดยใช้เครื่องมือ ดังนี้ กล้องจุลทรรศน์, XRD, Raman และ FTIR ส่วน  
องค์ประกอบทางเคมีโดยเครื่องมือ EPMA, XRF และ ICP-MS โดยตัวอย่างกากแร่สามารถแบ่งออกเป็น กากแร่สีเทา  
ส่วนบน และกากแร่สีเหลืองส่วนล่าง จากการศึกษาพบว่ากากแร่สีเทามีองค์ประกอบส่วนใหญ่เป็นแร่ซัลไฟด์ (พิโร  
ไทต์ ไพไรต์ และคาลโคไพไรต์) และแร่ซิลิเกต ดังนั้นกากแร่สีเทาจึงมีศักยภาพก่อให้เกิดน้ำเหมืองเป็นกรด ส่วนกาก  
แร่สีเหลืองประกอบด้วยแร่เกอไทต์ ควอตซ์ คลอไรต์ มัสโคไวต์ แคลไซต์ ฮีมาไทต์ และยังมีพบพิไรต์บ้างเล็กน้อย  
ซึ่งกากแร่ชนิดนี้ถูกจัดเป็นชนิดที่ไม่ก่อให้เกิดน้ำเหมืองเป็นกรด แต่อย่างไรก็ตามยังพบว่ากากแร่ตอนล่างนี้มี สารหนู  
(238–2870 มก./กก.) ทองแดง (750–2608 มก./กก.) และตะกั่ว (10–1506 มก./กก.) ในปริมาณสูง นอกจากนี้  
การศึกษาหินทิ้ง พบว่าหินทิ้งในพื้นที่ศึกษานี้ประกอบไปด้วย หินทราย หินทรายแป้ง หินกอสแซน หินสการ์น หิน  
สการ์น-ซัลไฟด์ หินซัลไฟด์เนื้อแน่น หินไดโอไรท์ และหินปูน/หินอ่อน จากการศึกษาพบว่าหินซัลไฟด์เนื้อแน่นและ  
หินสการ์น-ซัลไฟด์ที่ประกอบด้วยแร่ซัลไฟด์ (พิโรไทต์ ไพไรต์ คาลโคไพไรต์ และอาร์ซีโนไพไรต์) เมื่อถูกออกซิไดซ์จะ  
มีศักยภาพทำให้เกิดน้ำเหมืองเป็นกรด นอกจากนี้ยังพบว่าหินทั้งชนิดกอสแซนมีธาตุพิษสูง ได้แก่ สารหนู (334–810  
มก./กก.) ทองแดง (500–7500 มก./กก.) และสังกะสี (45–350 มก./กก.) ซึ่งหินทั้งชนิดกอสแซนนี้สามารถนำมาใช้  
สำหรับเป็นตัวดูดซับตามธรรมชาติ (ภายใต้สภาวะควบคุม ออกซิเดชันและ pH สูงกว่า 2) มีศักยภาพสูงในการใช้  
ฟื้นฟูพื้นที่รอบๆ ที่มีสารหนูและทองแดงปนเปื้อน จากผลการศึกษาที่ได้กล่าวไปแล้วจึงสรุปได้ว่ากากแร่สีเทาและหิน  
ทิ้งชนิดซัลไฟด์เนื้อแน่นและสการ์น-ซัลไฟด์ มีศักยภาพก่อให้เกิดน้ำเหมืองเป็นกรด ในขณะที่กากแร่สีเหลืองและหิน  
กอสแซนที่ประกอบด้วยธาตุพิษปริมาณสูง ซึ่งธาตุเหล่านี้จะไม่เสถียรในสภาวะน้ำเหมืองเป็นกรดและอาจถูก  
ปลดปล่อยออกสู่สิ่งแวดล้อมได้ ดังนั้นเพื่อเป็นการควบคุมไม่ให้เกิดน้ำเหมืองเป็นกรด จึงต้องปิดคลุมบ่อกักเก็บกาก  
แร่และกองหินทิ้ง (โดยเฉพาะกองหินทิ้งชนิดซัลไฟด์และกองหินทิ้งชนิดทรานซิชัน) ด้วยชั้นดินบดอัดทันทีหลังจากที่  
ปิดเหมือง เพื่อป้องกันการออกซิไดซ์ของแร่ซัลไฟด์

ภาควิชา	ธรณีวิทยา	ลายมือชื่อนิสิต .....
สาขาวิชา	ธรณีวิทยา	ลายมือชื่อ อ.ที่ปริกษาหลัก .....
ปีการศึกษา	2559	ลายมือชื่อ อ.ที่ปริกษาร่วม .....

# # 5472890823 : MAJOR GEOLOGY

KEYWORDS: TAILING / WASTE ROCK / GOLD MINE / TOXIC ELEMENT / THAILAND

THITIPHAN ASSAWINCHAROENKIJ: MINERALOGICAL AND GEOCHEMICAL CHARACTERISTICS OF WASTE ROCKS AND TAILINGS FROM A GOLD MINE IN NORTHEASTERN THAILAND: APPLICATION FOR ENVIRONMENTAL IMPACT PROTECTION. ADVISOR: ASSOC. PROF. CHAKKAPHAN SUTTHIRAT, Ph.D., CO-ADVISOR: ASSOC. PROF. CHRISTOPH A. HAUZENBERGER, Ph.D., 110 pp.

Gold mining activities have raised seriously concern on environment and health in the local communities, particularly in the northeastern Thailand. Although, gold mines in Thailand have been operated longer than decade, potentials of acid mine drainage (AMD) generation and toxic element releasing have not been investigated in detail. Various mining wastes may contain hazardous elements such as arsenic, lead, zinc, cadmium and cyanide. These elements may be released under AMD environment. Therefore, AMD is a severe environmental impact which often occurs in metal sulfide mines including gold mine. Mine wastes (i.e. tailings and waste rocks) from the study area in the northeastern Thailand are collected and investigated. Mineralogical and geochemical characteristics of these mine wastes were carried out using microscope, XRD, Raman, FTIR, EPMA, XRF and ICP-MS. The tailing samples can be divided into upper gray tailings and lower ochre tailings. The upper gray tailings mainly contain sulfide minerals (pyrrhotite, pyrite  $\pm$  chalcopyrite) and silicate minerals; consequently, they are defined as potential acid forming (PAF). On the other hand, the lower ochre tailings mainly contain goethite, quartz, chlorite, muscovite, calcite and hematite with minor pyrrhotite which they are classified as non-acid forming (NAF). However, the lower ochre tailings contain high contents of As (238–2870 mg kg<sup>-1</sup>), Cu (750–2608 mg kg<sup>-1</sup>) and Pb (10–1506 mg kg<sup>-1</sup>). Regarding to the waste rocks, they are characterized by sandstone, siltstone, gossan, skarn, skarn-sulfide, massive sulfide, diorite and limestone/marble. Among these rocks, the massive sulfide and skarn-sulfide rocks mainly consist of pyrrhotite, pyrite, arsenopyrite and chalcopyrite that are actual source of AMD. Moreover, the gossan rocks are composed of As (334–810 mg kg<sup>-1</sup>), Cu (500–7500 mg kg<sup>-1</sup>) and Zn (45–350 mg kg<sup>-1</sup>), which they can be used as a natural adsorbent (under controlled oxidizing condition and pH > 2) with high potential for remediation of As and Cu contamination within the surrounding areas. In conclusions, the upper tailings and the massive sulfide/skarn-sulfide rocks have potential of AMD generation whereas the lower tailings and gossan waste rock contain high contents of toxic elements. These toxic elements are unstable under acid drainage and they may be released into the environment. Therefore, the tailing storage is recommended to be covered to prevent the oxidizing processes of the upper tailings. For the waste rock dumping sites, particularly sulfide and transition dumps containing massive sulfide and skarn-sulfide rocks, they should also be cover by layer of compacted clay after the mine closure.

Department: Geology

Field of Study: Geology

Academic Year: 2016

Student's Signature .....

Advisor's Signature .....

Co-Advisor's Signature .....

## ACKNOWLEDGEMENTS

The most important acknowledgment of gratitude I wish to express is to my advisor Associate Professor Dr. Chakkaphan Sutthirat for the continuous support of my Ph.D. study and related research, for his patience, motivation, and immense knowledge. His guidance helped me in all the time of research and writing of this thesis. I could not have imagined having a better advisor and mentor for my Ph.D. study.

I would like to express my deepest thanks and sincere appreciation to my co-advisor, Associate Professor Dr. Christoph A. Hauzenberger, who provided me an opportunity to visit his university as exchange student of the University of Graz, and gave access to the laboratory and research facilities. Without his precious support it would not be possible to conduct this research.

I make this opportunity to thank all committees— such as Prof. Dr. Montri Choowong, Assoc. Prof. Dr. Wasant Pongsapich, Assoc. Prof. Dr. Punya Charusiri, Assoc. Prof. Dr. Srilert Chotpantarat and Dr. Chulalak Changul for their insightful comments and encouragement, but also for the hard question which incited me to widen my research from various perspectives.

I gratefully acknowledges the financial supports from Thailand Governments SAST from Master to Ph.D. for 4 years. In addition, this research was supported by the 90th Anniversary of Chulalongkorn University Fund (Ratchadaphiseksomphot Endowment Fund) Graduate School, Chulalongkorn University. Moreover, I would like to thank the Austrian Federal Ministry of Science, Research and Economy (BMWFW) for financial support ASEA-Uninet/Ernst Mach Grant (Ernst Mach weltweit TSOA) scholarship to visit the University of Graz for 6 months.

A special thanks goes to my fellow doctoral students, especially Mr. Alongkot Funka and Ms. Parisa Nimnate, for their feedback, cooperation and of course friendship. We had a difficult time and have happiness together. Moreover, I am grateful to Miss Somporn Wonglak for her assistance during sample collections.

In addition, I would like to thanks all staffs of Department of Geology, they give cordiality to me and I feel like living with family, especially Dr. Sakonvan Chawchai who always supported me and pushed me to be a confident person. In addition, I would like to thanks Mrs. Jiraprapa Niampun and Ms. Sopit Pumpuang for supporting my laboratory works in Department of Geology, Faculty of Science.

Last but not the least, I would like to acknowledge with gratitude, the support and love of my family – my parents, Nop-A Nun and Thipwipa; my younger sister, Athita and my younger brother, Pakanun. Moreover, I would like to thanks Mr. Akkarapon Sakjaroenying who has supported me throughout this process and has constantly encouraged me when the tasks seemed arduous and insurmountable. They all kept me going, and this research would not have not been possible without them.

## CONTENTS

	Page
THAI ABSTRACT .....	iv
ENGLISH ABSTRACT .....	v
ACKNOWLEDGEMENTS .....	vi
CONTENTS .....	vii
LIST OF TABLES .....	xi
LIST OF FIGURES .....	xiii
LIST OF ABBREVIATIONS .....	xvii
CHAPTER 1 INTRODUCTION .....	1
1.1 Introduction .....	1
1.2 Objectives .....	3
1.3 Scope of Work .....	4
1.4 Expected Outcomes .....	5
1.5 Theoretical Background and Relevant Research .....	5
1.5.1 Mine waste .....	5
1.5.2 Sulfidic mine waste .....	7
1.5.2.1 Pyrite ( $\text{FeS}_2$ ).....	7
1.5.2.2 Pyrrhotite ( $\text{Fe}_{(1-x)}\text{S}$ ) .....	8
1.5.2.3 Chalcopyrite ( $\text{CuFeS}$ ).....	8
1.5.2.4 Arsenopyrite ( $\text{FeAsS}$ ) .....	9
1.5.3 Acid mine drainage (AMD) or acid rock drainage (ARD).....	10
1.5.4 Toxic elements.....	12
1.5.5 Secondary minerals.....	12

	Page
1.5.6 The study area.....	15
CHAPTER 2 MINERALOGY AND GEOCHEMISTRY OF TAILINGS FROM A GOLD MINE IN NORTHEASTERN THAILAND .....	17
Abstract.....	18
2.1 Introduction.....	19
2.1.1 Site description and potential environmental impacts .....	21
2.1.2 Ore dressing and tailing generation.....	24
2.2 Methods and materials .....	25
2.2.1 Sampling and geochemical analyses.....	25
2.2.2 Acid forming potential analyses .....	26
2.3 Results .....	28
2.3.1 Mineral Assemblage .....	28
2.3.2 Mineral Chemistry.....	30
2.3.3 Bulk geochemistry .....	33
2.3.3.1 Major oxides .....	33
2.3.3.2 Trace elements.....	33
2.3.4 Acid forming potential (AFP).....	38
2.4 Discussion.....	39
2.4.1 Characteristics of Mine Tailings .....	39
2.4.2 AMD and Heavy Metal Contamination .....	42
2.5 Conclusions and recommendations.....	44
CHAPTER 3 MINERALOGICAL AND GEOCHEMICAL CHARACTERIZATION OF WASTE-ROCKS FROM A GOLD MINE IN NORTHEASTERN THAILAND: APPLICATION FOR ENVIRONMENTAL IMPACT PROTECTION .....	46



	Page
Abstract.....	47
3.1 Introduction.....	48
3.2 Geology and mineralization.....	52
3.3 Materials and methods.....	53
3.3.1 Rock wastes and dumping sites.....	53
3.3.2 Analytical methods.....	53
3.4 Results.....	55
3.4.1 Petrographical and geochemical characteristics.....	55
3.4.2 Mineral chemistry.....	59
3.5 Discussion.....	61
3.6 Conclusions and recommendations.....	67
3.7 Electronic Supplementary Material A: Petrographic Description.....	68
3.8 Electronic Supplementary Material B: Whole-rock Geochemistry.....	71
CHAPTER 4           MINERALOGICAL AND CHEMICAL CHARACTERISTICS OF GOSSAN WASTE ROCKS FROM A GOLD MINE IN NORTHEASTERN THAILAND.....	76
Abstract.....	77
4.1 Introduction.....	78
4.2 Materials and methods.....	79
4.3 Results.....	81
4.3.1 Mineral texture and assemblage.....	81
4.3.2 Chemical composition.....	84
4.4 Discussions.....	88
4.4.1 Characteristics.....	88

	Page
4.4.2 Sorption-desorption of toxic element.....	89
4.5 Conclusion .....	92
CHAPTER 5 CONCLUSION AND RECOMMENDATION .....	93
5.1 Conclusion .....	93
5.2 Recommendation.....	95
REFERENCES .....	96
VITA.....	110



## LIST OF TABLES

	Page
<b>Table 1.1</b> Relative resistance of sulfide minerals in oxidized waste materials [modified after Moncur et al. (2009) and Lindsay et al. (2015)]. .....	10
<b>Table 1.2</b> Simplified acid producing reactions in the complete oxidation of the sulfide minerals .....	11
<b>Table 1.3</b> Chemical formula of sulfide minerals and minor and trace element substitution. ....	13
<b>Table 1.4</b> Effect of pollutants on human health and permissible level modified from Singh et al. (2011); Kasprzak et al. (2003); Das et al. (2008). ....	14
<b>Table 2.1</b> Representative EPMA analyses of sulfide minerals from the upper and lower tailings. ....	31
<b>Table 2.2</b> Representative EPMA analyses of goethite from the lower tailings. ....	32
<b>Table 2.3</b> Bulk geochemical analyses (wt.% oxides) of the gold mine tailings, as determined by XRF analysis and loss on ignition (LOI) contents. ....	34
<b>Table 2.4</b> Trace element concentrations in the gold mine tailings, as determined by ICP-MS analysis.....	36
<b>Table 2.5</b> Analyses of acid forming potential (AFP) of the gold mine tailings in northeastern Thailand .....	40
<b>Table 2.6</b> Classification of acid forming potential (AFP) using various criteria for mine tailings from the gold mine in Northeastern Thailand.....	41
<b>Table 3.1</b> Summary of mineral assemblages in waste rocks taken from some well-known metal mines around the world. ....	49
<b>Table 3.2</b> Estimated amounts and volumes of all waste rock dumps from the main pit. Total rock waste was estimated at 2,552,170 metric tons (Mt) and 997,280 cubic meters (m <sup>3</sup> ) (Khon Kaen University Report, 2009). ....	53

<b>Table 3.3</b> Representative EPMA analyses (wt.%) of sulfide minerals in the massive sulfide and skarn-sulfide waste rocks.....	62
<b>Table 3.4</b> Representative EPMA analyses (wt.%) of amorphous hydrous ferric oxides (HFO) found in the gossan waste rocks.....	63
<b>Table 3.5</b> Summary of trace elements (mg/kg and wt.%) in waste rocks from the study area and other mine sites.....	66
<b>Table 3.6</b> Major and minor oxide contents (wt.%) of waste rocks from the studied gold mine in northeastern Thailand, analyzed from glass beads and some pressed powders using XRF.....	72
<b>Table 3.7</b> Trace elements (ppm except Au in ppb) in the waste rocks from the studied gold mine in northeastern Thailand, analyzed by ICP-MS using solution samples and some pressed powder samples analyzed by XRF. ....	74
<b>Table 4.1</b> Mineral assemblages and their ideal chemical formula. ....	84
<b>Table 4.2</b> Statistics of EPMA analyses of major and minor elements (Si, Al, Fe, Mg, Ca, Mn and Na), with some crucial trace elements (As, Cu and S) of all types selected from gossan samples, all concentrations in percent weight (%). ....	86

## LIST OF FIGURES

	Page
<b>Figure 1.1</b> Map of Thailand showing location of the study area, Thung Kham Gold mine in Loei Province, Northeastern Thailand (marked by red star).....	2
<b>Figure 1.2</b> (a) Locations of tailing storage, northern storage, waste rock dumping sites, plant and open pit of the Thung Kham mine (the Google Earth satellite image was taken on the 9 <sup>th</sup> February 2016); photographs (b) and (c) of the tailing storage and waste rock dumps, respectively (these photographs were taken on the 1 <sup>st</sup> May 2012).....	4
<b>Figure 1.3</b> Geological map of the study area in northeastern Thailand modified from Rodmanee (2000).....	16
<b>Figure 2.1</b> (a) (insert) The study area location in northeastern Thailand and (main panel) the local map showing the location of the mine (main pit), tailing pond, old pits and waste rock dumps (WRD). SP1–SP4 are the sites of the four drill cores. (b) Cross section of the main pit showing the locations of the different ore types modified after Khon Kaen University Report (2009). (c) Cross section showing the outline of tailing pond and locations of the four drill cores (SP1–SP4).....	22
<b>Figure 2.2</b> Satellite image of the study area (source: Google Earth on February 9, 2016) showing the location of collapsed tailing pond in October 2012.....	24
<b>Figure 2.3</b> Representative XRD patterns of (a) the upper tailings and (b) the lower tailings. Mineral abbreviations are Q:quartz, Di:diopside, Po:pyrrhotite, Ad:andradite, C:calcite, Py:pyrite, Ms: muscovite, Cl:chlorite and Gth:goethite.....	29
<b>Figure 2.4</b> Core specimens of (a) upper tailing and (d) lower tailing; photomicrographs of polished-sections under plane-polarized reflected light showing (b) and (c) pyrrhotite (Po), chalcopyrite (Ccp), pyrite (Py) and others in the upper tailing; (e) mainly goethite (Gth) and some quartz (Qz) and pyrrhotite (Po) in the lower tailing and (f) cracked grain intergrowth between pyrrhotite (Po), pyrite (Py) and covellite (Cv) (top left), concentric Fe-oxyhydroxide (top	

- right), colloform goethite (Gth) (bottom left) and oxidized pyrite regular grain (bottom right).....30
- Figure 2.5** Variation diagrams of selected major oxides against the level of SiO<sub>2</sub> for the samples in Table 2.3.....35
- Figure 2.6** Plots of the SiO<sub>2</sub> level against the potential selected toxic elements, As, Mn, Co, Cu, Pb and Ni, for the samples in Table 2.4.....37
- Figure 3.1** (a) The geological map of the study area showing the location of mining sites, including OXWD-1, -2 (oxide waste dumps 1 and 2), SFWD (sulfide waste dump) and TSWD (transition waste dump); (b) genesis model of the initial and following gold mineralization stages (modified from Rodmanee (2000)); (c) cross section of the main pit showing three different ore types (modified after Khon Kaen University Report (2009)).....51
- Figure 3.2** Waste rock dumps: (a) and (b) dump sites of oxide waste rocks (OXWD-1 and OXWD-2); (c) sulfide waste dump (SFWD); (d) transition waste dump (TSWD).....54
- Figure 3.3** Plots of FeO<sub>t</sub> (wt.%) contents against SiO<sub>2</sub>, Al<sub>2</sub>O<sub>3</sub>, CaO, MnO, MgO and SO<sub>3</sub> (wt.%) of sandstone/siltstone, diorite, gossan, skarn, skarn-sulfide and massive sulfide.....57
- Figure 3.4** Plots of FeO<sub>t</sub> (wt.%) versus As (arsenic), Cd (cadmium), Cr (chromium), Cu (copper), Hg (mercury) and Zn (zinc) levels (ppm) of sandstone/siltstone, diorite, gossan, skarn, skarn-sulfide and massive sulfide.....58
- Figure 3.5** Back Scattered Electron (BSE) Images and X-ray maps of gossan samples' levels of As, Cu, Fe and Mn in: (a) and (b) amorphous hydrous ferric oxides and (c) goethite and gypsum. Abbreviations are HFO: hydrous ferric oxide, Ox-Px: oxidized-pyroxene, Gth: goethite, and Gp: gypsum.....60
- Figure 3.6** Eh–pH diagram for the Fe–As–S–O system (25 °C, 1 atm) and plots of surface water collected from the ponds around the waste rock dumps (SFWD, TSWD and OXWD, data from ERIC (2012). The dashed box indicates typical near-surface conditions modified from Craw et al. (2003).....64
- Figure 3.7** Photomicrographs under transmitted-light of (a) fine-grained sandstone, (b) diorite and (c) garnet-pyroxene skarn rock. Photomicrographs under

reflected-light of (d) skarn-sulfide, (e) massive sulfide, (f) gossan showing colloform goethite and sulfide minerals, (g) gossan showing goethite enclosing gypsum and (h) gossan presenting some garnets with relic pyroxene surrounded by goethite or hydrous ferric oxide. Abbreviations are Qz: quartz, Bt: biotite, Rf: rock fragment, Kfs: K-feldspar, Hbl: hornblende, Pl: plagioclase, Px: pyroxene, Grt: garnet, Gth: goethite, Apy: arsenopyrite, Po: pyrrhotite, Ccp: chalcopyrite, Gp: gypsum, Ox-Silicate: oxidized-silicate mineral, Ox-Px: oxidized-pyroxene and HFO: hydrous ferric oxide..... 69

**Figure 3.8** Representative (a) Raman pattern of crystalline goethite and (b) FTIR patterns of hydrous ferric oxide (HFO) (top) and goethite (bottom) ..... 70

**Figure 4.1** Photographs of mining activities in the study area such as (a) gold processing plant, (b) mining pit showing location of dumped waste rocks of ore-barren gossan in (c) and (d) the dump sites. .... 80

**Figure 4.2** Photographs of gossan rock samples and selected areas for investigation. (a) sample-1 includes type-I: pale yellow, type-II: brownish yellow, and type-III: yellowish brown. (b) sample-2 includes type-IV: dusky red and type-V: red. .... 81

**Figure 4.3** Back Scattering Electron (BSE) images taken from SEM showing micromorphology of: (a) type-I and (b) type-II showing lath-shaped crystals of primary quartz; (c) type-III, (d) type-IV and (e) type-V showing flaky-shaped microcrystalline of goethite and secondary quartz (microcrystalline quartz). .... 82

**Figure 4.4** XRD patterns of the samples (a) type-I, (b) type-II, (c) type-III, (d) type-IV and (e) type-V collected selectively from the gossan rocks. Abbreviations of mineral were suggested by Whitney and Evans (2010) i.e., Qz (quartz), Ep (epidote), Grt (garnet), Amp (amphibole), Mnt (montmorillonite), Gth (goethite), Jrs (jarosite), Ank (ankerite), Mag (magnetite) and Gp (gypsum). .... 83

**Figure 4.5** Plots of Fe/Si versus other elemental ratios (Al, Mg, Ca, S, As and Cu against Si)..... 87

**Figure 4.6** Eh–pH diagram for the systems  $\text{Fe}_2\text{O}_3\text{--SO}_3\text{--H}_2\text{O}$  suggested by Majzlan et al. (2004) showing consistency of Fe-oxyhydroxide minerals (i.e., schwertmannite  $(\text{Fe}_8\text{O}_8(\text{OH})_6(\text{SO}_4)_n\text{H}_2\text{O})$ , ferrihydrite  $(\text{Fe}_5\text{HO}_8\cdot 4\text{H}_2\text{O})$  and

green rust ( $\text{Fe}^{\text{II}}\text{-Fe}^{\text{III}}(\text{OH})$ ) and the speciation of arsenic in the aqueous phase suggested by Majzlan et al. (2007).....91





## LIST OF ABBREVIATIONS

AMD	Acid mine drainage
ARD	Acid rock drainage
ABA	Acid base accounting
APF	Acid forming potential
MPA	Maximum potential acidity
ANC	Acid neutralizing capacity
NAG	Net acid generation
NAPP	Net acid-producing potential
NAF	Non-acid formation
PAF	Potential acid formation
UC	Uncertainly classified
NGO	Non-government organization
LOI	Loss on ignition
SEM	Scanning electron microscope
FTIR	Fourier transform infrared spectroscopy
EPMA	electron micro probe analyzer
XRD	X-ray powder diffraction
XRF	X-ray fluorescence
ICP-MS	Inductively coupled plasma mass spectrometry
n.d.	Non-detected
LD	Lower than detection limit
SD	Standard deviation
TTLIC	Total threshold limit concentration
TSQS	Thailand soil quality standard
TGQS	Thailand groundwater quality standard
TSWQ	Thailand surface water quality
HDPE	High-density polyethylene
SFWD	Sulfide waste dump
TSWD	Transition waste dump

OXWD	Oxide waste dump
Wt.%	Weigh percent
mg/kg, mg kg <sup>-1</sup>	Milligram per kilogram
µg/kg	Microgram per kilogram
mg/L	Milligram per liter
ppm	Part per million
m	Meter
cm	Centimeter
mm	Millimeter
°C	Degree Celsius
h	Hours



# CHAPTER 1

## INTRODUCTION

### 1.1 Introduction

Recently, environmental impacts from mining activities have been concerned seriously by local community, NGO, governmental agencies and private sectors. Various mining wastes may have been generated; some of them may contain hazardous components such as arsenic, lead, zinc, copper, mercury, cadmium and cyanide. These components can be released when acid drainage is generated. Subsequently, they may affect ecosystem and human health (Jackson and Parbhakar-Fox, 2016; Simate and Ndlovu, 2014). Acid drainage or acid mine drainage (AMD) is a serious environmental impact which is often occurred from sulfide-bearing wastes when they have exposed to the atmosphere (Lottermoser, 2010; Parbhakar-Fox and Lottermoser, 2015; Sutthirat, 2011). During mine operation, enormous mine wastes are generated and dumped around mine site.

Thung Kham Gold mine located in Loei province, northeastern Thailand as shown Figure 1.1 was selected for this study. Regarding to gold deposit, gold occurs mainly in skarn, massive sulfide and gossan rocks which form as small veins in sedimentary host rocks (Rodmanee, 2000). Thus, the enormous waste rocks and tailings, potentially contain sulfide minerals, have been presented within the mine site (Figure 1.2a). They may generate acid mine drainage (AMD) and release hazardous components. These situations were previously reported by many researchers (Akcil and Koldas, 2006; Carbone et al., 2013; Jackson and Parbhakar-Fox, 2016; Lengke et al., 2010; Lindsay et al., 2009; Lindsay et al., 2015; Lottermoser, 2010; Lottermoser, 2011; Simate and Ndlovu, 2014; Valente et al., 2013; Valente and Leal Gomes, 2009).

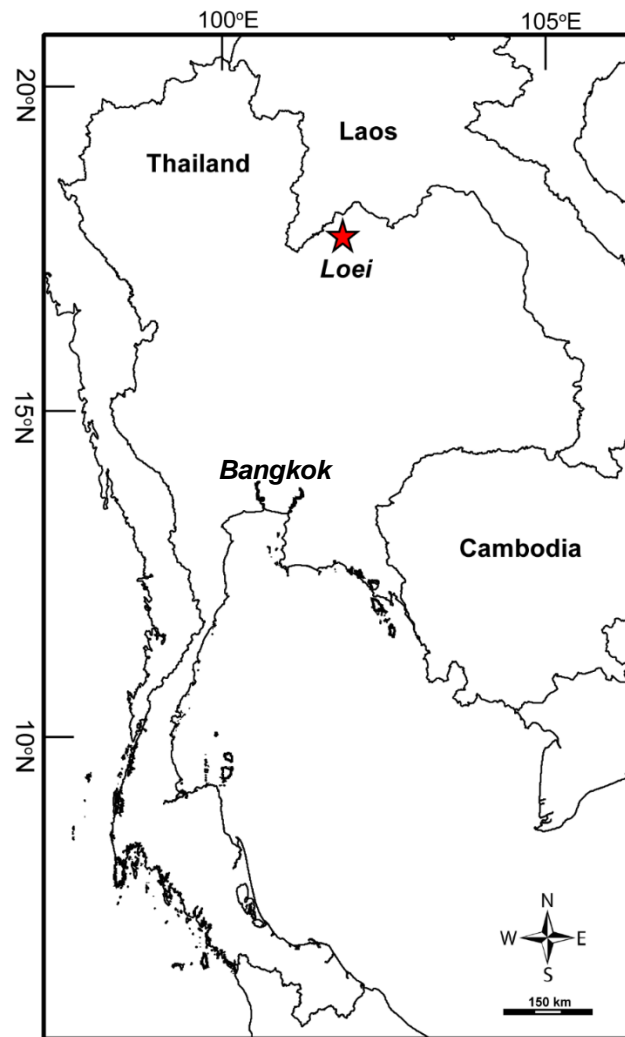


**Figure 1.1** Map of Thailand showing location of the study area, Thung Kham Gold mine in Loei Province, Northeastern Thailand (marked by red star).

Waste rocks are transported from the open pit and then dumped at the dumping sites (Figure 1.2c) while the tailings are flowed through the pipes to the tailing storage (Figure 1.2b).

Many protesters including NGO have complained that groundwater and surface water have been contaminated by arsenic and some other heavy metals which might leak out from the tailing storage or waste rock dumps. Therefore, the study of mine wastes is important because it can predict and monitor such mentioned environmental impacts. However, this aspect is quite new research theme in Thailand.

This report combines three manuscripts which have been published in standard international journals. These manuscripts had been carried out during this PhD study which emphasized on the solid mine wastes, both tailings and waste rocks. These waste materials were dumped in the Thung Kham gold mine. Because ores consist of massive sulfide and gossan rocks; therefore, these tailings and waste rocks potentially contain high sulfide minerals and toxic elements. Consequently, mineralogical and geochemical characteristics of these tailings and waste rocks should be investigated. All the results from this study are then reported in Chapter 2 to Chapter 4.

Characteristics of tailings are reported in Chapter 2, entitled “Mineralogy and geochemistry of tailings from a gold mine in northeastern Thailand”. Subsequently, investigation of waste rocks is present in Chapter 3 on the topic “Mineralogical and geochemical characterization of waste-rocks from a gold mine in northeastern Thailand: Application for environmental impact protection”. The topic in Chapter 3 has been revised and should be accepted by Environmental Science and Pollution Research to be published soon. Finally, the detailed experiment of gossan waste rocks is shown in Chapter 4, namely “Mineralogical and chemical characteristics of gossan waste rocks from a gold mine in northeastern Thailand”.

## 1.2 Objectives

The main objectives of the thesis research are:

1. To investigate petrography and whole-rock geochemistry of waste rocks in relation to AMD generation and metal releasing; and
2. To characterize mineral composition, mineral chemistry and bulk geochemistry of mine tailings in relation to AMD potential and metal source of contamination.

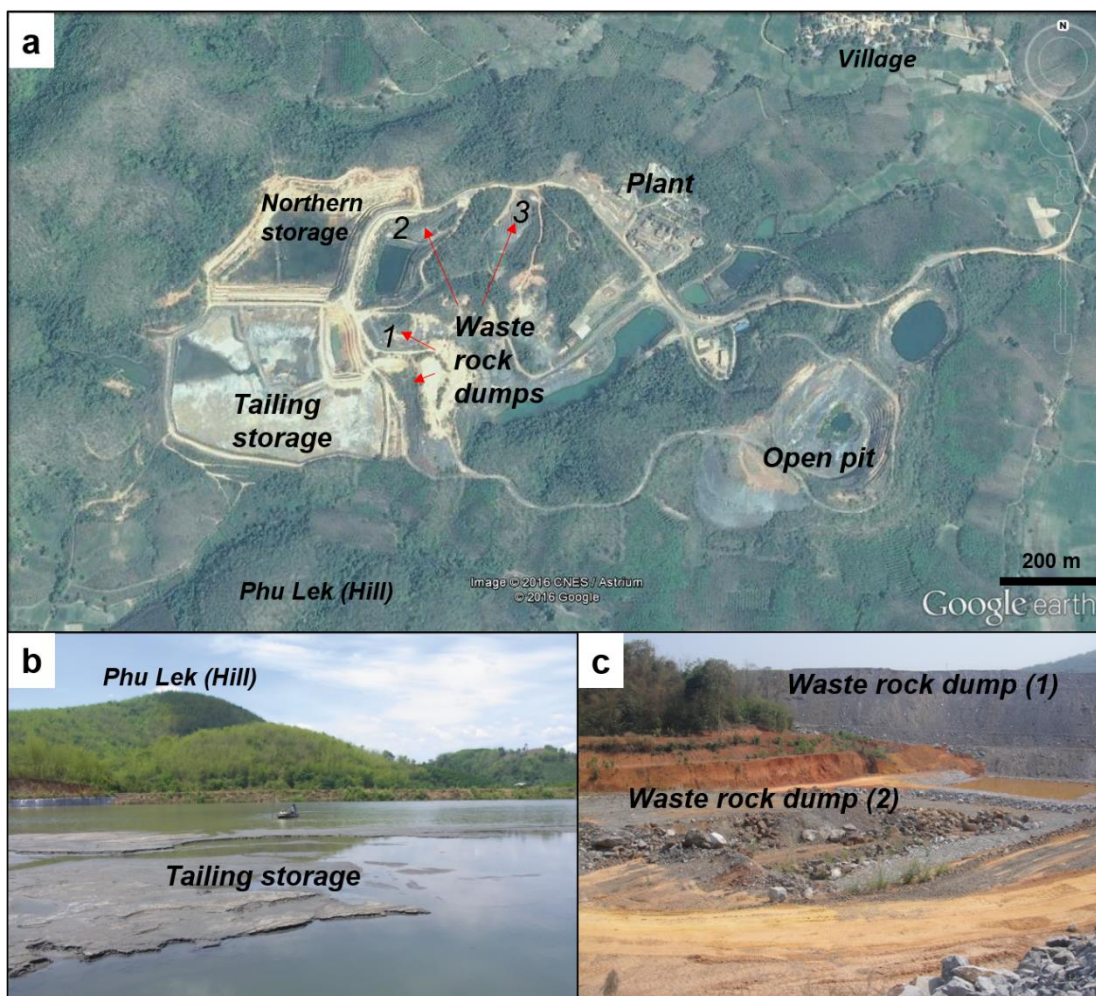


**Figure 1.2** (a) Locations of tailing storage, northern storage, waste rock dumping sites, plant and open pit of the Thung Kham mine (the Google Earth satellite image was taken on the 9<sup>th</sup> February 2016); photographs (b) and (c) of the tailing storage and waste rock dumps, respectively (these photographs were taken on the 1<sup>st</sup> May 2012).

### 1.3 Scope of Work

This research is focused on mineralogical compositions and geochemical characteristics of main mine wastes including waste rocks and tailings from the Thung Kham Gold mine in Northeastern Thailand. Potentials of acid mine drainage (AMD) of tailings are also examined.

## 1.4 Expected Outcomes

Results of this study may lead to risk reduction plans of the study gold mine. Mine closure and waste management should be well operated using information gained from the study. Eventually, environmental impacts, particularly generation of AMD and releasing of toxic elements, will never take place in this area.

## 1.5 Theoretical Background and Relevant Research

### 1.5.1 Mine waste

Mine wastes are either solid or liquid or gaseous phases produced by mining, mineral processing and metallurgical extraction. They are eventually dumped and left around the mining site after removing valuable metals from an ore and refining the extractable metals into a purer form; in general, they are unwanted materials without current economic value (Hudson-Edwards et al., 2011). Common solid mining wastes can be grouped as (1) waste rocks and (2) tailings in most cases.

(1) Waste rocks are removed from the mining sites, especially by quarrying and excavation. Various types of waste rocks found in different ore deposits should have different compositions that would be characterized using both mineralogical and geochemical compositions (Sutthirat, 2011). Acid generation of some waste rocks, which usually contain sulfide minerals, may take place depending on the environmental conditions, particularly oxidation of sulfides (Changul et al., 2009a; Nugraha et al., 2009; Parbhakar-Fox et al., 2013; Parbhakar-Fox et al., 2014; Smuda et al., 2007; Sracek et al., 2006).

(2) Tailings are mixture of milled rock and chemical fluids that may contain cyanide (CN<sup>-</sup>) in the case of gold mine (Jambor et al., 2009; Khodadad et al., 2008). These materials remain from mineral processing and metal extraction (Hudson-Edwards et al., 2011). They are similar to slurry that is a mixture of fine grained sediment and water, which they have been stored in a tailing storage facility. During the mineral processing, ores and their host rocks have to be ground and milled prior to mineral separation. Chemical additives may also be added during the process. Some of them may still remain in the tailings while most of these chemicals are usually recovered

and reused in the process. Moreover, some chemical additives (e.g., cyanide) are decomposed by the natural process within a short period; however, many of them may be bound strongly and long-lasting within the tailings. In addition, some tailings may also contain concentrations of non-economic minerals such as silicates, oxides, hydroxides, carbonates and sulfides that have never been collected throughout the dressing process (Sutthirat, 2011).

Many researchers studied about characteristics of mine waste related to acid mine drainage (AMD) generation and toxic elements releasing as summarized below.

Marescotti et al. (2008) suggested that the main source of the pollutant is represented by sulfide-bearing fragments contained in tailings and waste rocks from the Libiola Fe-Cu sulfide mine, Italy. They found that the tailing was dominated by secondary Fe-oxides and Fe-oxyhydroxides, known as stable mineral, which completely replaced primary sulfide clasts, so these tailings are practically inert material. On the other hand, the sulfide-bearing waste rocks still have a strong potential to produce long term AMD.

The study of low sulfide tailings from Hitura sulfide mine in Finland was reported by Heikkinen and Räsänen (2008). These mine tailings were composed largely of serpentine, talc, mica and amphibole with minor carbonate and accessories of sulfide minerals, such as pyrrhotite, pentlandite and chalcopyrite. This study shows that the Hitura tailings are either as 'non-potentially AMD generating', when the silicate buffer is taken into account, or as 'likely AMD producing', if only the carbonate buffer is considered. Because the carbonate buffer can be dissolved in the shallow tailings while sulfide minerals still remain; therefore, AMD generation and heavy metal releasing may likely happen in the future. As a result, the low sulfide tailings should be immediately covered after mine close to prevent sulfide oxidation.

Changul et al. (2009b) investigated mine tailing at Akara Gold mine in Thailand. They stated that chemical and mineral compositions of mine tailing are needed to investigate before leaching experiments of heavy metals from the tailing. The results of this study found that tailings mainly consist of primary minerals such as quartz, calcite and feldspar. All of these tailings are classified as 'non-acid formation' (NAF) and their total heavy metal concentrations fall within the Thailand Soil Quality Standards. Moreover, Changul et al. (2009a) also studied the potential AMD generating



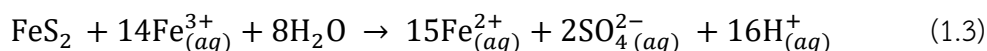
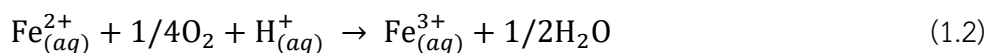
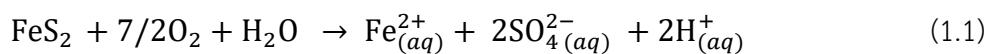
from waste rocks at Akara Gold mine. They found that the silicified lapilli tuff and sheared tuff have potential to generate acidity.

### 1.5.2 Sulfidic mine waste

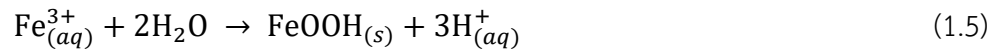
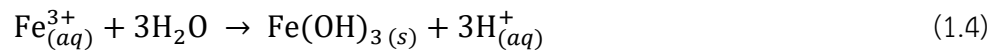
Coal and metal (e.g. Cu, Au, Pb, Zn, Ni, U and Fe) mines have high potential to environmental impact because they are mainly composed of sulfide minerals, especially iron-sulfide such as pyrite, pyrrhotite, arsenopyrite and chalcopyrite. These sulfide minerals are stable under reducing condition (Lottermoser, 2010). They are possibly oxidized, when they are exposed to the atmosphere, and may generate acid aquatic drainage ( $H^+$ ). The oxidation reaction of the common sulfide minerals is summarized below.

#### 1.5.2.1 Pyrite ( $FeS_2$ )

Pyrite is the most abundant sulfide minerals. It has been found in various geological environments. However, it is commonly associated with coal and metal ore deposits. Pyrite can be directly oxidized by oxygen and water to produce dissolved ferrous iron ( $Fe^{2+}$ ) (Eq. 1.1) (Evangelou and Zhang, 1995). Ferrous iron ( $Fe^{2+}$ ) is subsequently oxidized to ferric iron ( $Fe^{3+}$ ) (see Eq. 1.2). The  $Fe^{3+}$  is recognized as a more potent oxidant than oxygen even. In fact, below pH value of about 3, the oxidation of pyrite by  $Fe^{3+}$  is about 10–100 times faster than by  $O_2$  (Simate and Ndlovu, 2014). It can oxidize pyrite and further decreases pH (Simate and Ndlovu, 2014) (Eq. 1.3).

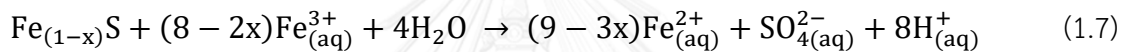
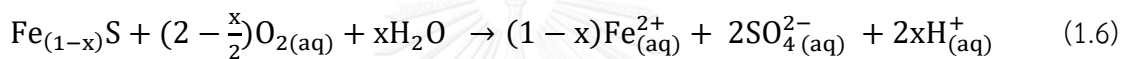


Solubility of ferric iron is usually low at neutral pH. Therefore, if the pH increases to higher than 3, the precipitations of hydroxides ( $Fe(OH)_3$ ), as a replacement for ferrihydrite [ $5Fe_2O_3 \cdot 9H_2O$ ] (Moncur et al., 2009), and oxy-hydroxides ( $FeOOH$ ) can be occurred as shown in equations (1.4) and (1.5), respectively (Lottermoser, 2010).



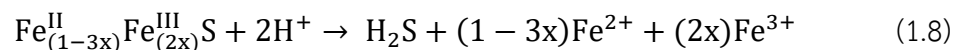
### 1.5.2.2 Pyrrhotite ( $\text{Fe}_{(1-x)}\text{S}$ )

Pyrrhotite is the second most abundant sulfide minerals occurred in the Earth crust (Belzile et al., 2004). When pyrrhotite is oxidized, pH may be reduced to > 4 (Belzile et al., 2004); consequently, ferrous and sulfuric acid will be generated (Eq. 1.6). Ferrous ion is oxidized to ferric ion (see Eq. 1.2) becoming an oxidant to react with pyrrhotite (Eq. 1.7).



In addition, relative resistance of the sulfide minerals, based on microscope investigation of several sulfide tailings, was suggested by Moncur et al. (2009) (Table 1.1). Therefore, the oxidation reduction of pyrrhotite is the quickest process compared to the other sulfides.

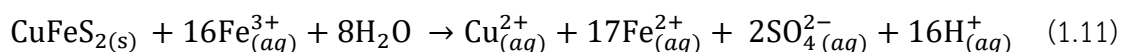
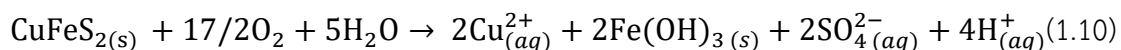
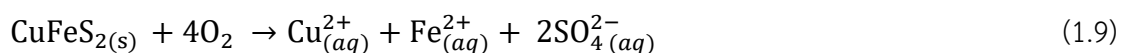
Pyrrhotite is iron deficient mineral, because the missing  $\text{Fe}^{2+}$  in the pyrrhotite structure is replaced by the  $\text{Fe}^{3+}$  (Chiriac and Rimstidt, 2014; Moncur et al., 2009; Murphy and Strongin, 2009), so the chemical formula of pyrrhotite can be written as  $\text{Fe}_{(1-3x)}^{\text{II}}\text{Fe}_{(2x)}^{\text{III}}\text{S}$  (Chiriac and Rimstidt, 2014). Therefore,  $\text{Fe}^{3+}$  might be released under acidic solution (Eq. 1.8), which it is used for oxidizing pyrrhotite (Eq. 1.7).



### 1.5.2.3 Chalcopyrite ( $\text{CuFeS}$ )

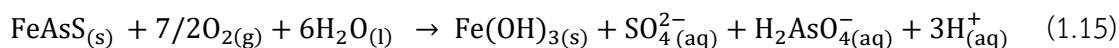
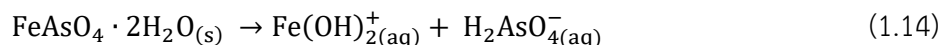
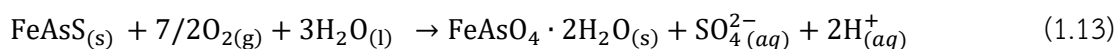
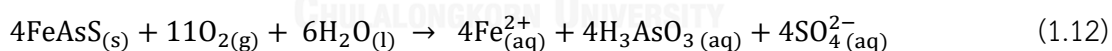
Chalcopyrites exposed to the atmosphere are oxidized by  $\text{O}_2$  (Eq. 1.9) (Anawar, 2015; Simate and Ndlovu, 2014); their oxidation can be induced by oxygen and water (Eq. 1.10) (Parbhakar-Fox and Lottermoser, 2015). Moreover, ferric ( $\text{Fe}^{3+}$ )

produced from ferrous ( $\text{Fe}^{2+}$ ) can also oxidize chalcopyrite (Eq. 1.11) (Anawar, 2015). Complete chalcopyrite oxidation will generate Fe-oxyhydroxide and Fe-hydroxide from hydrolysis of ferric (Eqs. 1.4 and 1.5).




#### 1.5.2.4 Arsenopyrite ( $\text{FeAsS}$ )

The oxidation of arsenopyrite by atmospheric  $\text{O}_2$  is present in equation 1.12 (Lindsay et al., 2015). Arsenopyrite may generate scorodite [ $\text{Fe}^{3+}\text{As}^5\text{O}_4 \cdot 2\text{H}_2\text{O}$ ] (Eq. 1.13) (Lottermoser, 2010). Scorodite, in turn, can dissolve and generate  $\text{Fe}^{3+}(\text{OH})_2^+$  along with  $\text{H}_2\text{As}^{5+}\text{O}_4^-$  (Eq. 1.14) (Anawar, 2015). Otherwise, complete oxidative reduction of arsenopyrite can produce iron-hydroxide, arsenate ( $\text{As}^{5+}$ ) and sulfuric acid (Eq. 1.15) (Parbhakar-Fox and Lottermoser, 2015). Ferrous ion ( $\text{Fe}^{2+}$ ) oxidizes to ferric ion ( $\text{Fe}^{3+}$ ) (Eq. 1.2). Under  $\text{pH} \geq 3$ , Fe-hydroxide can precipitate by hydrolysis of ferric ion (Eqs. 1.4 and 1.5) (Lottermoser, 2010).



In addition, the complete oxidations of the sulfide minerals (pyrite/marcasite, pyrrhotite, chalcopyrite, arsenopyrite, sphalerite and galena) are summarized in Table 1.2 that was modified from Lindsay et al. (2015), Lottermoser (2010) and Parbhakar-Fox and Lottermoser (2015).

**Table 1.1** Relative resistance of sulfide minerals in oxidized waste materials [modified after Moncur et al. (2009) and Lindsay et al. (2015)].

Mineral	Formula	Resistance	
Pyrrhotite	$\text{Fe}_{(1-x)}\text{S}$	Low	
Galena	$\text{PbS}$		
Sphalerite	$(\text{Zn}_{(1-x)}\text{Fe}_x)\text{S}$		
Bornite	$\text{Cu}_5\text{FeS}_4$		
Pentlandite	$(\text{Fe,Ni})_9\text{S}_8$		
Arsenopyrite	$\text{FeAsS}$		
Marcasite	$\text{FeS}_2$		
Pyrite	$\text{FeS}_2$		
Chalcopyrite	$\text{CuFeS}_2$		
Molybdenite	$\text{MoS}_2$		High

### 1.5.3 Acid mine drainage (AMD) or acid rock drainage (ARD)

Acid mine drainage (AMD) or acid rock drainage (ARD) may take place when sulfide minerals have exposed to the air as explained above. Under pH lower than 5.5, many elements including metals (e.g., Fe, Cu, Pb, Zn, Cd, Co, Cr, Ni, Hg), metalloids (e.g., As and Sb) and other elements (e.g., Al, Mn, Si, Ca, Na, K, Mg, Ba, F) can be dissolved from both sulfide and silicate minerals, and released into groundwater and surface water (Lottermoser, 2010). In general, coal mine, metal mine, open pit, ore stockpiles, tailing storages, as well as waste rock dumps are potential sources of AMD, if they contain the sulfide minerals.

**Table 1.2** Simplified acid producing reactions in the complete oxidation of the sulfide minerals

Mineral	Chemical reaction	References
Pyrite/ marcasite	$\text{FeS}_{2(s)} + 15/4 \text{O}_{2(g)} + 7/2 \text{H}_2\text{O}_{(l)} \rightarrow \text{Fe}(\text{OH})_{3(s)} + 2\text{SO}_4^{2-}{}_{(aq)} + 4\text{H}^+{}_{(aq)}$	(1), (3)
Pyrrhotite	$\text{Fe}_{0.9}\text{S}_{(s)} + 2.175\text{O}_{2(g)} + 2.35\text{H}_2\text{O}_{(l)} \rightarrow 0.9\text{Fe}(\text{OH})_{3(s)} + \text{SO}_4^{2-}{}_{(aq)} + 2\text{H}^+{}_{(aq)}$	(2)
Chalcopyrite	$2\text{CuFeS}_{2(s)} + 17/2\text{O}_{2(g)} + 5\text{H}_2\text{O}_{(l)} \rightarrow 2\text{Cu}^{2+}{}_{(aq)} + 2\text{Fe}(\text{OH})_{3(s)} + 4\text{SO}_4^{2-}{}_{(aq)} + 4\text{H}^+{}_{(aq)}$	(3)
Arsenopyrite	$\text{FeAsS}_{(s)} + 7/2\text{O}_{2(g)} + 3\text{H}_2\text{O}_{(l)} \rightarrow \text{FeAsO}_4 \cdot 2\text{H}_2\text{O}_{(s)} + \text{SO}_4^{2-}{}_{(aq)} + 2\text{H}^+{}_{(aq)}$	(2)
	or $\text{FeAsS}_{(s)} + 7/2\text{O}_{2(g)} + 6\text{H}_2\text{O}_{(l)} \rightarrow \text{Fe}(\text{OH})_{3(s)} + \text{SO}_4^{2-}{}_{(aq)} + \text{H}_2\text{AsO}_4^- + 3\text{H}^+{}_{(aq)}$	(3)
Sphalerite (Fe-rich)	$(\text{Zn, Fe})\text{S}_{(s)} + 3\text{O}_{2(g)} + \text{H}_2\text{O}_{(l)} \rightarrow \text{Zn}^{2+}{}_{(aq)} + \text{Fe}(\text{OH})_{3(s)} + \text{SO}_4^{2-}{}_{(aq)} + 2\text{H}^+{}_{(aq)}$	(2)
	or $\text{ZnS}_{(s)} + 2\text{O}_{2(g)} \rightarrow \text{Zn}^{2+}{}_{(aq)} + \text{SO}_4^{2-}{}_{(aq)}$	(3)
Galena	$\text{PbS}_{(s)} + 2\text{O}_{2(g)} \rightarrow \text{Pb}^{2+}{}_{(aq)} + \text{SO}_4^{2-}{}_{(aq)}$	(3)

(1) Lindsay et al. (2015); (2) Lottermoser (2010); (3) Parbhakar-Fox and Lottermoser (2015)

Most of the solid mine wastes, particular sulfide-bearing mine wastes, exposing to the atmosphere, may undertake weathering reactions and biological process (by microorganisms) and subsequently generate acid mine drainage (AMD) (Holmström et al., 2001; Janzen et al., 2000; Lindsay et al., 2015; Moncur et al., 2009; Moncur et al., 2015; Murciego et al., 2011; Smuda et al., 2007; Valente and Leal Gomes, 2009). The crucial microorganisms consist of *Acidithiobacillus ferrooxidans* (to oxidize  $\text{Fe}^{2+}$ ,  $\text{S}^0$ , metal sulfides and sulfur compounds), *Acidithiobacillus thiooxidans* (to oxidize  $\text{S}^0$  and sulfides to sulfuric acid) and *Leptospirillum ferrooxidans* (to oxidize  $\text{Fe}^{2+}$ ). These microorganisms are catalyst for AMD generation (Parbhakar-Fox and Lottermoser, 2015).

Acid mine drainage can affect indirectly to plants and human health. For instance, when AMD flow through down stream, the soil pH becomes decrease. The important elements (i.e., N, P, K) are tied up in the soil and not available to plants. Moreover, the essential plant nutrients (i.e., Ca and Mg) may be absent or deficient in low pH soils. In addition, toxic elements including Al, Fe and Mn are also released from soil particles, thus increasing their toxicity (Simate and Ndlovu, 2014).

### 1.5.4 Toxic elements

Metal, metalloid, heavy metal and toxic element may have some similarity and unclear terminology. Metals are elements that have potential to lose one or more electrons and property of ductility and malleability. They are usually thermal and electrical conductors. On the other hand, metalloids (e.g., As, Sb, Bi, Se and Te) are defined as elements that have ability to gain one or more electrons with lower ability to heat and electrical conductivities. Heavy metals are those metals with atomic density greater than  $6 \text{ g/cm}^3$  (e.g., Fe, Cu, Pb, Zn, Sn, Ni, Co, Mo, W, Hg, Cd, In, Tl) (Lottermoser, 2010; Thornton, 1995). Therefore, using the term of toxic elements in this study is more meaningful than heavy metals because it is defined as potential toxic elements, including heavy metals and metalloids that may threaten the ecosystem and human health, eventually.

Under acid drainage condition, the sulfide minerals can be dissolved and some toxic elements substituted in mineral structure can be released to the drainage. List of minor and trace elements associate with the sulfide minerals is present in Table 1.3. However, these toxic elements are usually from other sources. The major sources of the pollutants or toxic elements (e.g., As, Cd, Cr, Cu, Hg, Mn, Ni, Pb and Zn) with permissible level and their effects on human health are present in Table 1.4.

### 1.5.5 Secondary minerals

Secondary minerals are originated from weathering processes of sulfide minerals (see Table 1.2) that may have occurred before, during or after mine operation (Lottermoser, 2010). They comprise a large group of mineral found in mine wastes. In general, these minerals are fine particles with high capacity for toxic metal adsorption (Jamieson, 2011).

The crucial secondary minerals related to mining processes are goethite ( $\text{FeOOH}$ ), hematite ( $\text{Fe}_2\text{O}_3$ ), magnetite ( $\text{Fe}_3\text{O}_4$ ), ferrihydrite ( $\text{Fe}(\text{OH})_3$ ), schwertmannite ( $\text{Fe}_{16}\text{O}_{16}(\text{SO}_4)_2 \cdot n\text{H}_2\text{O}$ ) and jarosite groups ( $(\text{K}, \text{Na}, \text{H}_3\text{O})\text{Fe}_3(\text{SO}_4)_2(\text{OH})_6$ ). Moreover, hydrous ferric oxide (HFO) can also be produced by sulfide oxidation. HFO is a non-crystalline or amorphous iron oxide. Goethite, hematite and magnetite are extremely stable; moreover, they are often the end member of transformations of other iron oxides (Cornell and Schwertmann, 2003).

**Table 1.3** Chemical formula of sulfide minerals and minor and trace element substitution.

Mineral name	Chemical formula	Minor and trace element substitution	References
Arsenopyrite	FeAsS	Ag, Au, Bi, Co, Cu, Mn, Ni, Pb, Se, Sb, Te, W, Zn, Zr	(1), (2)
Chalcopyrite	CuFeS <sub>2</sub>	Ag, As, Bi, Cd, Co, Cr, In, Mn, Mo, Ni, Pb, Sb, Se, Sn, Ti, V, Zn	(3)
Galena	PbS	Ag, As, Bi, Cd, Cu, Fe, Hg, Mn, Ni, Sb, Se, Sn, Tl, Zn	(3)
Marcasite	FeS <sub>2</sub>	As, Hg, Se, Sn, Ti, Tl, Pb, V	(3)
Pyrite	FeS <sub>2</sub>	Ag, As, Au, Bi, Cd, Co, Ga, Ge, Hg, In, Mo, Ni, Pb, Sb, Se, Sn, Ti, Tl, V	(3)
Pyrrhotite	Fe <sub>1-x</sub> S	Ag, As, Co, Cr, Cu, Mo, Ni, Pb, Se, Sn, V, Zn	(3)
Sphalerite	ZnS	Ag, As, Ba, Cu, Cd, Co, Cr, Fe, Ga, Ge, Hg, In, Mn, Mo, Ni, Sb, Se, Sn, Tl, V	(3)

(1) Cook et al. (2013); (2) Liu et al. (2014); (3) Lottermoser (2010)



**Table 1.4** Effect of pollutants on human health and permissible level modified from Singh et al. (2011); Kasprzak et al. (2003); Das et al. (2008).

Pollutants	Major sources	Effect on human health	Permissible level (mg/L)
Arsenic	Pesticides, fungicides, metal smelters	Bronchitis, dermatitis, poisoning, carcinogen	0.02
Cadmium	Welding, electroplating, pesticide fertilizer, Cd and Ni batteries, nuclear fission plant	Renal dysfunction, lung disease, lung cancer, bone defects, increased blood pressure, kidney damage, bronchitis, bone marrow cancer, gastrointestinal disorder	0.06
Chromium	Mines, mineral sources	Damage to the nervous system, fatigue, irritability	0.05
Copper	Mining, pesticides production, chemical industry, metal piping	Anemia, liver and kidney damage, stomach and intestinal irritation	0.10
Lead	Paint, pesticide, smoking, automobile emission, mining, burning of coal	Mental retardation in children, developmental delay, fatal infant encephalopathy, congenital paralysis, sensor neural deafness, liver, kidney, and gastrointestinal damage, acute or chronic damage to the nervous system, epilepticus	0.10
Manganese	Welding, fuel addition, ferromanganese production	Inhalation or contact causes damage to nervous central system	0.26
Mercury	pesticide, batteries, paper industry	Damage to the nervous system, protoplasm poisoning, spontaneous abortion, minor physiological changes, tremors, gingivitis, acrodynia characterized by pink hands and feet	0.01
Nickel	*Mining, refining, alloy production, electroplating, and welding	*Carcinogen, lung fibrosis, cardiovascular and kidney diseases	**0.0002
Zinc	Refineries, bass manufacture, metal plating, plumbing	Damage to nervous membrane	15.00

\*Kasprzak et al. (2003); \*\*Das et al. (2008)



### 1.5.6 The study area

The study area is the second largest gold mine in Thailand named as Thung Kham Gold Mine. It is located in Wang Saphung District, Loei Province in the northeastern Thailand. This gold mine has been operated since 2006 (2549 BE) with an estimated mine life of at least 20 years. This gold mine has been suspected by many surrounding villagers, NGO, and also local community as cause of toxic element contamination in soil, surface water and groundwater longer than 8 years. Since 2008, the residents of six villages nearby this gold mine — Na Nong Bong, Phu Tab Fah, Huay Puk, Gog Sa Thon, Gang Hin and Fak Huay — became a protest group, named as Khon Rak Ban Kerd (KRBK), against and allege the Thung Kham Gold Mine for the damage and pollution (Transbordernews, 2014). Finally, this gold mine was officially closed in 2016 by the Thai Government. There are many websites that reported problems and incidents of this gold mine: <http://transbordernews.in.th/home/?p=4609>, <http://geographical.co.uk/people/development/item/1178-gold-diggers>, <http://isaanrecord.com/2014/05/20/gold-mine-protesters-hurt-by-armed-mob-and-shady-deals-3/>, and <http://www.nationmultimedia.com/news/national/aec/30279464>.

Geologically, the study area is mainly occupied by the Upper-Permian sedimentary rocks of the Pha Dua Formation, Saraburi Group. This formation consists of gray to dark gray siltstone, shale and sandstone (Figure 1.3). This formation was intruded by Triassic granodiorite which is a main source of hydrothermal fluid for metamorphism /metasomatism. Moreover, limestone lenses have been found in this area; they show coarse-grained crystals due to recrystallization involved directly by intrusion. Gold mainly occurred in skarns, massive sulfide ores and gossan rocks. Gold mineralization is skarn type deposit (Crow and Zaw, 2011; Rodmanee, 2000). Skarns are coarse-grained metamorphic rocks consisting of Ca-Fe-Mg-Mn-Al silicate minerals which were formed by replacement of carbonate-bearing rocks during contact metamorphism and metasomatism. Massive sulfide rock consists of pyrrhotite, chalcopyrite, arsenopyrite and pyrite. Gossan, consisting of limonite ( $\text{FeO}(\text{OH})\cdot n\text{H}_2\text{O}$ ), hematite ( $\text{Fe}_2\text{O}_3$ ) and magnetite ( $\text{Fe}_3\text{O}_4$ ), was weathered from massive sulfide rocks. It is yellow, yellow-brown, red-brown and dark brown, and shows porous to dense matrix with rock fragmental texture. Generally, skarn was formed along the contact zone between granodiorites and host sedimentary rocks. The skarn in the Thung Kham mine is fine-grained to coarse-grained rock with green and brown color (Rodmanee, 2000).

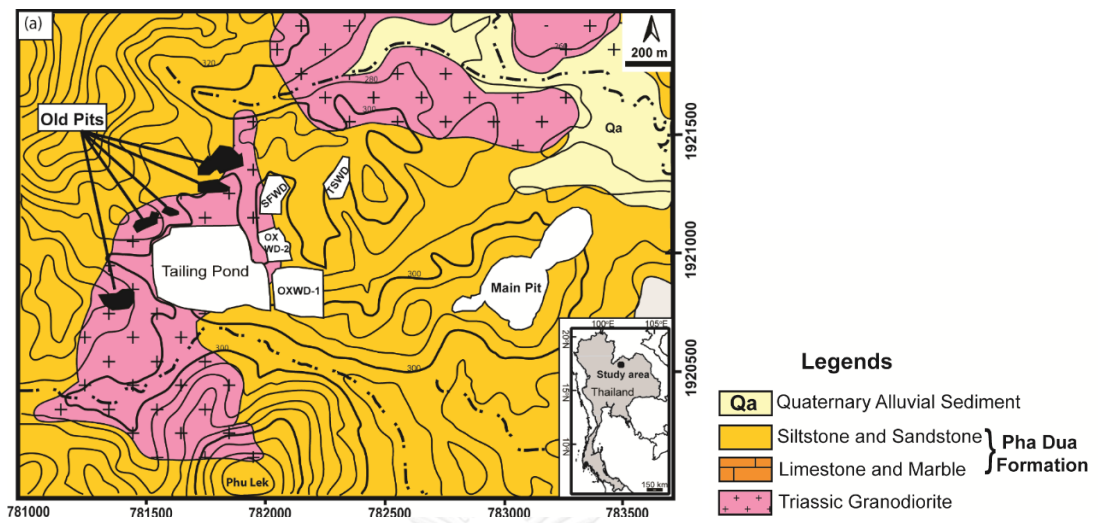


Figure 1.3 Geological map of the study area in northeastern Thailand modified from Rodmanee (2000)

CHAPTER 2  
MINERALOGY AND GEOCHEMISTRY OF TAILINGS FROM A GOLD MINE IN  
NORTHEASTERN THAILAND

Thitiphan Assawincharoenkij<sup>a</sup>, Christoph Hauzenberger<sup>b</sup>, Chakkaphan Sutthirat<sup>a,c,d\*</sup>

<sup>a</sup> Department of Geology, Faculty of Science, Chulalongkorn University, Bangkok 10330, Thailand

<sup>b</sup> NAWI Graz Geocenter, Petrology and Geochemistry, University of Graz, Universitätsplatz 2, 8010, Graz, Austria

<sup>c</sup> Research Program of Toxic Substance Management in the Mining Industry, Center of Excellence on Hazardous Substance Management (HSM), Bangkok 10330, Thailand

<sup>d</sup> Research Unit of Site Remediation on Metals Management from Industry and Mining (Site Rem), Environmental Research Institute, Chulalongkorn University, Bangkok 10330, Thailand

\* Corresponding author

Human and Ecological Risk Assessment: An International Journal 23(2) (2017):  
364-387

<http://dx.doi.org/10.1080/10807039.2016.1248894>

## Abstract

Mineralogical and geochemical characteristics of tailings from a gold mine in northeastern Thailand were investigated in relation to acid mine drainage (AMD) and the release potentials of toxic elements. The tailings can be divided into upper tailings and lower tailings. The upper tailings usually contain pyrrhotite, pyrite, chalcopyrite, calcite, quartz, andradite and diopside. The lower tailings mainly contain goethite, quartz, chlorite, muscovite, calcite and hematite pyrrhotite. These assemblages clearly relate to the original types of gold deposit prior to mining and mineral processing. The upper tailings are defined as potential acid forming (PAF), whereas the lower tailings are classified as non-acid forming (NAF). Regarding heavy metals, apart from high Mn level, the other heavy metals appear to have low concentrations in the upper tailings. On the other hand, the lower tailings contain high contents of As, Cu and Pb, which appear to be higher than the National Total Threshold Limit Concentrations. Goethite, the main mineral assemblage in the lower tailings, reveals characteristic of arsenic adsorbent. As a result, the tailing pond is recommended to be covered to prevent the oxidizing processes of the upper tailings; otherwise, AMD generation may take place soon after the mine closure. Land reclamation and monitoring plans must be planned very well and carried out with great care since arsenic contamination has been reported in stream water close to the tailing dam.

จุฬาลงกรณ์มหาวิทยาลัย  
CHULALONGKORN UNIVERSITY

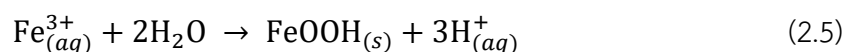
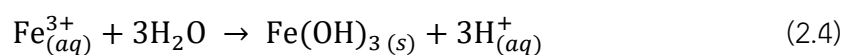
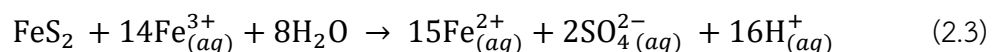
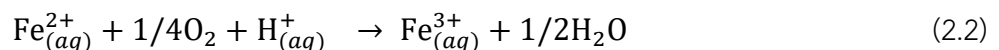
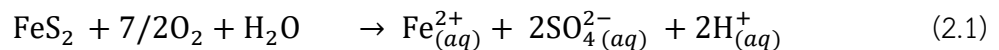
**Keywords:** acid mine drainage, AMD, gold mine, heavy metal, toxic element, tailing

## 2.1 Introduction

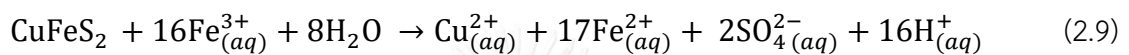
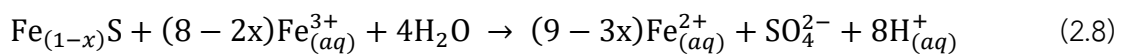
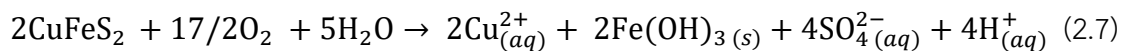
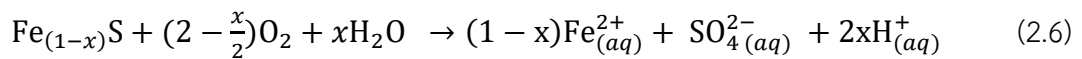
Mining activities can produce enormous quantities of waste materials, especially tailings which are the residues from the mineral processing and metal extraction (Changul et al., 2009b; Hudson-Edwards et al., 2011; Lindsay et al., 2015; Lottermoser, 2010; Parbhakar-Fox and Lottermoser, 2015; Sutthirat, 2011). Ore bearing-rocks are milled prior to mineral processing. Chemical additives are added during the extraction process; consequently, some of these chemicals may remain in the tailings. Moreover, the mine tailings usually contain gangue minerals, such as silicates, oxides, hydroxides, carbonates and sulfides (Hudson-Edwards et al., 2011; Lottermoser, 2010).

The most significant sulfide minerals in ore deposits are pyrite ( $\text{FeS}_2$ ), pyrrhotite ( $\text{Fe}_{(1-x)}\text{S}$ ), chalcopyrite ( $\text{CuFeS}_2$ ), arsenopyrite ( $\text{FeAsS}$ ), sphalerite ( $\text{ZnS}$ ) and galena ( $\text{PbS}$ ) which may remain in the mine tailings (Lapakko, 2002; Parbhakar-Fox and Lottermoser, 2015; Stumm and Morgan, 1981, 1996). The sulfide-bearing tailings have usually been oxidized during weathering prior to AMD generation with release of toxic metals and metalloids such as As, Cd, Co, Cr, Cu, Fe, Hg, Mn, Ni, Pb and Zn (Anawar, 2015; Hudson-Edwards et al., 2011; Lottermoser, 2011; Simate and Ndlovu, 2014).

For example, pyrite oxidation reactions are given in Equations (2.1)–(2.5). The first equation (Eq. 2.1) occurs when the surface of pyrite is exposed to the atmosphere. Under excess oxygen, Fe(II) will be subsequently oxidized to Fe(III) (Eq. 2.2). Under acid condition ( $\text{pH} < 4.5$ ), ferric iron can remain in solution and become the dominant oxidant (Eq. 2.3) (Singer and Stumm, 1970). Hydrolysis of Fe(III) will occur at pH value greater than 5, and generates precipitation of Fe(III) hydroxide ( $\text{Fe}(\text{OH})_3$ ) and Fe(III) oxyhydroxides ( $\text{FeOOH}$ ) as shown in Equations (2.4) and (2.5) (Evangelou and Zhang, 1995; Lottermoser, 2010; Parbhakar-Fox and Lottermoser, 2015).



The oxidation of pyrrhotite presented in Equations (2.6) was suggested by Nicholson and Scharer (1993). Similarly, chalcopyrite is oxidized by O<sub>2</sub> and water (Eq. 2.7) (Parbhakar-Fox and Lottermoser, 2015). In both minerals iron is further oxidized by Fe(III) (Eqs. 2.8 and 2.9), (Janzen et al., 2000; Lindsay et al., 2015), which probably occur from ferrous oxidization (Eq. 2.2).



Under the condition of pH > 5 secondary minerals precipitate and thus remain within the mine tailings, e.g., hydrous oxides of Fe, Mn and Al; goethite [ $\alpha$ -FeOOH]; lepidocrocite [ $\gamma$ -FeOOH]; jarosite [KFe<sub>3</sub>(SO<sub>4</sub>)<sub>2</sub>(OH)<sub>6</sub>]; schwertmannite [Fe<sub>8</sub>O<sub>8</sub>(OH)<sub>6</sub>SO<sub>4</sub>]; ferrihydrite [Fe<sub>5</sub>O<sub>8</sub>.4H<sub>2</sub>O]; hematite; clay minerals; gypsum and ochreous precipitates (Hudson-Edwards et al., 2011; Lindsay et al., 2015; Lottermoser, 2010). These secondary minerals can adsorb and co-precipitate with metal and metalloid elements (i.e., As, Cd, Co, Cr, Cu, Fe, Hg, Mn, Ni, Pb and Zn); consequently, mobility of these elements should be retarded in the general environment (Carbone et al., 2013).

Characterization of the mine tailings is very crucial for predicting and monitoring the environmental impacts as well as remediation plans. This work is a new research theme for the mining management in Thailand despite the fact that contamination with heavy metals and toxic elements (particularly As) in the groundwater and surface water from mining activities have been documented in this country (Choprapawon and Rodcline, 1997; Williams et al., 1997). Moreover, in Thailand, the tailings produced from the biggest gold mine (Akara Gold mine) were investigated by Changul et al. (2009b). They found that these tailings were classified as NAF potential but contained Mn (2082 mg/kg) that exceeded the Thailand Soil Quality Standards for Habitat and Agriculture (1800 mg/kg).

This study area is a gold mine located within the northeastern Thailand (Figure 2.1a). The environmental impacts from the gold mine and its processing plant are of concern, and have led to several protests (<http://geographical.co.uk/people/>

development/item/1178-gold-diggers; <http://isaanrecord.com/2014/05/20/gold-mine-protesters-hurt-by-armed-mob-and-shady-deals-3/>).

Due to the nature of this gold deposit, enormous tailings may contain sulfide minerals and possibly cause AMD generation and release of toxic elements. Therefore, the aim of this research is to examine the mineralogical and geochemical characteristics of these mine tailings. Subsequently, managing and mine closure plans focused on the mine tailings are suggested. The information of study may be used for decision-making of the governmental and environmental agencies for land reclamation and conflict reduction.

### **2.1.1 Site description and potential environmental impacts**

The gold mine of this study, located in northeastern Thailand (Figure 2.1a), is known as the “Phu Thab Fah gold deposit,” which contains quite low gold grade (Crow and Zaw, 2011; Rodmanee, 2000) compared to the other commercial world gold deposits. The mine excavation started in 2006 with a planned mining operation for 20 years. Geologically, it is hosted by sedimentary sequences of the Permian Pha Dua Formation, which consist mainly of sandstone, siltstone, shale and limestone. These host rocks were intruded by Triassic granodiorite (Rodmanee, 2000).

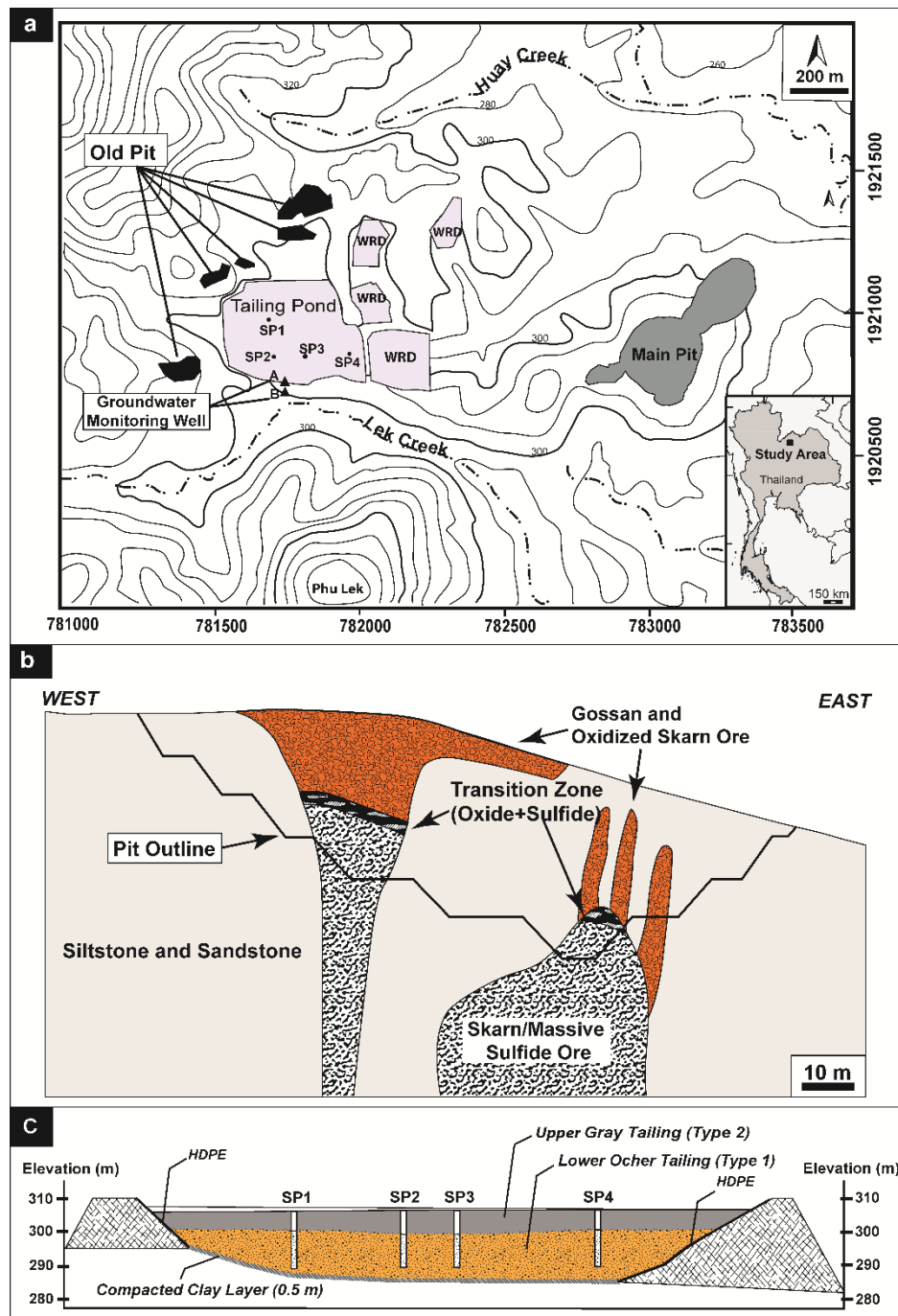


**Figure 2.1** (a) (insert) The study area location in northeastern Thailand and (main panel) the local map showing the location of the mine (main pit), tailing pond, old pits and waste rock dumps (WRD). SP1–SP4 are the sites of the four drill cores. (b) Cross section of the main pit showing the locations of the different ore types modified after Khon Kaen University Report (2009). (c) Cross section showing the outline of tailing pond and locations of the four drill cores (SP1–SP4).



Gold deposits of the area (Figure 2.1b) occurred at significant levels in skarn, massive sulfide rock and gossan with the economically cutoff grade of 0.5 g/t and a maximum concentration of about 6.7 g/t gold. Primary ore zones including skarn and massive sulfide have been altered to hydroxide gossan zone usually having ochre color. This natural process may take a very long period of time, perhaps thousands of years. This oxidized ore zone typically occurred close to the surface, which is then mined initially (see Figure 2.1b); consequently, its tailings were dumped at the bottom of the tailing pond formed as lower tailings (Figure 2.1c). Subsequently, the primary ore zone (skarn and massive sulfide) set in the deeper part (Figure 2.1b) was then processed and its tailings were dumped on top of the lower tailings (Figure 2.1c); so then they are called upper tailings, as they are generated from the primary ore zone. The tailing pond was designed at 1,983,300 cm<sup>3</sup>, which can facilitate a maximum volume of 1,071,598 cm<sup>3</sup> of tailings over the mining operation (ERIC, 2012). However, the tailing pond is surrounded by floodplain and close to a small hill (Phu Lek, another gold deposit) in the south (see Figure 2.1a). Rice paddy fields and rubber plantations are the main agricultural activities in the area.

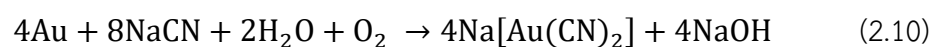
In October 2012, the tailing pond collapsed partly close to the northern pond (see Figure 2.2). Leakage of the tailing pond flowed directly into the northern pond (Figure 2.2). After this accident, the water in the northern pond were collected and analyzed for specific toxic elements (e.g., As, Cd, Cu, Pb, Mn and Hg) and also cyanide (CN<sup>-</sup>) (Department of Primary Industries and Mines's Report, 2012). They subsequently reported 0.0059–0.0076 mg/L As, ≤0.003 mg/L Cd, 0.011–0.033 mg/L Cu, ≤0.005 mg/L Pb, 1.20–1.25 mg/L Mn, ≤0.0005 mg/L Hg, and 0.006–0.055 mg/L CN<sup>-</sup> in the water samples, which were lower than the Thailand Industrial effluent standard (1996) ([http://www.pcd.go.th/info\\_serv/en\\_reg\\_std\\_water04.html](http://www.pcd.go.th/info_serv/en_reg_std_water04.html)).



**Figure 2.2** Satellite image of the study area (source: Google Earth on February 9, 2016) showing the location of collapsed tailing pond in October 2012.

### 2.1.2 Ore dressing and tailing generation

Gold occurs, although already enriched compared to common rocks, in relatively low concentrations in the mine deposit. Ore dressing, involving both physical and chemical processes, is typically engaged at gold mines in order to concentrate gold prior to final processing. After rock crushing, the ore-bearing rocks go through semi-autogenous grinding and ball milling. Grinded ore (53–106  $\mu\text{m}$ ) is then processed using a flotation process with a hydrocyclone. The two-step flotation is designed to separate copper sulfide ( $\text{CuS}$ ) and iron sulfide ( $\text{FeS}$ ) from gold-bearing ore. The gold-bearing ore, concentrated in gold and silver, is then fed into the carbon-in-pulp process along with lime ( $\text{Ca}(\text{OH})_2$ ) and sodium cyanide ( $\text{NaCN}$ ) solution (200–400 ppm) at pH 10. Activated carbon is used to adsorb the gold and silver from the resulting slurry mixture. The gold dissolution is described by the Elsener's equation, shown in Equation (2.10):



Gold and silver adsorbed onto the activated carbon (called loaded carbon) are then eluted using NaOH and NaCN solution, and the eluate is then processed by electro-winning. The gold sludge is refined, smelted and made into dore (55–80% pure gold) bars. Tailings and slurry from the mixed wastewater and solid waste that remain from all the processes are discharged into the tailing pond. However, prior to transportation to the tailing pond, the tailings are treated to reduce the cyanide and heavy metal levels using the INCO Process (SO<sub>2</sub>/Air Process). This reduces the total cyanide in the tailings and wastewater to less than 20 ppm. This INCO process was developed by INCO Limited in the 1980's (see Botz (1999)).

## 2.2 Methods and materials

### 2.2.1 Sampling and geochemical analyses

In May 2012, four core samples (SP1–SP4) were collected from the tailing pond (Figure 2.1c). Core drilling was performed to a depth of 17 m and samples were taken at every 1-m depth. Core sampling tubes were sealed immediately with plastic film and placed in a plastic ziplock bag. In the laboratory, all samples were dried in an oven at 105 °C for 30 min to remove moisture to avoid oxidization (Wolfe et al., 2007). The samples were then hand crushed and sieved through a 0.09-mm mesh prior to their characterization.

Polished sections were prepared in epoxy resin prior to investigation of mineralogical characteristics. Reflected-light microscope and a Bruker X-ray Diffractometer (XRD) based at the Department of Geology, Chulalongkorn University, Bangkok, Thailand, were initially used for mineral identification. Mineral identification under microscope was carried out, based on mineral texture, shape, color and optical characteristics following the procedure as instructed in Optical Mineralogy (Kerr, 1959) and Ore Mineral Atlas (Marshall et al., 2004). Moreover, mineral chemistry was analyzed using a JEOL JXA-8800R Electron Probe Micro-Analyzer (EPMA) at ICREMER, Akita University, Japan. Quantitative chemical analyses were carried out at an accelerating voltage of 20 kV with a beam current of about 20 nA for sulfide and oxide minerals. Counting times were typically 30 s on peak and total background. Natural minerals were used as standards. For quality assurance and quality control (QA/QC), three spot

analyses were proceeded and interposed by an analysis of standard reference. Detection limits were estimated at about 330 ppm As, 320 ppm Cu, 1030 ppm Co, 270 ppm Fe, 220 ppm Mn, 300 ppm Ni, and 60 ppm S.

Thirty-one samples were tested for geochemical analyses. Major/minor oxides ( $\text{SiO}_2$ ,  $\text{TiO}_2$ ,  $\text{FeO}_t$ , MnO, MgO, CaO,  $\text{Na}_2\text{O}$ ,  $\text{K}_2\text{O}$  and  $\text{P}_2\text{O}_5$ ) were determined by a Bruker S4 X-ray Fluorescence (XRF) spectrometer at the Department of Geology, Chulalongkorn University. Calibration curves were prepared from the reference rock standards supplied by the U.S. Geological Survey (USGS) and the Geological Survey of Japan (GSJ). The loss on ignition was measured from the weight differences between the dried powder and after ignition at 1000 °C for 3 h in a TMF-200 electric furnace.

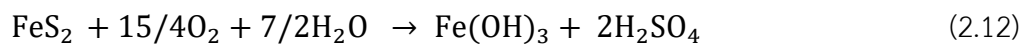
The solutions of samples and reference standards (i.e., BHVO-2, SGR-1, GSP-2, Sco-1, SDO-1, DTS-2, MAG-1, JKL-1, JSd-1, JA-2 and LG-2) were prepared by the total digestion method using mixed acid of HF-HClO<sub>4</sub>-HNO<sub>3</sub>, manually heated on a hot plate, as suggested by Satoh et al. (1999). These solutions were subsequently analyzed for trace elements (Ag, As, Au, Cd, Co, Cr, Cu, Hg, Mn, Ni, Pb and Zn) by Thermo-CapQ Inductively Coupled Plasma-Mass Spectrometer (ICP-MS) at the Scientific and Technological Research Equipment Centre, Chulalongkorn University. Calibration curves were prepared using reference standards supplied by USGS and GSJ. The detection limits of all elements range from 0.002 to 0.05 mg/kg.

### 2.2.2 Acid forming potential analyses

Acid forming potential (AFP) of tailings was also estimated using acid base accounting (ABA) and net acid generation (NAG) tests. The ABA method is the most common static test method (Ferguson and Erickson, 1988) that reports the net acid-producing potential (NAPP), whereas the NAG test was evaluated from the final pH of the samples after the oxidation process between  $\text{H}_2\text{O}_2$  and iron sulfide minerals (Changul et al., 2009b; Miller et al., 1997). From the ABA results, the samples were classified as being either potential acid formation (PAF) or non-acid formation (NAF). The NAPP was calculated by subtracting the acid neutralizing capacity (ANC) from the maximum potential acidity (MPA) using Equation (2.11):

$$\text{NAPP (kg H}_2\text{SO}_4\text{/t)} = \text{MPA (kg H}_2\text{SO}_4\text{/t)} - \text{ANC (kg H}_2\text{SO}_4\text{/t)} \quad (2.11)$$

The MPA, reported as kg H<sub>2</sub>SO<sub>4</sub>/t (where t = tonnage), was calculated from the total %S multiplied by 30.6 to reflect the reaction stoichiometry for the complete-oxidation of sulfide minerals. This assumes that all sulfur is present as reactive pyrite following stoichiometry for pyrite oxidation (Eq. 2.12). For instance, one tonnage of rock which contains 1 wt.% pyrite may generate 30.6 kg of H<sub>2</sub>SO<sub>4</sub>.

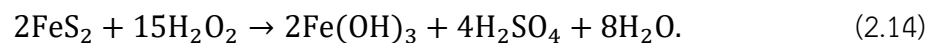


The total sulfur contents of these tailing samples were measured using a Leco Sulfur analyzer at Mae Moh Mine laboratory of the Electricity Generating Authority of Thailand, Lampang, Thailand. The ANC was performed using the Sobek method (Sobek et al., 1978), which determines the amount of neutralizing materials, such as CaCO<sub>3</sub> and other carbonates, and then was recalculated from the amount of HCl required to neutralize the sample after evaluating the residual HCl level by titration with NaOH. The volume of acid consumed represents the ANC of the sample. The calculation was performed using Equation (2.13) and reported in kg H<sub>2</sub>SO<sub>4</sub>/t (Sobek et al., 1978). The volume and concentration of HCl added to each sample was based on the results of the fizzing level, as reported previously (Sobek et al., 1978).

$$\text{ANC (kg H}_2\text{SO}_4\text{/t)} = \left( A - B \times \frac{C}{D} \right) \times 25 \times E, \quad (2.13)$$

where A and B are the volume of HCl and NaOH added, respectively; C and D are the volume of HCl and NaOH in the blank, respectively; and E is the normality of the added HCl.

The initial pH of the tailing samples was measured immediately after adding 5 mL of 0.01 mol/L CaCl<sub>2</sub> to 5 g of tailing samples, as suggested (Miller and Kissel, 2010). The pH of the NAG (NAGpH) was directly measured after completion of the oxidation of iron sulfide minerals with H<sub>2</sub>O<sub>2</sub>, as shown in Equation (2.14),



To this end, 2.5 g of tailing samples was added into 250 mL of 15% H<sub>2</sub>O<sub>2</sub> and left in a fume hood for 24 h at room temperature. Samples were allowed to react for a minimum of 2 h at 100 °C until the effervescence stopped and then cooled to room temperature before measurement of the solution pH (Lawrence et al., 1988; Miller et al., 1997).

## 2.3 Results

Tailings were physically characterized as having a gray color from top to 6–7 m depth whereas, from 7- to 12-m depth, an ocher color can be observed (Figure 2.1c). The color differences are related to the types of the initial ore zones. The average grain size of the upper gray tailings ranged from 20 to 60 µm, while the grain size of the lower ocher tailings ranges from 30 to 200 µm. The upper gray tailings (Figure 2.4a) are the product from ore processing of the skarn and massive sulfide zones, which occur in the deeper levels of the mined deposit (see Figure 2.1b). On the other hand, the lower ocher tailings (Figure 2.4d) are the remains from the processing of gossan ore which formed in the oxidation zone of the deposit (ERIC 2012). Consequently, these tailings were subdivided into two types including lower ocher tailings (Type 1) and upper gray tailings (Type 2). Mineralogical characteristics of both tailing types and their original ore zones are reported below.

### 2.3.1 Mineral Assemblage

The main gangue minerals were identified by XRD yielding characteristic peaks of calcite, quartz, pyrrhotite and andradite with minor amounts of pyrite and diopside in the upper gray tailings, whereas the lower ocher tailings mainly consist of quartz, muscovite, chlorite, goethite and minor pyrrhotite. The XRD patterns are shown in Figures 2.3a and b.

Photomicrographs taken from polished sections under reflected light show different assemblages between the upper gray tailings and the lower ocher tailing. Sulfides in the gray tailings consist mainly of pyrrhotite and pyrite (Figures 2.4b and c), which usually form separate grains. However, intergrowth pyrrhotite–chalcopyrite grain is sometimes observed (Figure 2.4b). Concerning the lower ocher tailings, goethite is

the most dominant iron ore phase (Figure 2.4e). In addition, sulfide minerals are also found in the lower ocher tailings; however, these sulfides are partially oxidized and altered from the original grains. Figure 2.4f shows typical metal-bearing grains and their textures observed in the lower ocher tailings, including intergrowth grain between pyrrhotite, pyrite and covellite (top left); concentric texture of Fe-oxyhydroxide (top right); oxidized pyrite (bottom right); and colloform goethite (bottom left).

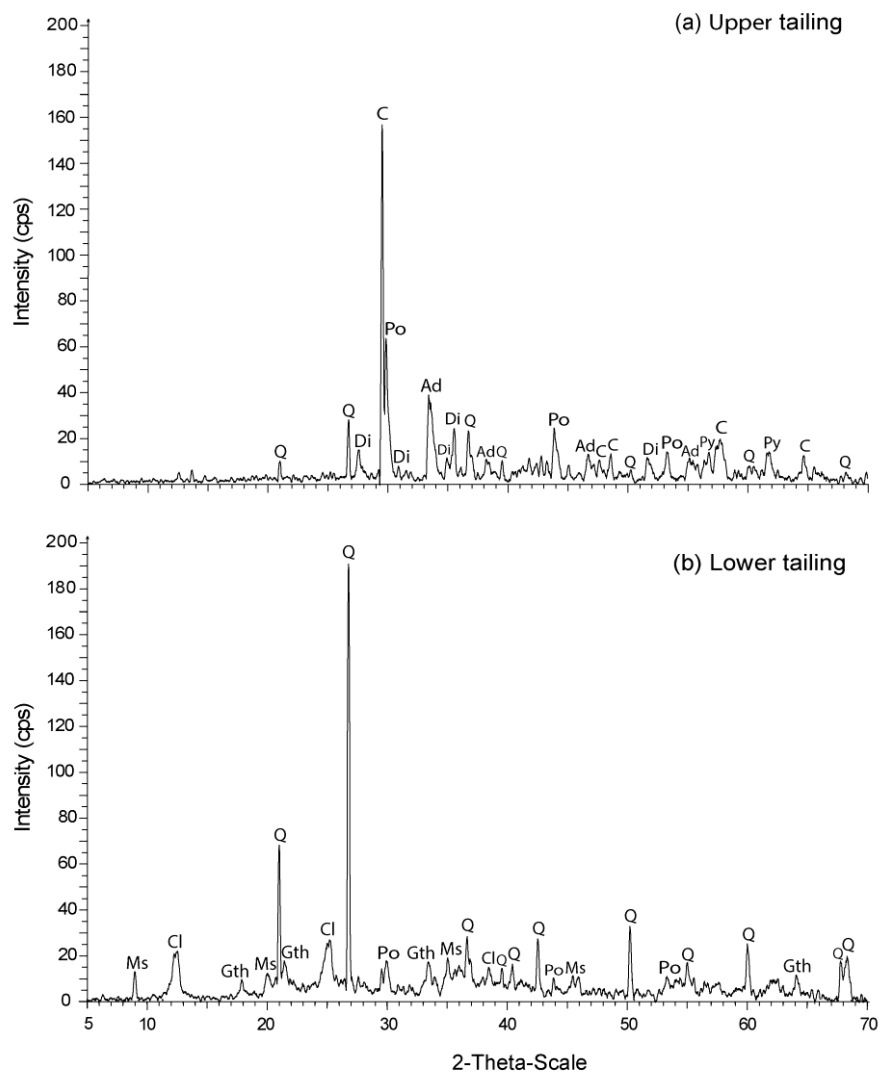


**Figure 2.3** Representative XRD patterns of (a) the upper tailings and (b) the lower tailings. Mineral abbreviations are Q:quartz, Di:diopside, Po:pyrrhotite, Ad:andradite, C:calcite, Py:pyrite, Ms:muscovite, Cl:chlorite and Gth:goethite.

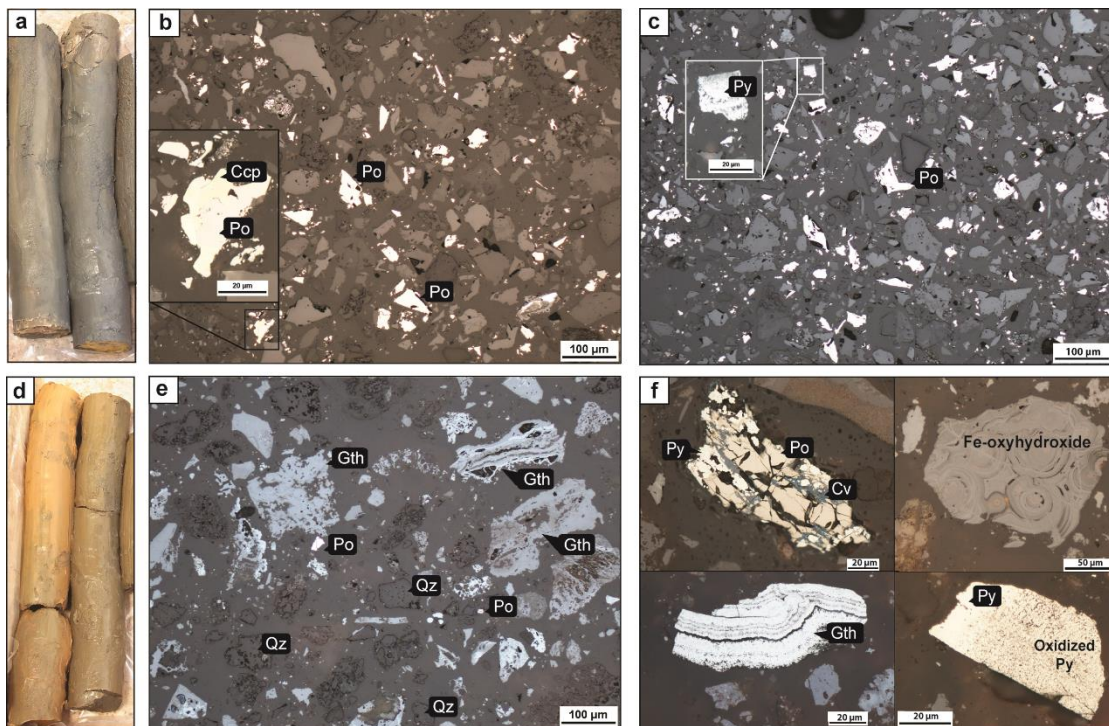


**Figure 2.4** Core specimens of (a) upper tailing and (d) lower tailing; photomicrographs of polished-sections under plane-polarized reflected light showing (b) and (c) pyrrhotite (Po), chalcopyrite (Ccp), pyrite (Py) and others in the upper tailing; (e) mainly goethite (Gth) and some quartz (Qz) and pyrrhotite (Po) in the lower tailing and (f) cracked grain intergrowth between pyrrhotite (Po), pyrite (Py) and covellite (Cv) (top left), concentric Fe-oxyhydroxide (top right), colloform goethite (Gth) (bottom left) and oxidized pyrite regular grain (bottom right).

### 2.3.2 Mineral Chemistry

EPMA analyses of sulfide minerals found in both tailings are present in Table 2.1. Pyrite and pyrrhotite (two different forms of iron sulfide minerals) in the upper tailings and the lower tailings do not show any significant variation in their chemical composition. Some trace elements such as Co ( $\leq 0.16$  wt.%) and Cu ( $\leq 0.04$ – $0.54$  wt.%) are noticeable. Chalcopyrite (copper iron sulfide mineral) found in the upper tailings contains minor amounts of Co ( $<0.1$  wt.%).

Goethite (Fe-oxyhydroxide mineral), the main iron-bearing assemblage in the lower tailings, is mainly composed of Fe (av. 78.90 wt.%) with trace amounts of Cu ( $<1.5$  wt.%), As ( $<1.2$  wt.%), and S (0.02–0.14 wt.%), and negligible Co and Mn (Table



2.2), which are similarly reported elsewhere (Asta et al., 2009; Carbone et al., 2012). Based on these mineral chemistries, Fe appears to be the main metal in mineral assemblages of both tailing groups.

**Table 2.1** Representative EPMA analyses of sulfide minerals from the upper and lower tailings.

Samples	Minerals	Elements (wt.%)						
		Fe	S	As	Co	Cu	Mn	Ni
Upper tailing	Pyrite	45.86	52.11	n.d.	n.d.	0.04	n.d.	0.04
		46.49	51.79	n.d.	n.d.	0.04	n.d.	n.d.
		45.76	52.91	n.d.	n.d.	n.d.	n.d.	n.d.
	Pyrrhotite	59.88	39.32	n.d.	0.11	0.12	n.d.	n.d.
		59.86	39.11	n.d.	0.08	0.05	n.d.	n.d.
		59.75	39.04	n.d.	0.16	n.d.	0.04	0.04
	Chalcopyrite	36.46	39.50	n.d.	0.08	23.82	0.04	n.d.
		36.32	38.98	n.d.	0.06	23.82	n.d.	n.d.
		36.13	40.17	n.d.	0.06	23.08	n.d.	n.d.
Lower tailing	Pyrite	46.01	52.09	n.d.	0.10	0.30	0.05	n.d.
		46.13	51.99	n.d.	0.10	0.54	0.02	n.d.
		45.57	52.45	n.d.	0.08	n.d.	0.04	n.d.
	Pyrrhotite	60.71	38.34	n.d.	0.13	0.15	n.d.	n.d.
		60.33	38.32	n.d.	0.10	0.22	n.d.	n.d.
		60.28	37.87	n.d.	n.d.	n.d.	n.d.	n.d.

n.d.: non-detected

**Table 2.2** Representative EPMA analyses of goethite from the lower tailings.

Elements (wt%)	Si	Ti	Al	Fe(III)	Mn	Mg	Ca	Na	S	As	Co	Cr	Cu	Ni
Goethite	1.67	n.d.	0.33	82.23	n.d.	n.d.	0.59	0.22	0.11	0.91	0.08	n.d.	1.40	n.d.
from	4.44	n.d.	2.18	77.44	0.02	0.08	0.90	0.11	0.07	0.08	0.08	0.03	0.58	n.d.
Lower	6.09	0.12	0.16	77.40	0.02	n.d.	0.47	0.11	0.03	0.19	0.05	0.03	0.07	n.d.
tailings	2.44	0.03	1.14	77.10	n.d.	0.02	0.39	0.08	0.11	0.05	0.08	n.d.	0.68	n.d.
	1.81	n.d.	0.11	84.70	0.04	n.d.	0.19	0.12	0.10	0.07	0.07	n.d.	0.06	n.d.
	4.13	0.12	0.35	76.29	0.07	0.01	0.27	0.23	0.05	0.17	0.06	n.d.	0.15	n.d.
	2.03	0.09	0.39	74.94	0.13	n.d.	0.74	0.18	0.04	0.97	0.06	n.d.	0.29	n.d.
	3.03	0.06	1.43	82.65	0.04	n.d.	0.23	0.21	0.06	0.18	0.02	n.d.	0.27	n.d.
	1.56	0.03	0.07	81.63	n.d.	n.d.	0.16	0.05	0.09	0.06	0.06	n.d.	0.17	n.d.
	1.35	n.d.	0.39	78.58	0.01	n.d.	0.38	0.13	0.07	0.77	0.07	n.d.	n.d.	n.d.
	2.01	n.d.	3.42	68.52	0.07	0.16	0.57	0.06	0.06	0.15	0.04	n.d.	0.34	n.d.
	1.26	0.02	0.02	80.32	n.d.	n.d.	0.11	0.10	0.06	0.11	0.03	n.d.	0.17	n.d.
	1.88	n.d.	0.07	85.21	0.07	n.d.	0.24	0.09	0.07	0.32	0.07	n.d.	0.04	n.d.
	1.63	n.d.	0.13	78.04	0.01	0.01	0.10	0.09	0.14	0.14	0.07	n.d.	0.81	n.d.
	1.28	n.d.	0.05	89.52	0.01	n.d.	0.14	0.12	0.10	0.04	0.06	0.04	n.d.	n.d.
	2.72	n.d.	0.73	76.99	0.04	0.03	0.15	0.13	0.09	0.15	0.05	n.d.	0.40	n.d.
	3.83	0.08	1.13	74.77	n.d.	n.d.	0.43	0.08	0.04	0.49	0.07	n.d.	0.32	n.d.
	3.36	n.d.	4.14	77.34	0.31	0.17	0.54	0.30	0.05	0.10	0.08	n.d.	0.40	n.d.
	0.91	0.04	0.07	78.99	0.03	n.d.	0.29	0.06	0.06	0.34	0.06	n.d.	0.06	n.d.
	2.29	n.d.	1.10	82.02	0.12	n.d.	0.29	0.20	0.08	0.41	0.08	n.d.	0.33	n.d.
	5.04	n.d.	2.06	69.28	0.22	0.24	0.44	0.37	0.02	0.22	0.08	n.d.	0.17	n.d.
	1.16	0.11	0.05	80.29	0.01	0.02	0.27	0.05	0.10	0.05	0.07	n.d.	0.10	n.d.
	1.42	0.02	0.09	79.92	0.01	n.d.	0.16	0.10	0.10	0.10	0.04	n.d.	0.09	n.d.
	1.51	0.02	0.87	79.48	0.10	n.d.	0.72	0.11	0.05	1.11	0.07	n.d.	0.32	n.d.
Av.	2.45	0.06	0.85	78.90	0.07	0.08	0.37	0.14	0.07	0.30	0.06	0.03	0.33	-
Sd.	1.37	0.04	1.11	4.61	0.08	0.09	0.22	0.08	0.03	0.32	0.02	0.01	0.32	-

n.d.: non-detected

### 2.3.3 Bulk geochemistry

#### 2.3.3.1 Major oxides

The bulk geochemical compositions of representative tailings are determined by XRF analysis and summarized in Table 2.3. These geochemical data are also plotted in Figure 2.5 in comparison with the  $\text{SiO}_2$  contents that range between 21 and 43 wt.% from both tailing groups with averages of  $29 \pm 4.8$  wt.% in upper tailings and  $34 \pm 5.3$  wt.% in lower tailings. In general, the upper tailings yield about 10–21 wt.% CaO, 2–3 wt.% MgO, 0.1–0.3 wt.% MnO and 0.3–0.9 wt.%  $\text{Na}_2\text{O}$ , which are higher than those of the lower tailings (<10 wt.% CaO, <1.5 wt.% MgO,  $\leq 0.15$  wt.% MnO and <0.5 wt.%  $\text{Na}_2\text{O}$ ). On the other hand, the upper tailings contain about 0.2–0.4 wt.%  $\text{TiO}_2$ , 0.3–1.4 wt.%  $\text{K}_2\text{O}$  and 3.5–10 wt.%  $\text{Al}_2\text{O}_3$ , which are lower than those of the lower tailings ( $\geq 0.4$  wt.%  $\text{TiO}_2$ , 0.8–2 wt.%  $\text{K}_2\text{O}$  and 5–19 wt.%  $\text{Al}_2\text{O}_3$ ). The  $\text{P}_2\text{O}_5$  contents of both tailing groups are very low and negligible. Only the  $\text{FeO}_{\text{total}}$  contents are found in a large scattered pattern, ranging from about 16 to 40 wt.% (av.  $28 \pm 7.9$  wt.%) in the lower tailings and from 15 to 21 wt.% (av.  $18 \pm 1.9$  wt.%) in the upper tailings.

#### 2.3.3.2 Trace elements

The Ag, As, Au, Cd, Co, Cr, Cu, Hg, Mn, Ni, Pb and Zn concentrations of representative tailing samples are shown in Table 2.4. The variation plots between As, Mn, Co, Cu, Pb and Ni, as potential toxic elements, against  $\text{SiO}_2$  are present in Figure 2.6. Some characteristics of both tailing groups can be distinguished below.

Trace elements in the upper tailings range between 0.5–0.8, 39–268, 0.2–0.4, 23–40, 222–425, 226–1111, 2–12, 1421–3524, 15–29, 4–19 and 53–158 mg/kg for Ag, As, Cd, Co, Cr, Cu, Hg, Mn, Ni, Pb and Zn, respectively. Moreover, 2–15  $\mu\text{g}/\text{kg}$  Au still remains in these tailings.

The lower tailings consist of 0.5–3.9, 238–2870, 0.2–1.3, 9–42, 82–282, 750–2608, 1–11, 120–1508, 11–34, 10–1506 and 48–470 mg/kg for Ag, As, Cd, Co, Cr, Cu, Hg, Mn, Ni, Pb and Zn, respectively, whereas 2–27  $\mu\text{g}/\text{kg}$  Au is also observed in these tailings.

**Table 2.3** Bulk geochemical analyses (wt.% oxides) of the gold mine tailings, as determined by XRF analysis and loss on ignition (LOI) contents.

Type	Sample No. <sup>a</sup>	Composition (wt.%)										
		SiO <sub>2</sub>	TiO <sub>2</sub>	Al <sub>2</sub> O <sub>3</sub>	FeOt	MnO	MgO	CaO	Na <sub>2</sub> O	K <sub>2</sub> O	P <sub>2</sub> O <sub>5</sub>	LOI
Upper tailings	SP1-1	30.11	0.23	5.93	16.82	0.23	3.12	20.99	0.52	0.54	0.12	2.00
	SP1-3	28.48	0.26	6.48	19.34	0.20	2.53	15.77	0.58	0.64	0.12	3.93
	SP1-5	32.20	0.30	7.01	19.04	0.16	3.08	14.31	0.76	0.97	0.09	2.77
	SP1-6	30.08	0.27	6.67	20.42	0.17	2.79	14.72	0.68	0.80	0.09	3.31
	SP2-1	20.98	0.16	3.54	17.63	0.22	1.98	21.31	0.30	0.25	0.06	4.37
	SP2-3	27.71	0.22	5.45	16.28	0.22	2.52	20.17	0.48	0.51	0.12	3.59
	SP2-5	29.49	0.23	5.82	19.64	0.21	2.76	15.03	0.64	0.63	0.09	3.76
	SP2-7	31.01	0.26	6.52	14.99	0.28	2.34	20.31	0.57	0.48	0.14	3.13
	SP3-1	24.32	0.18	4.28	17.33	0.21	2.25	20.99	0.41	0.38	0.08	4.83
	SP3-3	28.57	0.22	5.57	15.85	0.22	2.75	20.38	0.53	0.57	0.11	3.76
	SP3-4	36.44	0.36	8.69	15.44	0.16	2.60	13.88	0.79	1.15	0.13	3.57
	SP3-7	24.91	0.21	4.56	21.16	0.16	2.40	15.96	0.48	0.51	0.07	5.02
	SP4-1	23.13	0.20	4.11	17.00	0.22	2.10	20.38	0.34	0.37	0.08	4.37
	SP4-3	39.79	0.40	10.11	15.68	0.13	2.79	10.06	0.92	1.43	0.13	3.92
	SP4-5	29.70	0.30	6.73	16.37	0.23	2.22	19.31	0.52	0.59	0.13	4.50
	Lower tailings	SP1-7	35.83	0.91	17.82	18.65	0.12	1.08	4.34	0.31	1.11	0.09
SP1-10		33.74	0.56	6.64	33.29	0.03	0.46	1.81	0.30	1.36	0.15	8.81
SP1-13		29.92	0.80	13.08	35.52	0.08	0.36	1.66	0.20	0.94	0.15	10.29
SP1-17		32.25	0.68	12.79	27.69	0.13	1.00	4.92	0.36	1.22	0.09	9.12
SP2-9		32.19	0.50	9.76	21.56	0.12	1.36	9.44	0.50	1.26	0.14	9.23
SP2-11		41.44	0.78	16.78	23.42	0.15	0.54	1.24	0.24	2.01	0.13	8.32
SP2-13		28.22	0.73	11.04	36.53	0.09	0.37	1.98	0.20	0.79	0.15	10.91
SP2-17		33.80	0.70	14.06	27.12	0.15	0.85	4.99	0.31	1.42	0.08	9.63
SP3-8		39.18	0.74	14.36	15.71	0.11	0.81	4.20	0.30	1.17	0.08	6.57
SP3-9		41.31	0.82	18.24	19.48	0.10	0.52	1.02	0.20	2.12	0.12	8.25
SP3-13		30.53	0.71	9.98	36.83	0.06	0.36	1.33	0.20	1.18	0.17	9.64
SP3-17		31.72	0.65	11.54	31.29	0.12	0.73	4.27	0.30	1.09	0.08	9.99
SP4-7		42.82	0.86	19.21	18.19	0.09	0.56	0.82	0.22	2.21	0.11	8.64
SP4-9		30.81	0.57	5.38	37.81	0.02	0.25	1.06	0.17	0.82	0.16	8.87
SP4-14	33.98	0.71	13.74	25.40	0.12	0.90	5.00	0.27	1.39	0.08	9.40	
SP4-17	22.87	0.43	6.16	39.33	0.07	0.46	5.02	0.21	0.81	0.09	10.74	

<sup>a</sup>SPX-Y; where X is the core number (1–4 see Figure 2.1) and Y is the depth in meters below the surface (1–17)

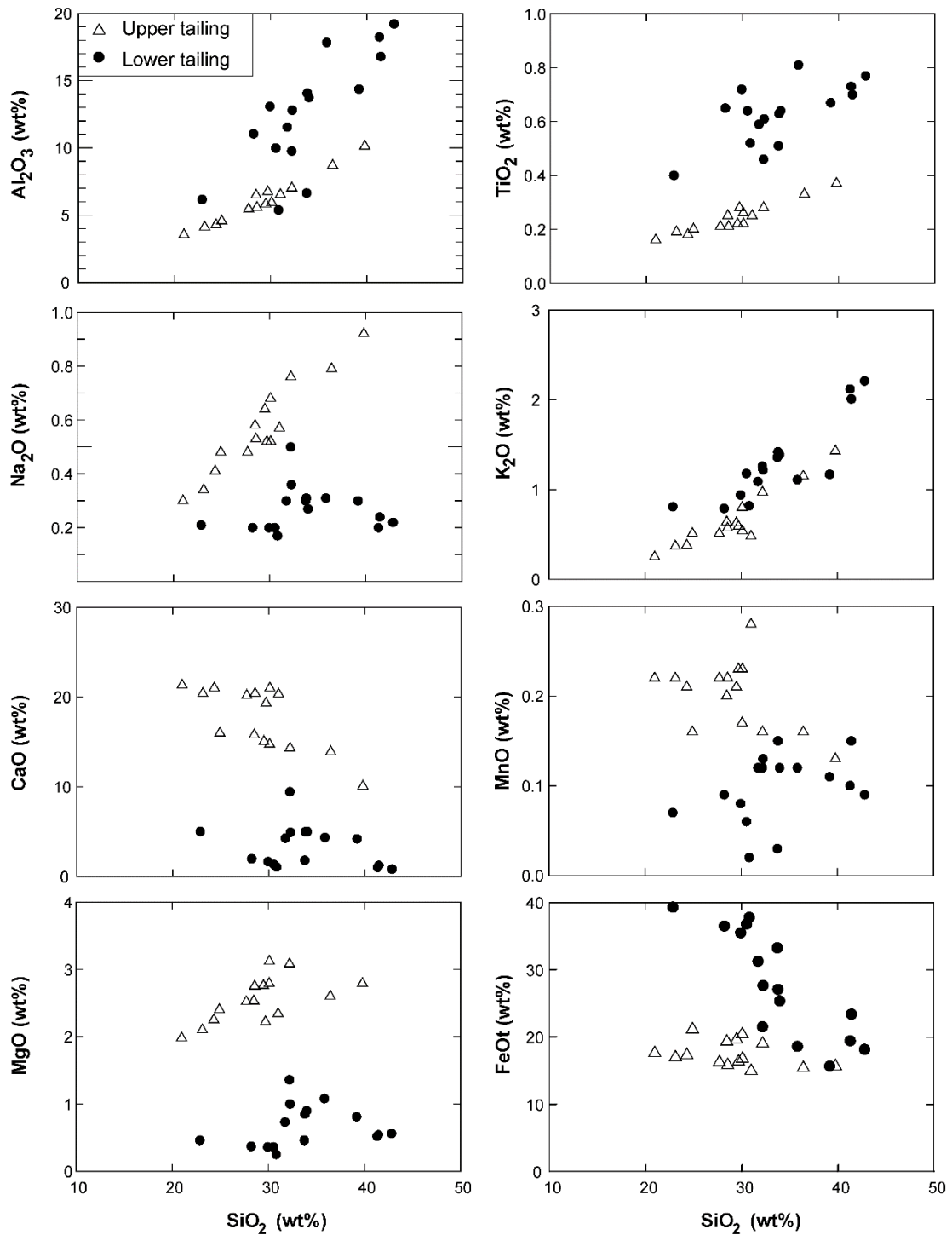


Figure 2.5 Variation diagrams of selected major oxides against the level of SiO<sub>2</sub> for the samples in Table 2.3.

**Table 2.4** Trace element concentrations in the gold mine tailings, as determined by ICP-MS analysis

Type	Sample No. <sup>a</sup>	Composition (mg/kg)											
		Ag	As	Au <sup>b</sup>	Cd	Co	Cr	Cu	Hg	Mn	Ni	Pb	Zn
Upper tailings	SP1-1	0.5	214	9.6	0.19	22.9	264	290	1.9	2730	20.7	5.9	158
	SP1-3	0.5	222	7.0	0.18	33.1	315	334	12.4	2441	20.8	4.9	81
	SP1-5	0.5	160	3.0	0.21	29.9	309	726	3.2	1825	14.9	13.9	65
	SP1-6	0.8	151	6.7	0.25	30.2	300	824	4.7	2009	16.6	19.3	69
	SP2-1	0.5	133	5.0	0.21	32.6	222	241	6.2	2824	24.5	4.2	82
	SP2-3	0.5	195	9.2	0.41	39.3	425	515	2.0	2889	29.3	5.2	115
	SP2-5	0.8	39	15.1	0.17	34.9	329	1111	2.9	2573	18.0	8.5	73
	SP2-7	0.6	117	9.8	0.25	33.7	267	272	1.1	3524	26.7	15.6	98
	SP3-1	0.5	126	3.1	0.39	31.2	283	226	1.7	2636	28.4	4.6	133
	SP3-3	0.5	50	2.3	0.21	34.2	405	414	1.7	2580	26.3	4.6	107
	SP3-4	0.5	268	2.6	0.25	33.3	373	266	3.1	1888	24.4	6.1	53
	SP3-7	0.5	75	4.9	0.19	32.8	261	605	2.7	2016	15.7	9.2	65
	SP4-1	0.8	88	2.4	0.18	29.6	261	271	1.5	2833	27.2	5.7	122
	SP4-3	0.5	67	2.6	0.36	31.7	377	275	3.5	1421	27.2	6.0	70
	SP4-5	0.5	69	2.7	0.22	26.2	257	528	2.8	2800	20.1	14.1	75
	Lower tailings	SP1-7	0.5	1670	2.7	0.53	34.7	282	846	10.9	1030	26.9	109
SP1-10		1.1	301	14.1	0.17	14.5	133	2585	7.1	206	12.6	11.4	66
SP1-13		1.0	278	4.2	0.25	11.1	174	1600	4.1	703	19.4	9.7	61
SP1-17		0.7	1244	7.2	0.25	20.1	223	1630	2.9	1017	22.0	18.3	55
SP2-9		1.1	291	26.7	1.29	31.6	197	1878	5.0	1099	27.3	28.9	80
SP2-11		1.9	681	6.8	1.13	42.2	229	928	2.7	1226	34.4	654	384
SP2-13		1.2	662	5.3	0.29	13.7	178	1893	9.8	724	21.1	26.4	51
SP2-17		0.7	1312	3.7	0.27	22.5	138	1594	3.3	1508	30.0	13.7	81
SP3-8		0.7	878	11.3	0.40	30.9	281	876	1.0	1062	24.7	66.4	470
SP3-9		3.9	1232	7.5	1.16	27.4	224	750	2.3	860	24.8	1506	300
SP3-13		0.6	238	3.8	0.21	13.7	153	1722	7.5	448	16.5	10.4	68
SP3-17		0.6	2677	2.6	0.32	18.9	130	1537	3.5	1067	22.5	13.0	55
SP4-7		0.7	2870	1.5	0.26	11.5	82	1716	4.0	595	11.2	10.1	61
SP4-9		0.7	1405	3.0	0.24	8.6	236	2608	6.2	120	12.9	14.7	48
SP4-14	0.7	1100	2.7	0.23	16.2	143	1647	2.3	1097	20.9	16.1	59	
SP4-17	2.7	1018	3.9	0.94	23.6	233	834	2.4	741	25.7	1098	267	
<sup>c</sup> TTL		500	500	-	100	8000	500	2500	20	-	2000	1000	5000

<sup>a</sup>SPX-Y; where X is the core number (1–4 see Figure 2.1) and Y is the depth in meters below the surface (1–17)

<sup>b</sup>µg/kg

<sup>c</sup>TTL: National Total Threshold Limit Concentration

In comparison, the upper tailings have lower As, Cu and Pb levels and higher Mn and Co levels than those of the lower tailings, but the Ni contents in the upper tailings are not different from the lower tailings (Figure 2.6).

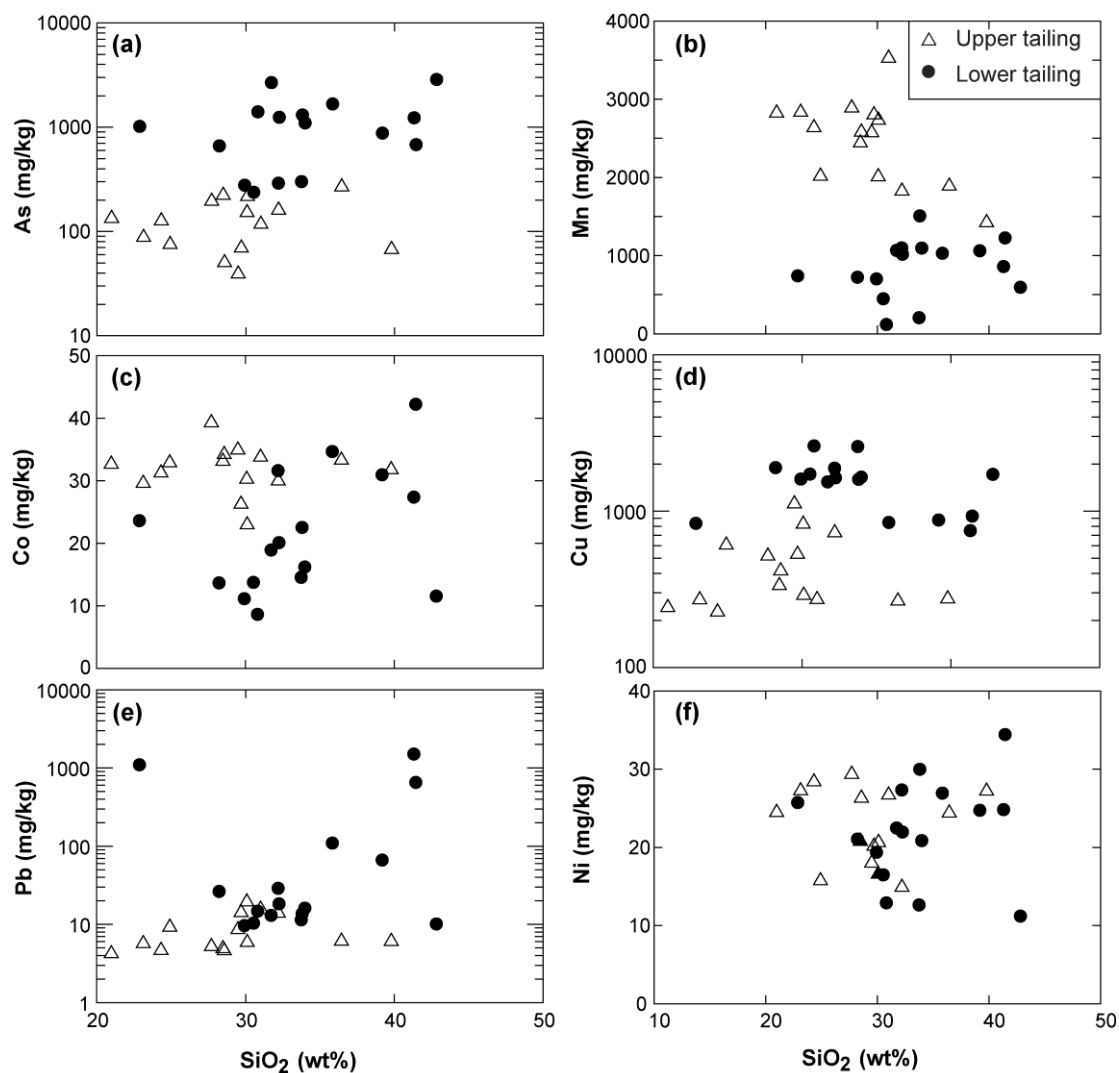


**Figure 2.6** Plots of the SiO<sub>2</sub> level against the potential selected toxic elements, As, Mn, Co, Cu, Pb and Ni, for the samples in Table 2.4.

### 2.3.4 Acid forming potential (AFP)

The results of the ABA test, as the forms of net neutralization potential (NAPP = MPA - ANC) and ANC/MPA ratio, and NAG test are presented in Table 2.5. Moreover, the initial pH and total sulfur are also reported. The upper tailings have higher total sulfur contents (4–9%) than the lower tailings (< 3%). Thus, the MPA range and average of the upper tailings (127–274;  $194.0 \pm 44.6$  kg H<sub>2</sub>SO<sub>4</sub>/t) are higher than those of the lower tailings (5–83;  $25.3 \pm 23.7$  kg H<sub>2</sub>SO<sub>4</sub>/t). In addition, the ANC values of the upper tailings (73–183;  $115.7 \pm 28.4$  kg H<sub>2</sub>SO<sub>4</sub>/t) are higher than those of the lower tailings (2–84;  $44.7 \pm 28.5$  kg H<sub>2</sub>SO<sub>4</sub>/t). Consequently, the NAPP in the upper tailings (–18 to 166;  $77.3 \pm 56.9$  kg H<sub>2</sub>SO<sub>4</sub>/t) is higher than those in the lower tailings (–60 to 42;  $-19.4 \pm 34.4$  kg H<sub>2</sub>SO<sub>4</sub>/t). Moreover, the average ANC/MPA ratio in the lower tailings ( $3.55 \pm 3.14$ ) is higher than that in the upper tailings ( $0.63 \pm 0.22$ ). The average initial pH values across all samples are broadly similar between the upper and lower tailings at  $6.23 \pm 0.29$  and  $6.19 \pm 0.38$ , respectively. Finally, for the NAG test, the NAGpH values range between 2.14 and 2.78 and 2.86 and 5.98 in the upper and lower tailings, respectively. The classification of AFP under the ABA and NAG criteria for the mine tailings is shown in Table 2.6.

According to Table 2.6, three categories of AFP can be classified, based on the NAPP values (suggested by Hutchison and Ellison (1992)), as 1) PAF, 2) NAF and 3) uncertainly classified (UC). Positive NAPP (> 20) is classified as PAF, whereas negative NAPP (<–20) is defined as NAF and a NAPP range between –20 and +20 is defined as UC (Hutchison and Ellison, 1992). The ANC/MPA ratio can also indicate AFP, where a ratio of < 2.5 is defined as PAF and a ratio of  $\geq 2.5$  is defined as NAF (Miller et al., 2006). The criteria of the NAG test suggested by EGI (2005) cited in Changul et al. (2009a) are that NAGpH  $\leq 4.5$  would be considered acid forming or PAF and a range of NAGpH > 4.5 would be considered non-acid forming or NAF. Sample SP3-3 from the upper tailings and Samples SP2-10 and SP3-13 from the lower tailings yielded inconsistency between the ABA and NAG tests. By taking two from three criteria, the Samples SP3-3 and SP2-10 could be PAF, whereas the sample SP3-13 should be classified as NAF. Moreover, samples SP1-17 and SP4-9 appear to be UC. Consequently, the summary of AFP categories of each sample are shown on the last column of Table 2.6 where all of the upper tailings fall within PAF; on the other hand, the lower tailings are mostly grouped as NAF and a few samples are UC (SP1-17 and SP4-9).



## 2.4 Discussion

### 2.4.1 Characteristics of Mine Tailings

Although many minerals in the bulk tailing samples are identified by XRD, the main metal gangues can be identified as pyrrhotite in the upper tailings and goethite in the lower tailings. Apart from quartz, which is found in both tailings, the other gangues in both types of tailings are compatible to the original deposits including skarn/massive sulfide in the deeper deposits and gossan in the shallower deposits (see Figure 2.1b). For instance, in the upper tailings, andradite, calcite and diopside occur typically in skarn assemblage, whereas pyrrhotite  $\pm$  pyrite/chalcopyrite is the main iron sulfide of the massive sulfide. On the other hand, goethite (the main iron ore), quartz associated with chlorite, muscovite and a few sulfide minerals are found in the lower tailings which these minerals are typically found as main components of the gossan deposit (Romero et al., 2006; Valente et al., 2013; Velasco et al., 2013). Although goethite is also the by-product of AMD as in Equations (2.4) and (2.5), this is not the case in the study tailing pond. However, the huge amount of sulfide minerals remained in the upper tailings may be more oxidized and altered to goethite with AMD generation as supported by García et al. (2005). Therefore, goethite in the lower must be from original source instead of further oxidizing process, which should not take place stronger in the deeper part.

**Table 2.5** Analyses of acid forming potential (AFP) of the gold mine tailings in northeastern Thailand

Type	Sample No. <sup>a</sup>	Initial pH	Total S (%S)	MPA (kg H <sub>2</sub> SO <sub>4</sub> /t)	ANC (kg H <sub>2</sub> SO <sub>4</sub> /t)	NAPP (kg H <sub>2</sub> SO <sub>4</sub> /t)	ANC/MPA	NAGpH
Upper tailings	SP1-3	6.72	7.12	217.87	95.76	122.11	0.44	2.55
	SP1-5	6.13	5.30	162.18	99.54	62.64	0.61	2.78
	SP1-6	6.38	6.33	193.70	104.58	89.11	0.54	2.73
	SP2-3	6.17	6.00	183.60	146.25	37.35	0.80	2.54
	SP2-5	6.12	7.82	239.29	73.08	166.21	0.31	2.54
	SP2-7	6.44	4.14	126.68	89.46	37.22	0.71	2.14
	SP3-3	6.16	5.37	164.32	182.50	-18.18	1.11	2.58
	SP3-6	5.61	8.95	273.87	115.00	158.87	0.42	2.74
	SP3-7	5.95	8.01	245.11	126.25	118.86	0.52	2.27
	SP4-1	6.23	5.30	162.18	121.25	40.93	0.75	2.38
	SP4-3	6.34	6.68	204.41	113.75	90.66	0.56	2.60
	SP4-5	6.54	4.66	142.60	120.97	21.63	0.85	2.56
Average		6.23	6.31	192.98	115.70	77.28	0.63	2.53
SD		0.29	1.46	44.62	28.37	56.86	0.22	0.19
Lower tailings	SP1-7	6.22	1.21	37.03	10.90	26.12	0.29	5.85
	SP1-9	5.79	1.43	43.76	1.77	41.99	0.04	2.86
	SP1-17	5.94	1.55	47.43	51.66	-4.23	1.09	4.70
	SP2-10	6.00	2.70	82.62	83.75	-1.13	1.01	3.35
	SP2-13	6.86	0.25	7.65	66.78	-59.13	8.73	5.55
	SP2-17	6.42	0.40	12.24	68.75	-56.51	5.62	5.49
	SP3-8	6.19	0.98	29.99	56.25	-26.26	1.88	5.46
	SP3-13	6.22	0.21	6.43	25.70	-19.28	4.00	5.63
	SP3-17	6.31	0.36	11.02	64.26	-53.25	5.83	5.92
	SP4-7	6.82	0.17	5.20	34.02	-28.82	6.54	5.98
	SP4-9	5.87	0.35	10.71	2.97	7.74	0.28	5.90
	SP4-15	5.66	0.31	9.49	69.30	-59.82	7.31	5.32
Average		6.19	0.83	25.30	44.68	-19.38	3.55	5.17
SD		0.38	0.77	23.71	28.54	34.39	3.14	1.03

<sup>a</sup>SPX-Y; where X is the core number (1–4 see Figure 2.1) and Y is the depth in meters below the surface (1–17).

**Table 2.6** Classification of acid forming potential (AFP) using various criteria for mine tailings from the gold mine in Northeastern Thailand

Type	<sup>a</sup> Sample No.	ABA				NAG Test		Summary	
		NAPP	<sup>b</sup> Hutchison	ANC/MPA	<sup>c</sup> Miller	NAGpH	<sup>d</sup> EGI		
Upper tailings	SP1-3	122.11	PAF	0.44	PAF	2.55	PAF	PAF	
	SP1-5	62.64	PAF	0.61	PAF	2.78	PAF	PAF	
	SP1-6	89.11	PAF	0.54	PAF	2.73	PAF	PAF	
	SP2-3	37.35	PAF	0.80	PAF	2.54	PAF	PAF	
	SP2-5	166.21	PAF	0.31	PAF	2.54	PAF	PAF	
	SP2-7	37.22	PAF	0.71	PAF	2.14	PAF	PAF	
	SP3-3	-18.18	UC	1.11	PAF	2.58	PAF	PAF	
	SP3-6	158.87	PAF	0.42	PAF	2.74	PAF	PAF	
	SP3-7	118.86	PAF	0.52	PAF	2.27	PAF	PAF	
	SP4-1	40.93	PAF	0.75	PAF	2.38	PAF	PAF	
	SP4-3	90.66	PAF	0.56	PAF	2.60	PAF	PAF	
	SP4-5	21.63	PAF	0.85	PAF	2.56	PAF	PAF	
	Lower tailings	SP1-7	26.12	PAF	0.29	PAF	5.85	NAF	PAF
		SP1-9	41.99	PAF	0.04	PAF	2.86	PAF	PAF
SP1-17		-4.23	UC	1.09	PAF	4.70	NAF	UC	
SP2-10		-1.13	UC	1.01	PAF	3.35	PAF	PAF	
SP2-13		-59.13	NAF	8.73	NAF	5.55	NAF	NAF	
SP2-17		-56.51	NAF	5.62	NAF	5.49	NAF	NAF	
SP3-8		-26.26	NAF	1.88	PAF	5.46	NAF	NAF	
SP3-13		-19.28	UC	4.00	NAF	5.63	NAF	NAF	
SP3-17		-53.25	NAF	5.83	NAF	5.92	NAF	NAF	
SP4-7		-28.82	NAF	6.54	NAF	5.98	NAF	NAF	
SP4-9		7.74	UC	0.28	PAF	5.90	NAF	UC	
SP4-15	-59.82	NAF	7.31	NAF	5.32	NAF	NAF		

<sup>a</sup> SPX-Y; where X is the core number (1–4 see Figure 2.1) and Y is the depth in meters below the surface (1–17).

<sup>b</sup> Hutchison and Ellison (1992)

<sup>c</sup> Miller et al. (2006)

<sup>d</sup> Environmental Geochemistry International PTY LTD (EGI) (2005)

Regarding bulk chemical composition, some major oxides are directly associated with the mineral assemblages of both tailing groups. For instance, FeO<sub>t</sub> contents are clearly related to pyrrhotite, pyrite and chalcopyrite in the upper tailings

and goethite (Fe-oxyhydroxide) in the lower tailings. The high CaO content in the upper tailings is compatible with calcite ( $\text{CaCO}_3$ ) that is crucially found in the upper tailings. Although the  $\text{SiO}_2$  content shows an essentially equal value in both layers of tailings, it is likely affected by the difference in the primary mineral assemblage. In the upper tailings, the  $\text{SiO}_2$  content constitutes several silicate minerals, such as andradite, diopside and quartz; moreover, the  $\text{SiO}_2$  content in the lower tailings is mainly restricted to residual quartz that is a major composition of the initial gossan deposit (Romero et al., 2006; Valente et al., 2013; Velasco et al., 2013).

Arsenic is found at high concentrations (238–2870 mg/kg, Table 2.4) in the bulk composition of lower tailings, which seems to have related to goethite chemistry. Mineral chemical analysis shows that the goethite composition contains arsenic contents (0.04–1.11 wt.%, Table 2.2), which may have formed as either co-precipitation or surface adsorption as suggested by Campbell and Nordstrom (2014) and Lottermoser (2010). All sulfide minerals, pyrrhotite, pyrite and chalcopyrite, in the upper tailings do not contain arsenic (see Table 2.1). However, their bulk composition still contains relatively low arsenic content (39–268 mg/kg), which may relate arsenopyrite that was found in the sulfide deposit (Rodmanee, 2000), the original source of upper tailings. Since bulk compositions directly reflect the mineral assemblage in the tailings, they can be used for risk assessment. Goethite is a possible main source of arsenic under acid drainage. In addition, the As (238–2870 mg/kg), Cu (750–2608 mg/kg) and Pb (10–1506 mg/kg) concentrations in the lower tailings are higher than the Total Threshold Limit Concentration (TTL) of hazardous waste announced by the Ministry of Industry Thailand (2006) (i.e.,  $\leq 500$  mg/kg As,  $\leq 2500$  mg/kg Cu,  $\leq 1000$  mg/kg Pb); therefore, the lower tailings must be declared as hazardous waste.

#### **2.4.2 AMD and Heavy Metal Contamination**

According to mineral chemistry, the upper tailings contain sulfide gangues, particularly pyrrhotite, pyrite and chalcopyrite, which can be further oxidized after mine closure. This may take a shorter time period compared to the process that occurs in the original ore deposit because particle sizes of the mine tailings are significantly reduced to very fine grains during the processing, thus it is more reactive. Although the upper tailings contain neutralizing minerals, such as calcite, their PAF properties were

highly evaluated as reported earlier. Consequently, acid mine drainage (AMD) will occur unless protection is well planned and implemented. Even though the lower tailings appear to have low potential of AMD generation, they must be declared as hazardous waste because they contain high contents of toxic elements, e.g., As, Cu and Pb and have been covered by the AFP material (the upper tailings). Although the toxic elements in upper tailings are lower than the TTL, the testing on Soluble Threshold Limit concentration of these tailings need to be further investigated.

During mining activity, this tailing pond was soaked by wastewater and also rain. Since 2016, after excessive conflict including partial collapse of tailing dam (in 2012), this mine has already been temporarily suspended, and may be permanently closed. Consequently, this tailing pond has been evaporated and dried out (see Figure 2.2). The upper tailings may be oxidized and led to AMD generation, which may in turn infiltrate into the lower tailings and remobilize some toxic elements such as arsenic (As) and copper (Cu) from goethite (Lottermoser, 2010; Nordstrom and Alpers, 1999; Smedley and Kinniburgh, 2002). Therefore, leaching experiments under acid condition (pH 2) of these tailings were studied by Boonsrang et al. (2013). Subsequently, they reported that As, Cu, Mn and Pb can be leached from the lower tailings (0.007–0.570 mg/L As, 0.016–3.398 mg/L Cu, 0.594–23.333 mg/L Mn and 0.0001–2.251 mg/L Pb). In comparison, the upper tailings release significantly lower amounts of these toxic metals (0.001–0.004 mg/L As, 0.008–0.263 mg/L Cu, 0.582–1.692 mg/L Mn and 0.0001–0.017 mg/L Pb). As shown in the leaching experiments (Boonsrang et al., 2013), the lower tailings appear to be more mobilized under the acidic conditions compared to the same condition for the upper tailings. Eventually, this may cause harmful heavy metal contamination throughout the area. This process is considered to have the highest risk impact.

Recently, this gold mine has been accused by some surrounding villagers as the main contamination source of toxic elements (As, Cu, Cd, Hg, Mn and Pb) and cyanide ( $\text{CN}^-$ ) (<http://sea-globe.com/digging-for-gold-striking-resistance-thailand-gold-mining-isaan-loei-cyanid/> and <http://en.nationalhealth.or.th/node/186>). Thus, four groups of sample (i.e., soil, stream sediment, surface water and groundwater) were collected and examined by Chotipong et al. (2014a). Subsequently, they suggested that the backgrounds of As in this area (<14 mg/kg in soils and <24 mg/kg in stream sediments) were quite high and definitely exceeding the Thailand Soil Quality Standard

(TSQS;  $\leq 3.9$  mg/kg). They also reported the high Mn background in the soil and stream sediment; however, Mn showed insignificant leaching from the tailing pond (Chotipong et al., 2014b). Although the TSQS has never been suggested for copper threshold limit, they found the high copper concentrations (6–385 mg/kg) in soils and (7–278 mg/kg) in stream sediments comparing to the natural soil (30 mg/kg) suggested by Bowen (1979) cited in (Kim et al., 2005). Moreover, Cd, Hg, Pb and cyanide ( $\text{CN}^-$ ) in soils and stream sediments yielded quite low concentrations (Chotipong et al., 2014a, b).

Chotipong et al. (2015) reported that As contents in the surface water samples (both collections before and after mining operation) exceeded the Thailand Surface Water Quality (TSWQ). These results corresponded to the high As contents in stream sediments. In addition, Mn contents in surface water surrounding the mine were found to be exceeding the TSWQ, whereas those within the mine were lower than the TSWQ. Cyanide contents (0.2–2 mg/L) in the tailing pond water samples were higher than the TSWQ (0.005 mg/L) but still lower than the tolerable level (20 ppm) suggested by Environmental Impact Assessment (EIA) report (Khon Kaen University Report, 2009). Cu, Cd, Hg and Pb contents in surface water samples were mostly lower than the TSWQ (Chotipong et al., 2015). In addition, Chotipong et al. (2016) reported that Mn contents in groundwater samples collected within the mine and its surrounding area were higher than the Thailand Groundwater Quality Standard. Cyanide was also found in groundwater sample from the monitoring well located at the southern tailing pond (see Figure 2.1a), only. Finally, they concluded that the background contents of As, Cu and Mn were naturally high and there is insignificant evidence of leaching from the tailing pond. However, cyanide in the groundwater samples surrounded the tailing pond should be monitored continuously with great care.

Although these tailings are recently low impact to the environment; however, they will be a large potential source of AMD and also toxic elements (e.g., As, Cu, Mn and Pb), especially arsenic unless protection plan is designed and implemented well.

## 2.5 Conclusions and recommendations

Based on physical appearances, the tailings from this gold mine can be divided into two groups: the upper gray and lower ochre tailings. The upper gray tailings are

composed of pyrrhotite, pyrite, chalcopyrite, andradite, diopside, calcite and quartz reflecting the initial ore material that consists of massive sulfide and skarn. The lower ocher tailings are mainly composed of quartz and goethite from the gossan ore deposit.

The characteristics of minerals can be related to their AFP. The upper gray tailings are, however, defined as PAF despite the fact that they contain calcite as a basic material. The lower ocher tailings are classified as NAF (non-acid forming) because they have a low content of total sulfide. Therefore, in the study site, the upper gray tailings may generate AMD. Although, the lower ocher tailings appear to be low potential source of AMD; they contain some toxic metals, particularly As, Cu and Pb at higher levels than the recommended contents of the TTLC and consequently classified as “hazardous waste”. The leaching test undertaken for these tailings yielded low soluble metal contents. This indicates low potential of metal transportation into the environment.

The tailing pond should be immediately covered soon after the mine closure to prevent oxidizing process and erosion. Since the upper tailings mainly consist of pyrrhotite and other sulfides, the dried tailing pond should be covered by the multi-layer structure as suggested by Lottermoser (2010). This tailing pond should be covered by compacted clay (at least 50 cm thick) to prevent water/oxygen reaction, and the compacted clay layer should be covered by a gravel layer (30 cm thick) to facilitate the drainage during rainy season. The top soil layer (1–2 m) must be covered before plantation. In addition, an AMD treatment system should be designed for prevention, where alkaline materials, such as limestone, hydrated lime, soda ash, caustic soda, ammonia, calcium peroxide, kiln dust and fly ash (Akcil and Koldas, 2006), can also be applied, initially at bottom layer (30 cm). Moreover, as the result of groundwater, Mn and cyanide was found in groundwater well located at the southern tailing pond (see Figure 2.1a); therefore, groundwater wells surrounding the tailing pond should be monitored continuously with great care.

CHAPTER 3  
MINERALOGICAL AND GEOCHEMICAL CHARACTERIZATION OF WASTE-ROCKS  
FROM A GOLD MINE IN NORTHEASTERN THAILAND: APPLICATION FOR  
ENVIRONMENTAL IMPACT PROTECTION

Thitiphan Assawincharoenki<sup>a</sup>, Christoph Hauenberger<sup>b</sup>, Karl Ettinger<sup>c</sup>,  
Chakkaphan Sutthirat<sup>a,c,d\*</sup>

<sup>a</sup> Department of Geology, Faculty of Science, Chulalongkorn University, Bangkok 10330, Thailand

<sup>b</sup> NAWI Graz Geocenter, Petrology and Geochemistry, University of Graz, Universitätsplatz 2, 8010, Graz, Austria

<sup>c</sup> Research Program of Toxic Substance Management in the Mining Industry, Center of Excellence on Hazardous Substance Management, Environmental Research Institute, Chulalongkorn University, Bangkok 10330, Thailand

<sup>d</sup> Research Unit of Site Remediation on Metals Management from Industry and Mining (Site Rem), Chulalongkorn University, Bangkok 10330, Thailand

\* Corresponding author

Environmental Science and Pollution Research (*Revised*)



## Abstract

Waste rocks from gold mining in northeastern Thailand are classified as sandstone, siltstone, gossan, skarn, skarn-sulfide, massive sulfide, diorite and limestone/marble. Among these rocks, skarn-sulfide and massive sulfide rocks have the potential to generate acid mine drainage (AMD) because they contain significant amounts of sulfide minerals, i.e., pyrrhotite, pyrite, arsenopyrite and chalcopyrite. Moreover, both sulfide rocks present high contents of As and Cu, which are caused by the occurrence of arsenopyrite and chalcopyrite, respectively. Another main concern is gossan contents, which are composed of goethite, hydrous ferric oxide (HFO), quartz, gypsum and oxidized pyroxene. X-ray maps using Electron Probe Micro-Analysis (EPMA) indicate distribution of some toxic elements in Fe-oxyhydroxide minerals in the gossan waste rock. Arsenic (up to 1.37 wt.%) and copper (up to 0.60 wt.%) are found in goethite, HFO and along the oxidized rim of pyroxene. Therefore, the gossan rock appears to be a source of As, Cu and Mn. As a result, massive sulfide, skarn-sulfide and gossan have the potential to cause environmental impacts, particularly AMD and toxic element contamination. Consequently, the massive sulfide and skarn-sulfide waste rocks should be protected from oxygen and water to avoid an oxidizing environment, whereas the gossan waste rocks should be protected from the formation of AMD to prevent heavy metal contamination.

จุฬาลงกรณ์มหาวิทยาลัย  
CHULALONGKORN UNIVERSITY

**Keywords:** AMD, gold mine, heavy metal, waste rock, gossan

### 3.1 Introduction

As natural gold deposits have a very low concentration in host rocks, enormous waste rocks have been produced and disposed of in surface dumps during mine operation. Consequently, these waste rocks are directly exposed to the atmosphere and may in turn cause a negative environmental impact (Changul et al., 2009a; Cidu et al., 2012; Da Pelo et al., 2009; Marescotti et al., 2009; Sutthirat and Changul, 2012). To demonstrate this, common waste rocks and their mineral assemblages from some crucial mining sites located in Spain, Peru, Canada, Australia and the USA (Álvarez-Valero et al., 2008; Ashley et al., 2004; Hunt et al., 2016; Koski et al., 2008; Smuda et al., 2007; Sracek et al., 2004; Sracek et al., 2006; Velasco et al., 2013) are summarized in Table 3.1. Sulfide minerals, e.g., pyrite, pyrrhotite, chalcopyrite, arsenopyrite, sphalerite and galena, appear to be crucial primary minerals, whereas goethite, hematite and Fe-oxyhydroxide are often found as secondary assemblages in these waste rocks. The sulfides may contain toxic elements such as As, Cu, Co, Ni, Pb and Zn that are formed within a crystal structure or occur as micro-inclusions (Lottermoser, 2010; Parbhakar-Fox et al., 2013). Although, they are stable under reducing conditions beneath the earth's surface, an oxidizing reaction may take place after they are exposed by mine operations (Lindsay et al., 2015; Lottermoser, 2010; Parbhakar-Fox and Lottermoser, 2015). In addition, secondary minerals, goethite and hematite, are also enriched in toxic elements (e.g., As, Cu and Pb) which were discovered, for example, in the Iberian Pyrite Belt in Southwest Spain (Romero et al., 2006; Valente et al., 2013; Velasco et al., 2013). Therefore, sulfide-bearing waste rocks have high potential to release toxic elements because of acid rock drainage formation and subsequent element mobilization (Changul et al., 2009a; Lapakko, 2002; Marescotti et al., 2009; Nugraha et al., 2009; Smith et al., 2013). Acid rock drainage (ARD), or acid mine drainage (AMD), is the formation of acid caused by an oxidizing reaction of sulfide-bearing waste materials (Hudson-Edwards et al., 2011; Lottermoser, 2010; Sutthirat, 2011).

**Table 3.1** Summary of mineral assemblages in waste rocks taken from some well-known metal mines around the world.

Mine/Country	Ore deposit	Waste rocks	Mineral assemblage		Reference
			Primary	Secondary	
<i>Iberian Pyrite Belt (IPB), Spain</i>	Ag-Au-Cu Massive sulfide	Gossan/ country rocks (volcanics and shales)	Quartz, halloysite, kaolinite, K-feldspar, muscovite	Goethite, beudantite, hematite, jarosite, gypsum, scorodite	Álvarez-Valero et al. (2008); Velasco et al. (2013); Hunt et al. (2016)
<i>Prince William Sound, Alaska, United States</i>	Cu-Volcano- genic massive sulfide	Massive sulfide	Pyrrhotite, pyrite, chalcopyrite, sphalerite, galena, arsenopyrite, cobaltite	Goethite, Fe-oxyhydroxide ( <i>amorphous</i> ), marcasite, lepidocrocite, covellite	Koski et al. (2008)
<i>Cerro de Pasco, Central Andes, Peru</i>	Polymetallic Pb-Zn-(Ag-Bi- Cu)	Quartz- pyrite/ volcanic/ dolomitic rocks	Quartz, hematite, pyrite, muscovite	Gypsum, jarosite, Fe hydroxide, kaolinite, dolomite	Smuda et al. (2007)
<i>Restigouche, New Brunswick Mine Doyon, Québec, Canada</i>	Au-vein-type mineralization	Sericite schist	Pyrite, muscovite, chlorite	Gypsum, jarosite, Fe-oxyhydroxide	Sracek et al. (2004); Sracek et al. (2006)
<i>Webbs Consols mine, New South Wales, Australia</i>	Polymetallic Pb-Zn-Ag sulfide-rich deposit	Granite/ altered- granite	Quartz, feldspars, biotite, arsenopyrite, sphalerite, galena, chalcopyrite	Illite, sericite, chlorite, scorodite, anglesite, smectite, Fe-oxyhydroxide	Ashley et al. (2004)

The toxic elements can potentially have a severe impact on human health and ecosystems (Simate and Ndlovu, 2014; Singh et al., 2011; Yadav, 2010). Arsenic, in particular, is a high toxic element with certain chemical forms (e.g., As<sup>3+</sup>) which is also known as a carcinogen even at very low concentrations (Paktunc, 2013). The gold mine under this study has been suspected to cause toxic element contamination in surface

water and groundwater (<http://geographical.co.uk/people/development/item/1178-gold-diggers> and <http://isaanrecord.com/2014/05/20/gold-mine-protesters-hurt-by-armed-mob-and-shady-deals-3/>). Many previous researchers have also reported the distribution of toxic elements in surface water and groundwater surrounding this study area (ERIC, 2012; Huagul, 2007; Khamthat, 2007; Nonthee, 2010; Tuisakda, 2008). For instance, Fe, Cu and Mn in surface water and groundwater have been shown to exceed the Thailand Surface Water Quality (TSWQ) and Thailand Groundwater Quality Standard (TGQS). However, these contaminants can be released from either the mine site or naturally exposed rocks in the area. There is still unclear evidence to indicate the real cause of the contamination. Characterizations of waste materials are therefore crucial in a study that aims at providing information for proper planning in prevention and remediation.

The study area for this research is “Phu Thap Fah Gold Deposit” (Crow and Zaw, 2011; Rodmanee, 2000) located in Wang Saphung district, Loei province in northeastern Thailand (Figure 3.1a). Gold mining has been operating here since 2006, with an estimated mine life of at least 25 years. The study area is located within a tropical monsoon climate with an average temperature of 25 °C that can range from about 10 °C to 40 °C. Average rainfall is about 1,300 mm/y (Thai Meteorological Department, 2012). During mining, huge amounts of waste rock are left in the area. Therefore, the main aims of this study are (1) to investigate petrography, mineral chemistry and whole-rock geochemistry of various waste rocks for determination of AMD generation and toxic element release and (2) to apply advanced geochemical analyses to indicate location and distribution of crucial toxic elements in the main mineral assemblages of particular waste rocks.

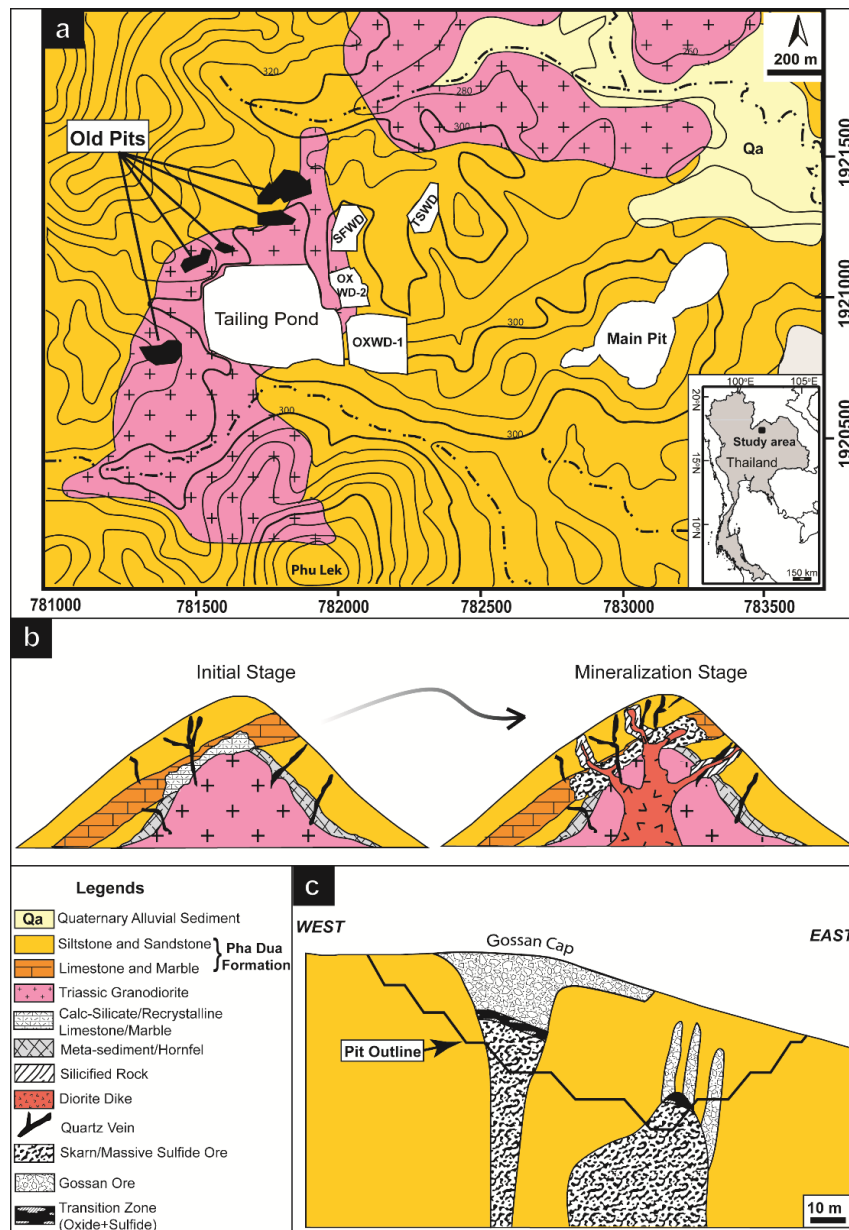


**Figure 3.1** (a) The geological map of the study area showing the location of mining sites, including OXWD-1, -2 (oxide waste dumps 1 and 2), SFWD (sulfide waste dump) and TSWD (transition waste dump); (b) genesis model of the initial and following gold mineralization stages (modified from Rodmanee (2000)); (c) cross section of the main pit showing three different ore types (modified after Khon Kaen University Report (2009)).

### 3.2 Geology and mineralization

Geologically, the gold mine is occupied by Pha Dua Formation of the Permian Saraburi Group, consisting mainly of thin-bedded shale, siltstone and sandstone with minor limestone intruded by Triassic granodiorite (Figure 3.1a) (Chonglakmani, 1984; Rodmanee, 2000). Figure 3.1b presents the genesis model of Phu Thap Fah gold mineralization which was proposed by Rodmanee (2000). Two stages of gold mineralization, including the initial stage and mineralization stage, were recognized. The initial stage was started when the Pha Dua Formation was intruded by Triassic granodiorite, leading to recrystallization of surrounding sedimentary rocks to meta-sediment/hornfel and marble. Subsequently, hydrothermal solution was derived from the granodiorite that caused an extensive metasomatism of skarn with a high content of garnet and pyroxene. The mineralization stage was indicated by diorite dike intruded into the early garnet-pyroxene skarn. The hydrothermal fluids derived from this late stage were pervasive throughout, causing retrograde alteration in the primary skarn. These hydrothermal fluids caused mineralization of massive sulfides (e.g., pyrrhotite, pyrite, arsenopyrite and chalcopyrite) and formation of gold, bismuth and telluride minerals (Rodmanee, 2000).

This gold deposit is significantly characterized by oxide (gossan) and sulfide (skarn-sulfide/massive sulfide) ores minerals (Rodmanee, 2000). Figure 3.1c displays a cross section of the main mining pit showing gossan cap (classified as oxide ore layers) on the surface covering siltstone and sandstone. In general, gossan rocks located over the main orebody were formed by erosion and oxidation of massive sulfide (Romero et al., 2006; Velasco et al., 2013). This gossan usually presents mushroom-like morphology contacting with the underlying massive sulfide orebody (Figure 3.1c) similar to the gossan deposits in the Iberian Pyrite Belt (IPB), Southwest Spain (Velasco et al., 2013). Sulfide ore (classified as “skarn-sulfide/massive sulfide ore”) is located at depths of about 40 m to 200 m (Rodmanee, 2000) in which it yields the highest gold grade at 3.54 g/t (in massive sulfide) and 7.97 g/t (in skarn-sulfide). In addition, the ore zone between oxide and sulfide ores, typically combining both oxide and sulfide ores, is classified as a transition ore zone (Figure 3.1c).

### 3.3 Materials and methods

#### 3.3.1 Rock wastes and dumping sites

Based on different ore types (i.e., oxide ore, transition ore and sulfide ore), waste rocks related to these ores are separated and disposed of on different dumping sites (Khon Kaen University Report, 2009), including oxide waste dumps (OXWD-1 and OXWD-2), transition waste dump (TSWD) and sulfide waste dump (SFWD) (see Figures 3.1a and 3.2). Estimated amounts and volumes of these waste dumps are summarized in Table 3.2 (Khon Kaen University Report, 2009). Waste rock samples were collected from all dump sites as shown in Figure 3.2. Moreover, some waste rock samples relating to the sulfide ore were additionally collected from the main mining pit. Limestone, marble, sandstone, siltstone, mudstone, gossan, diorite, granodiorite and massive sulfide were found and collected from the oxide waste dumps (OXWD-1 and OXWD-2). Siltstone, limestone/marble, diorite, skarn, massive sulfide and gossan were collected from the TSWD. Massive sulfide and skarn-sulfide rocks with some siltstones were sampled from the SFWD. More samples of siltstone, granodiorite, skarn, massive sulfide, skarn-sulfide and limestone/marble were additionally collected from the main pit.

#### 3.3.2 Analytical methods

Representative rock samples were then cut and prepared for thin sectioning and polished thin sectioning. Petrographic investigation was carried out using transmitted light and reflected-light microscopes at the Geology Department, Faculty of Science, Chulalongkorn University.

**Table 3.2** Estimated amounts and volumes of all waste rock dumps from the main pit. Total rock waste was estimated at 2,552,170 metric tons (Mt) and 997,280 cubic meters (m<sup>3</sup>) (Khon Kaen University Report, 2009).

Oxide waste rocks		Transition waste rocks		Sulfide waste rocks	
Amount (Mt)	Volume (m <sup>3</sup> )	Amount (Mt)	Volume (m <sup>3</sup> )	Amount (Mt)	Volume (m <sup>3</sup> )
1,658,910	674,450	382,830	140,380	510,430	182,450

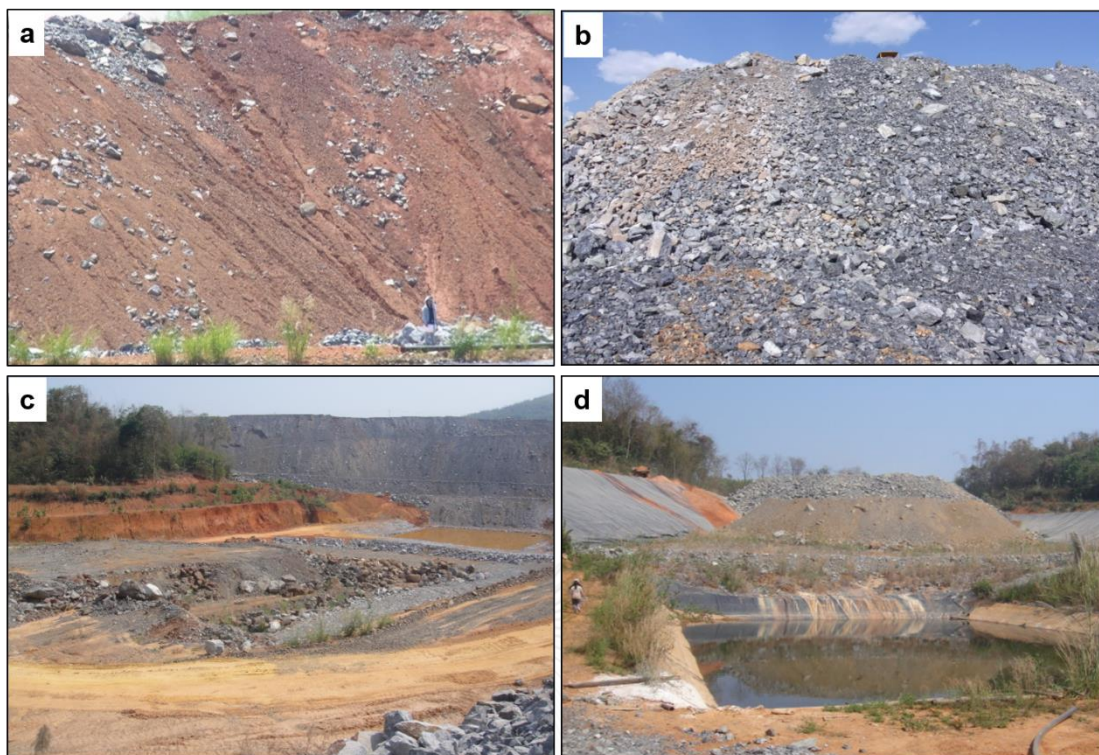


**Figure 3.2** Waste rock dumps: (a) and (b) dump sites of oxide waste rocks (OXWD-1 and OXWD-2); (c) sulfide waste dump (SFWD); (d) transition waste dump (TSWD)

Sixty one samples were selected representatively before crushing and milling. Powdered rock samples were dried to remove moisture in an oven at 60 °C for 8 h to prevent alterations of chemical and physical properties prior to further analyses (EPA, 2004). These powdered samples were pressed and analyzed for major/minor oxides (i.e., SiO<sub>2</sub>, TiO<sub>2</sub>, Al<sub>2</sub>O<sub>3</sub>, FeO<sub>t</sub>, MgO, MnO, K<sub>2</sub>O, Na<sub>2</sub>O and P<sub>2</sub>O<sub>5</sub>) using a X-ray fluorescence spectrometer (XRF) (Bruker AXS S4 Pioneer) at the Geology Department, Faculty of Science, Chulalongkorn University. Calibration curves for the XRF data were prepared from rock standards provided by the US Geological Survey (USGS) and Geological Survey of Japan (GSJ). Moreover, glass beads were prepared and analyzed using a Bruker AXS S4 Pioneer XRF at the NAWI Graz Geocenter, University of Graz, Austria.

In addition, mineral compositions were identified using a Bruker D8 Advance X-ray diffractometer (XRD) at the Geology Department, Faculty of Science, Chulalongkorn University. Mineral chemistry of sulfide and Fe-oxyhydroxide minerals was analyzed by a JEOL JXA-8200 electron probe micro analyzer (EPMA) at the Eugen-Stumpfl microprobe facility, UZAG (Mining University Leoben, University of Graz, Graz University



of Technology). A probe current of 20 nA and accelerating voltage of 20 kV and 25 kV were applied for sulfide and oxide minerals, respectively. Counting times were typically set at 30 seconds on peak and total background analyses. Natural minerals were used as standards.

Thirty-nine selected samples were digested for trace element analyses (e.g., As, Ag, Au, Cd, Co, Cr, Cu, Hg, Mn, Ni, Pb and Zn) using a Thermo-CapQ inductively coupled plasma-mass spectrometry (ICP-MS) at the Scientific and Technological Research Equipment Centre, Chulalongkorn University. The calibration curves were also prepared using well-characterized international reference standards supplied by USGS and GSJ. The relative standard deviations of these data were <5%. All samples and standards were digested totally using a HF-HClO<sub>4</sub>-HNO<sub>3</sub> mixed acid dissolution procedure under the same conditions as previously reported by Satoh et al. (1999). The detection limits of all elements ranged from 0.002 to 0.05 ppm.

### 3.4 Results

#### 3.4.1 Petrographical and geochemical characteristics

According to petrographic description, various kinds of waste rock under this study are identified; they are composed of fine-grained sandstone, siltstone, mudstone, massive sulfide, skarn-sulfide, skarn, gossan, diorite and limestone/marble. Their essential mineral assemblages observed under microscope and Fe-oxyhydroxide phases, i.e., goethite and hydrous ferric oxide (HFO), identified by Raman and FTIR patterns are reported in “3.7 Electronic Supplementary Material A”.

Major and minor chemical compositions (e.g., SiO<sub>2</sub>, TiO<sub>2</sub>, Al<sub>2</sub>O<sub>3</sub>, FeO<sub>t</sub>, MgO, MnO, K<sub>2</sub>O, Na<sub>2</sub>O, P<sub>2</sub>O<sub>5</sub> and SO<sub>3</sub>) of the waste rocks are summarized in Table 3.6, whereas their trace element analyses (e.g., As, Ag, Au, Cd, Co, Cr, Cu, Hg, Mn, Ni, Pb and Zn) are reported in Table 3.7. To understand variation of chemical composition of all rock types, the variation diagrams are plotted using FeO<sub>t</sub> against the other oxides as shown in Figure 3.3. Moreover, some selective trace elements (i.e., As, Cd, Cr, Cu, Hg and Zn) are also plotted versus FeO<sub>t</sub> as shown in Figure 3.4.

Limestone, sandstone/siltstone and diorite, collected from different dump sites and from the main pit have relatively low FeO<sub>t</sub> contents with narrow ranges of

individual main compositions (see Figure 3.3 and Table 3.6) which appear to have no correlation between  $\text{FeO}_t$  and other major oxides in these rock types. On the other hand, skarn, skarn-sulfide, gossan and massive sulfide contain higher ranges of  $\text{FeO}_t$ , respectively, and their  $\text{FeO}_t$  ranges seem to have continuously negative correlation with  $\text{SiO}_2$ ,  $\text{Al}_2\text{O}_3$ ,  $\text{CaO}$ ,  $\text{MnO}$  and  $\text{MgO}$  and positive correlation with  $\text{SO}_3$  (Figure 3.3) and also Cu (Figure 3.4). Only one gossan sample taken from the TSWD (TK23) revealed the highest  $\text{FeO}_t$  contents (48.48 wt.%), Au (8.4 ppb) and Cu (7480 ppm) with quite low  $\text{SO}_3$  content (1.34 wt.%) (Tables 3.6 and 3.7), which seem unlikely to have good correlation (Figures 3.3 and 3.4). Other gossan samples taken from the OXWD also show positive correlation between  $\text{FeO}_t$  and As, whereas skarn, skarn-sulfide and massive sulfide mostly show negative correlation of both elements (Figure 3.4). The other elements appear to have no correlation with  $\text{FeO}_t$ .



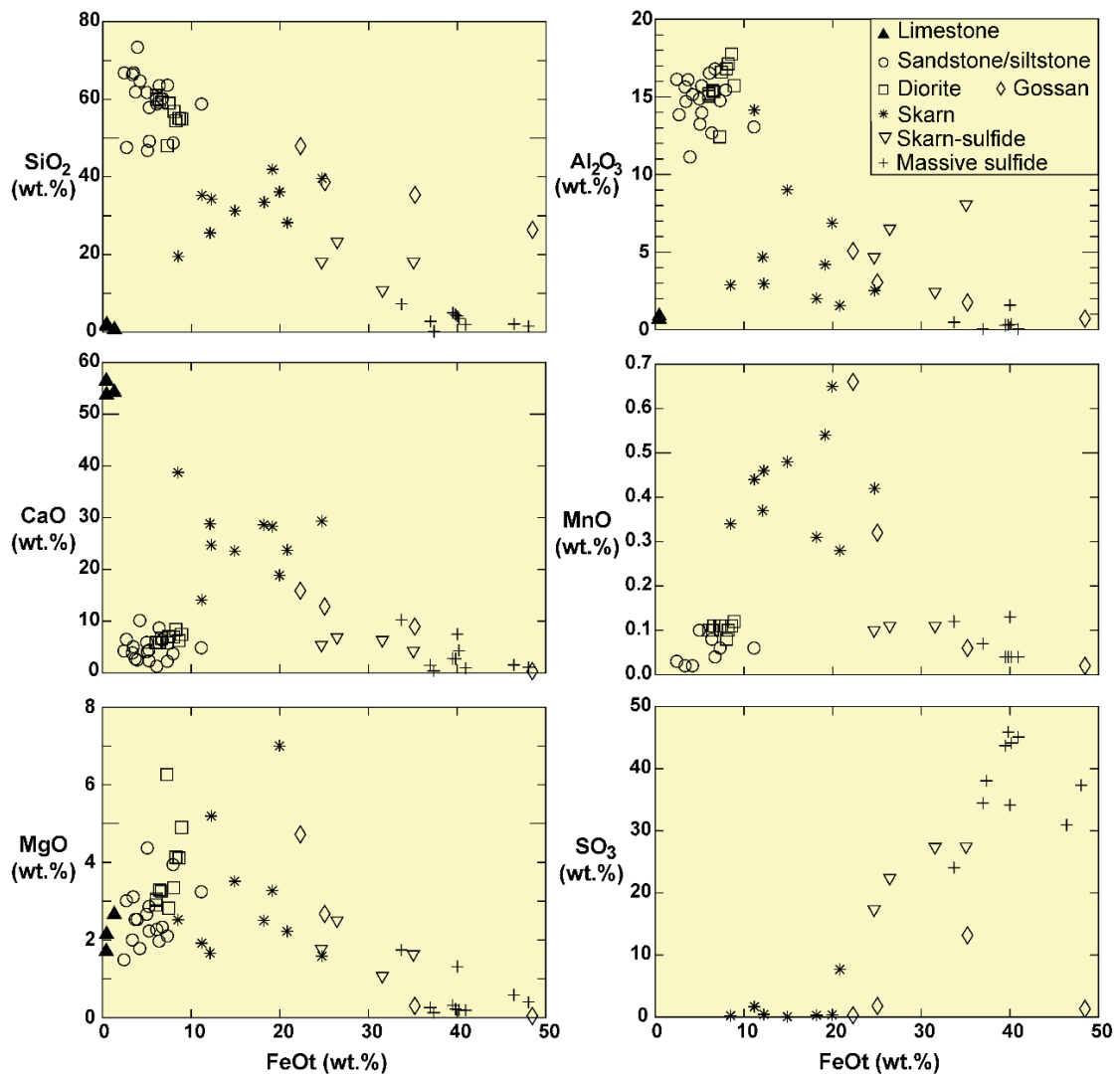
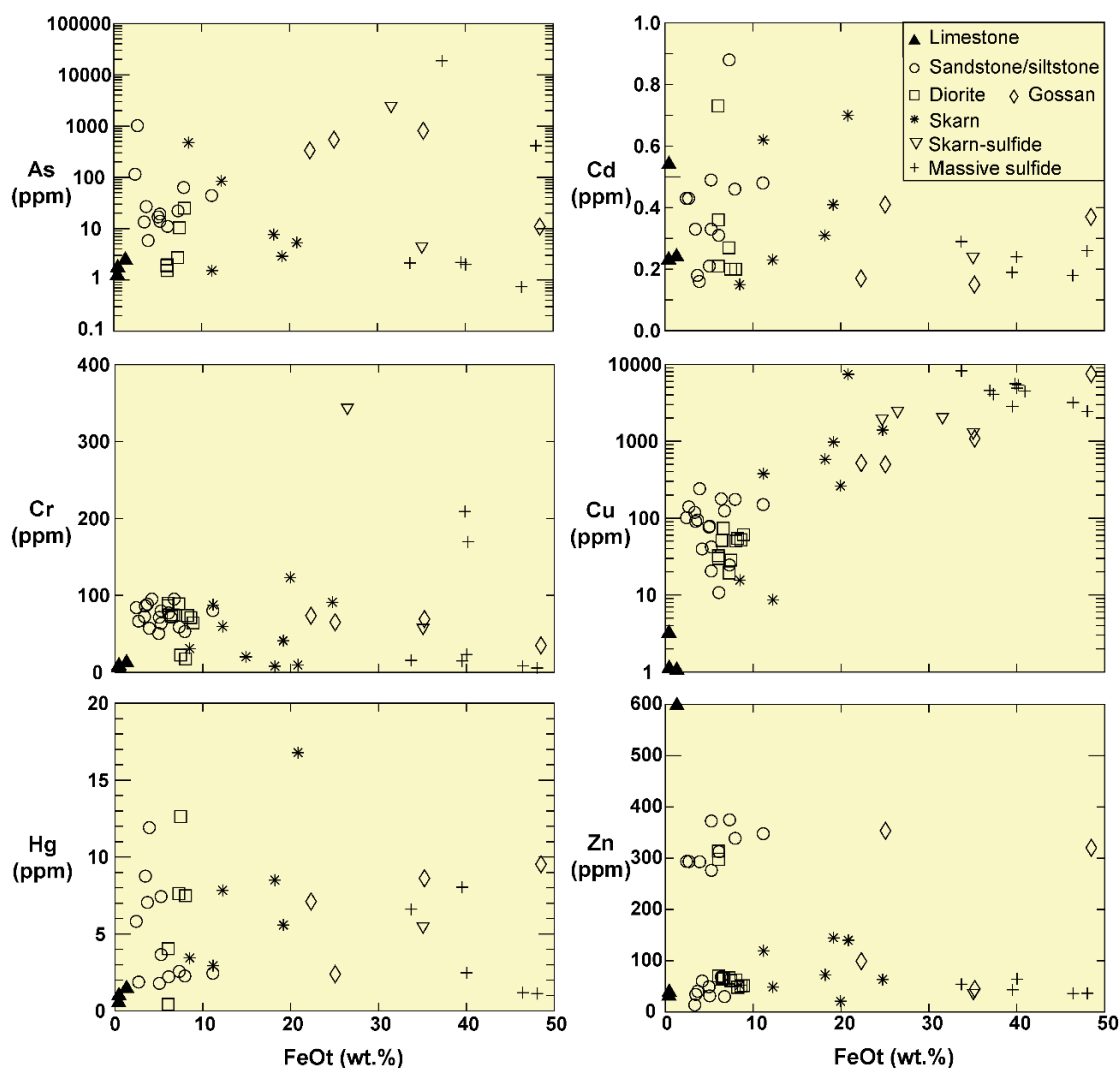


Figure 3.3 Plots of  $\text{FeO}_t$  (wt.%) contents against  $\text{SiO}_2$ ,  $\text{Al}_2\text{O}_3$ ,  $\text{CaO}$ ,  $\text{MnO}$ ,  $\text{MgO}$  and  $\text{SO}_3$  (wt.%) of sandstone/siltstone, diorite, gossan, skarn, skarn-sulfide and massive sulfide.



**Figure 3.4** Plots of FeO<sub>t</sub> (wt.%) versus As (arsenic), Cd (cadmium), Cr (chromium), Cu (copper), Hg (mercury) and Zn (zinc) levels (ppm) of sandstone/siltstone, diorite, gossan, skarn, skarn-sulfide and massive sulfide.

According to the results, the massive sulfide, skarn-sulfide, skarn and gossan rocks have higher average FeO<sub>t</sub> content (29±11 wt.%), whereas the sandstone/siltstone, diorite and limestone have lower average FeO<sub>t</sub> content (5±3 wt.%). The massive sulfide, skarn-sulfide and gossan rocks appear to be potential sources of toxic elements which may originate as major or minor compositions of pyrrhotite, pyrite, chalcopyrite, arsenopyrite, or Fe-oxyhydroxide phases. Therefore, some of these phases were also analyzed by EPMA for mineral chemistry analyses as reported in the next section.

### 3.4.2 Mineral chemistry

Massive sulfide, skarn-sulfide and gossan rocks were selected, based on their high contents of toxic elements, for mineral chemical analyses. Table 3.3 presents chemical compositions (i.e., Fe, S, As, Cu, Co and Ni) of sulfide minerals such as pyrrhotite, pyrite, chalcopyrite and arsenopyrite that are found in massive sulfide and skarn-sulfide rocks. Moreover, chemical analyses of goethite and HFO of gossan are also reported in Table 3.4.

The massive sulfide rocks are significantly composed of pyrrhotite and chalcopyrite. Pyrrhotite is composed of  $61\pm 0.07$  wt.% Fe,  $39\pm 0.35$  wt.% S with minor amounts of Co (0.03 wt.%). Chalcopyrite consists of  $35\pm 0.22$  wt.% Cu,  $31\pm 0.28$  wt.% Fe and  $35\pm 0.05$  wt.% S with negligible As ( $\leq 0.08$  wt.%).

The skarn-sulfide rocks consist of arsenopyrite, pyrrhotite, pyrite and chalcopyrite. Arsenopyrite has average contents of  $35\pm 0.26$  wt.% Fe,  $46\pm 0.28$  wt.% As and  $19\pm 0.31$  wt.% S with minor contents of Co (0.05–0.28 wt.%) and Ni (0.05–0.12 wt.%). Pyrrhotite contains  $60\pm 0.51$  wt.% Fe,  $39\pm 0.41$  wt.% S with minor contents of  $\leq 0.08$  wt.% Cu, 0.09–0.12 wt.% Co and  $\leq 0.05$  wt.% Ni. Pyrite has  $47.02\pm 0.04$  wt.% Fe,  $53\pm 0.39$  wt.% S with 0.07–0.08 wt.% Co. In addition, chalcopyrite is composed of  $35\pm 0.20$  wt.% Cu,  $31\pm 0.14$  wt.% Fe and  $35\pm 0.36$  wt.% S with negligible contents of As ( $\leq 0.07$  wt.%) and Co (0.03–0.05 wt.%).

X-ray mapping of gossan (Figure 3.5) clearly displays the distribution of different mineral phases and their element contents. This method is a key technique to understand variations of toxic elements in mineral phases. The distribution of toxic elements in some crucial mineral can be recognized. Arsenic and manganese are found obviously in HFO (amorphous or poorly crystalline ferric oxide phase) (Figures 3.5a, b); on the other hand, goethite shows clear distribution of Cu and Mn (Figure 3.5c). Two phases of the Fe-oxyhydroxide are distinguished, based on Raman and FTIR patterns, into goethite (crystalline phase) and HFO (see Figure 3.8 in Supplementary Material A). HFO cannot be observed using Raman spectroscopy because it lacks a crystalline structure.

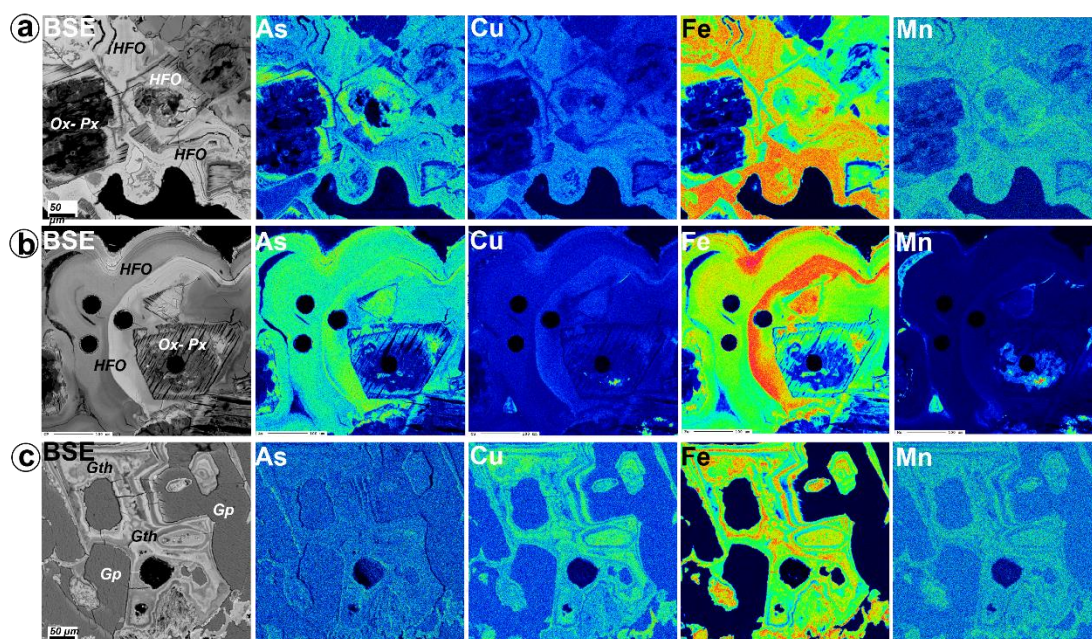
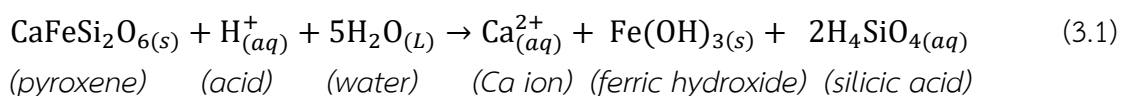


**Figure 3.5** Back Scattered Electron (BSE) Images and X-ray maps of gossan samples' levels of As, Cu, Fe and Mn in: (a) and (b) amorphous hydrous ferric oxides and (c) goethite and gypsum. Abbreviations are HFO: hydrous ferric oxide, Ox-Px: oxidized-pyroxene, Gth: goethite, and Gp: gypsum.

Although, Fe-oxyhydroxide may have originated through oxidation of iron sulfide minerals, it can also be formed by weathering of iron silicate minerals; for example, pyroxene ( $\text{CaFeSi}_2\text{O}_6$ ) (see equation (3.1) modified from Lottermoser (2010) and Noack et al. (1993)).



The chemical analyses of goethite and HFO in gossan are shown in Table 3.4. The goethite is composed of  $83 \pm 4.28$  wt.%  $\text{FeO}_t$ ,  $7 \pm 2.58$  wt.%  $\text{SiO}_2$  and  $0.07 \pm 0.08$  wt.%  $\text{MnO}$  with minor contents of As ( $0.16 \pm 0.01$  wt.%) and Cu ( $0.26 \pm 0.25$  wt.%). The HFO consists of  $71 \pm 5.30$  wt.%  $\text{FeO}_t$ ,  $14 \pm 3.76$  wt.%  $\text{SiO}_2$ ,  $4 \pm 2.69$  wt.%  $\text{Al}_2\text{O}_3$ ,  $0.12 \pm 0.06$  wt.%  $\text{MnO}$  with relatively high contents of As ( $0.76 \pm 0.38$  wt.%) and Cu ( $0.41 \pm 0.13$  wt.%). Moreover, HFO that occurred around the pyroxene rim contains  $65 \pm 3.41$  wt.%  $\text{FeO}_t$ ,  $18 \pm 4.02$  wt.%  $\text{SiO}_2$ ,  $4 \pm 0.66$  wt.%  $\text{Al}_2\text{O}_3$ ,  $0.3 \pm 0.11$  wt.%  $\text{MnO}$  with high contents of As ( $1.10 \pm 0.12$  wt.%) and Cu ( $0.34 \pm 0.04$  wt.%).

### 3.5 Discussion

The waste rocks mainly fall within boulder size, usually ranging from about 20 to 100 cm in diameter. The boulder waste rocks usually produce significant pore spaces in the dump sites. Consequently, water and oxygen can flow into the deeper parts and react with most of the waste rocks (Lottermoser, 2010; Marescotti et al., 2009). Thus, it seems likely that these waste rocks can still be oxidized even in the deeper part of the dump sites.

Based on mineral assemblages, the massive sulfide and skarn-sulfide waste rocks, mainly containing sulfide minerals, may generate AMD due to an oxidizing reaction (Marescotti et al., 2009; Parbhakar-Fox et al., 2014; Parbhakar-Fox et al., 2011) which has been confirmed by previous studies such as on acid-base accounting (ABA) and weathering cell methods (Charuseiam, 2012; Charuseiam et al., 2013; Das et al., 2008; ERIC, 2012). Consequently, the massive sulfide and skarn-sulfide waste rocks are classified as potential acid forming (PAF). On the other hand, the gossan, skarn and clastic rocks are classified as non-acid forming (NAF) (Charuseiam, 2012; Charuseiam et al., 2013; ERIC, 2012). Moreover, the present study indicates that the massive sulfide rocks contain high  $\text{SO}_3$  content, which is compatible with total S ranging from 18.8% to 34.5% (ERIC, 2012). Therefore, the massive sulfide rocks will be the main source of AMD unless a prevention plan is well implemented.

**Table 3.3** Representative EPMA analyses (wt.%) of sulfide minerals in the massive sulfide and skarn-sulfide waste rocks.

Rock type	Mineral	Fe	S	As	Cu	Co	Ni	Total
Massive sulfide	Po	60.51	39.20	<0.03	<0.02	<0.01	<0.02	99.81
	Po	60.65	39.71	<0.03	<0.02	<0.01	<0.02	100.41
	Po	60.57	39.04	<0.03	<0.02	0.03	<0.02	99.68
	Ccp	30.92	35.18	<0.03	34.63	<0.01	<0.02	100.75
	Ccp	30.93	35.30	<0.03	34.77	<0.01	<0.02	101.02
	Ccp	30.45	35.27	0.08	34.40	<0.01	<0.02	100.23
	Ccp	30.43	35.24	<0.03	34.27	<0.01	<0.02	99.99
Skarn-sulfide	Apy	35.23	19.11	45.78	<0.02	0.18	<0.02	100.31
	Apy	35.42	19.42	45.92	<0.02	0.17	<0.02	100.96
	Apy	35.63	19.36	45.63	<0.02	0.12	<0.02	100.76
	Apy	35.06	18.96	46.07	<0.02	0.17	0.12	100.40
	Apy	35.54	19.74	45.42	<0.02	0.28	0.05	101.06
	Apy	35.77	19.70	45.36	<0.02	0.05	<0.02	100.90
	Po	60.01	38.40	<0.03	<0.02	0.12	<0.02	98.55
	Po	59.94	38.26	<0.03	0.08	0.10	<0.02	98.41
	Po	59.97	38.83	<0.03	<0.02	0.10	<0.02	98.94
	Po	60.14	39.31	<0.03	<0.02	0.09	<0.02	99.60
	Py	46.99	52.29	<0.03	<0.02	0.07	<0.02	99.36
	Py	47.04	52.85	<0.03	<0.02	0.08	<0.02	100.01
	Ccp	31.40	34.55	<0.03	35.43	0.05	<0.02	101.45
	Ccp	31.22	34.66	<0.03	35.31	0.04	<0.02	101.24
	Ccp	31.17	34.55	0.07	34.90	0.04	<0.02	100.73
Ccp	31.15	34.15	<0.03	35.16	0.03	<0.02	100.49	

Po: pyrrhotite; Py: pyrite; Ccp: chalcopyrite; Apy: arsenopyrite



**Table 3.4** Representative EPMA analyses (wt.%) of amorphous hydrous ferric oxides (HFO) found in the gossan waste rocks.

Mineral	Texture/ Form	SiO <sub>2</sub>	FeO <sub>t</sub>	Al <sub>2</sub> O <sub>3</sub>	CaO	MgO	MnO	SO <sub>3</sub>	As	Cu	Co	Ni	Total
Goethite	Colloform	8.93	85.48	0.57	0.23	<0.01	0.02	<0.01	0.15	0.09	<0.01	<0.01	95.48
Goethite	Colloform	9.02	85.88	0.65	0.20	<0.01	<0.01	2.14	0.15	0.07	<0.01	<0.01	98.12
Goethite	Colloform	3.06	87.71	0.55	0.33	<0.01	0.02	2.06	0.17	0.07	<0.01	<0.01	93.96
Goethite	Colloform	8.63	78.43	0.94	0.10	<0.01	<0.01	1.82	<0.03	0.58	<0.01	<0.01	90.50
Goethite	Colloform	6.13	78.96	2.63	0.22	<0.01	0.16	2.09	<0.03	0.48	<0.01	<0.01	90.67
HFO	Colloform	14.47	64.42	5.32	0.55	<0.01	0.18	<0.01	1.12	0.33	<0.01	0.02	86.42
HFO	Colloform	11.27	73.78	2.84	0.55	<0.01	0.15	<0.01	1.37	0.40	<0.01	<0.01	90.36
HFO	Colloform	22.47	57.08	12.10	0.44	0.06	0.11	<0.01	0.86	0.26	<0.01	<0.01	93.38
HFO	Colloform	19.30	66.76	2.64	0.65	0.04	0.26	<0.01	1.05	0.28	0.05	<0.01	91.02
HFO	Colloform	15.37	72.60	2.61	0.60	0.05	0.20	<0.01	1.19	0.29	<0.01	0.02	92.93
HFO	Colloform	19.56	69.66	2.66	0.54	0.09	0.16	<0.01	0.88	0.25	<0.01	0.03	93.83
HFO	Colloform	13.34	73.79	2.94	0.52	0.04	0.16	<0.01	1.11	0.27	<0.01	0.02	92.18
HFO	Colloform	15.55	68.76	5.90	0.33	0.10	0.07	<0.01	0.63	0.53	<0.01	<0.01	91.87
HFO	Colloform	12.35	72.67	2.72	0.31	<0.01	0.06	<0.01	0.53	0.50	<0.01	<0.01	89.14
HFO	Colloform	11.24	75.95	2.13	0.45	<0.01	0.09	<0.01	0.85	0.43	<0.01	0.02	91.16
HFO	Colloform	9.82	74.36	1.80	0.36	<0.01	0.12	<0.01	0.66	0.38	<0.01	<0.01	87.51
HFO	Colloform	11.30	75.48	1.73	0.28	0.06	0.05	<0.01	0.27	0.56	<0.01	<0.01	89.73
HFO	Colloform	12.90	75.48	2.11	0.18	0.04	0.04	<0.01	0.19	0.49	<0.01	<0.01	91.43
HFO	Colloform	9.82	76.23	1.42	0.19	0.04	0.08	<0.01	0.22	0.60	<0.01	<0.01	88.59
HFO	Colloform	15.37	68.31	4.30	0.38	0.11	0.07	<0.01	0.43	0.58	<0.01	<0.01	89.55
HFO	Px-Rim*	25.59	59.15	5.32	0.59	0.27	0.24	<0.01	0.92	0.28	<0.01	0.02	92.38
HFO	Px-Rim*	15.55	67.48	4.43	0.46	0.17	0.41	<0.01	1.14	0.39	<0.01	<0.01	90.03
HFO	Px-Rim*	16.60	66.03	3.78	0.83	0.21	0.21	<0.01	1.19	0.33	<0.01	<0.01	89.18
HFO	Px-Rim*	15.50	65.17	4.11	0.57	0.14	0.36	<0.01	1.09	0.33	<0.01	<0.01	87.27
HFO	Px-Rim*	19.66	64.91	4.41	0.62	0.27	0.37	<0.01	1.03	0.34	<0.01	<0.01	91.62
HFO	Px-Rim*	15.50	69.16	3.39	0.76	0.16	0.12	<0.01	1.24	0.34	<0.01	<0.01	90.67

\*: Hydrous ferric oxide (HFO) formed along pyroxene rim (Px-Rim)

Concrete ponds were constructed to collect overflow from the rock dump sites (Figure 3.2). Therefore, AMD infiltration into the runoff and groundwater could be protected, accordingly. In 2012, surface water in a concrete SFWD pond had pH (6.13) and Eh (-0.012 V); moreover, As concentration was reported at 0.0113 ppm (ERIC, 2012). Based on an Eh-pH diagram for the Fe-As-S-O system (Figure 3.6) (Corkhill and Vaughan, 2009; Craw et al., 2003), arsenite (As<sup>3+</sup>) could be detected with the SFWD pond possibly caused by oxidizing of arsenopyrite. In addition, the Eh/pH values of

surface water in the TSWD and OXWD ponds were also reported at 0.234 V/6.49 and 0.251 V/6.51, respectively (ERIC, 2012), with water samples under such recorded conditions instead being arsenate ( $\text{As}^{5+}$ ) (Figure 3.6). Since the arsenite ( $\text{As}^{3+}$ ) has higher mobility and toxicity than arsenate ( $\text{As}^{5+}$ ) (Smedley and Kinniburgh, 2002), the SFWD pond requires greater care.

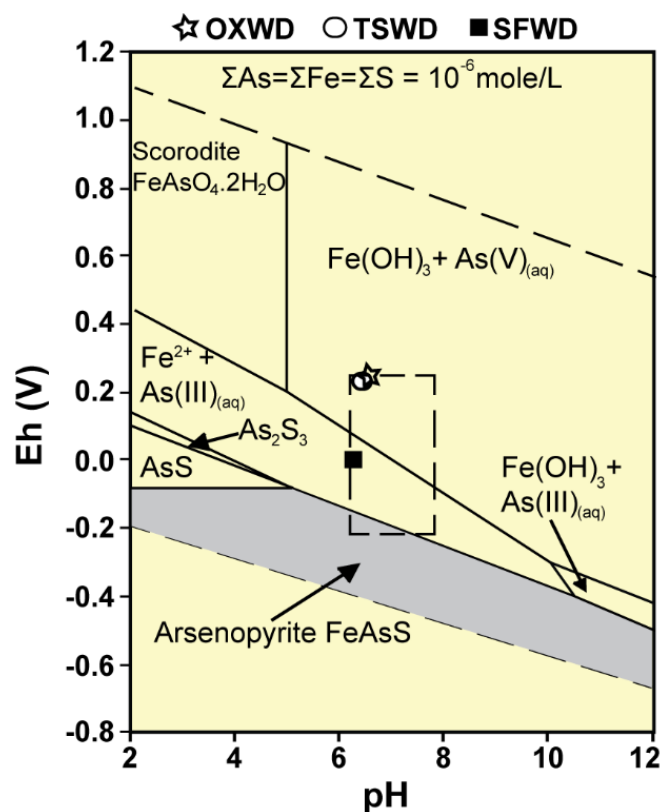


**Figure 3.6** Eh–pH diagram for the Fe–As–S–O system (25 °C, 1 atm) and plots of surface water collected from the ponds around the waste rock dumps (SFWD, TSWD and OXWD, data from ERIC (2012)). The dashed box indicates typical near-surface conditions modified from Craw et al. (2003).

To categorize the class of hazardous waste, the Total Threshold Limit Concentration (TTL) standard announced by the Ministry of Industry Thailand (2006) is applied to these rock wastes. Arsenic contents are recorded in siltstone (TK50: 1017 ppm), gossan (540–810 ppm) and massive sulfide/skarn-sulfide rocks (M15: 18600 ppm and M18: 2470 ppm) exceeding the TTL standard ( $\leq 500$  ppm As). Arsenic may be absorbed by clay mineral in siltstone (Smedley and Kinniburgh, 2002) and by HFO in

gossan (Murciego et al., 2011). On the other hand, arsenopyrite is a major initial source of As in the massive sulfide/skarn-sulfide rocks as found in samples no. M15 and M18. Moreover, Cu contents in gossan (7480 ppm) and massive sulfide (2500–8200 ppm) are high contents, exceeding the TTL standard ( $\leq 2500$  ppm Cu). Therefore, the massive sulfide/skarn-sulfide rocks and gossan must be declared as “hazardous waste”. Trace element (i.e., Ag, As, Cd, Cu, Mn, Pb and Zn) analyses in waste rocks from the study area in comparison with other mine sites are summarized in Table 3.5. Apart from Cu and Mn, the other trace elements found in this study area are lower than other mining sites as shown in the table. However, these waste rocks should be prevented from oxidizing to reduce a risky impact to the ecosystem. It should be notified that distribution of different trace elements (Table 3.5) are clearly related to specific ore deposits and rock types (see also Table 3.1).

Contents of As, Cu and Zn found in most sandstone/siltstone waste rocks from all dump sites appear to be higher than the average of background levels of sandstone, for instance, 1–13 ppm As (Smedley and Kinniburgh, 2002),  $\leq 57$  ppm Cu and 15–95 ppm Zn suggested by Turekian and Wedepohl (1961) and Rosler and Lange (1972). Therefore, the sandstone/siltstone waste rocks are of environmental concern. Although, these rock types have relatively low total As concentrations, they can be easily leached under acidic condition (0.024–0.172 ppm As) reported by Klongsamran et al. (2014).

The gossan samples have higher total concentrations and higher leachable contents of As, Cu, Mn and Zn than the other waste rocks as reported by Klongsamran et al. (2014). Hence, the gossan samples are unstable and risky to the environment, particularly in AMD condition. Acidic effluents ( $\text{pH} < 2$ ) can dissolve Fe-oxyhydroxides from the gossan and release high amounts of toxic elements (Romero et al., 2006). On the other hand, the massive sulfide and skarn waste rocks are quite stable even under high acidic condition (Klongsamran et al., 2014).

**Table 3.5** Summary of trace elements (mg/kg and wt.%) in waste rocks from the study area and other mine sites.

Location	Trace elements (mg/kg)							Reference
	Ag	As	Cd	Cu	Mn	Pb	Zn	
<b>Thailand</b>								
Phu Thap Fah								The present study
- <i>Massive/skam-sulfide</i>	1.30	70.7	0.20	3809	633	5.70	45.2	
- <i>Gossan</i>	1.40	424	0.28	2395	2337	6.75	204	
Chatree gold mine	0.57	17.57	0.23	95.91	1169	10.67	41.66	Sutthirat and Changul (2012)
<b>Spain</b>								
Iberian Pyrite Belt (IPB)								
- <i>Gossan</i>	8.49	1331	0.14	1246	31	841	-	Hunt et al. (2016)
- <i>Country rock</i>	-	1250	-	-	-	2700	-	Álvarez-Valero et al. (2008)
<b>United States</b>								
Prince William Sound, Alaska	46.95	1594	35.73	10%	560	877	-	Koski et al. (2008)
<b>Peru</b>								
Cerro de Pasco, Central Andes	-	2030	23	1100	2300	1.10%	0.87%	Smuda et al. (2007)
<b>Australia</b>								
Webbs Consols mine	357	12.38%	254	1130	1292	6.29%	3.99%	Ashley et al. (2004)

Based on X-ray mapping, arsenic and copper are found in goethite and HFO (Figure 3.5). Arsenic can be coprecipitate in goethite as arsenate ( $As^{5+}$ ) (Asta et al., 2009; Basu and Schreiber, 2013; Carbone et al., 2012), whereas Cu can substitute  $Fe^{3+}$  in the goethite structure (Carbone et al., 2012; Gerth, 1990) or be adsorbed on the goethite surface (Peacock and Sherman, 2004). The hydrous ferric oxide (HFO) can adsorb very high contents of As and Cu because of its poor crystalline structure (Cornell and Schwertmann, 2003; Lottermoser, 2010; Majzlan et al., 2007), small particle size, large surface area and high sorption capacity (Majzlan et al., 2007; Mohan and Pittman, 2007; Wilkie and Hering, 1996). In addition, many previous researchers, e.g., Murciego et al. (2011) and Rancourt et al. (2001), suggested that natural hydrous ferric oxide (HFO) usually has high potential to absorb arsenic, so called As-HFO. Subsequently, the observed high concentrations of these concerned elements can also be seen in the whole-rock geochemical analyses of gossan samples (see Table 3.7).

Nevertheless, the structure of HFO can be transformed to goethite by reprecipitation (Cornell and Schwertmann, 2003). During these processes, unit cells of iron oxide particle will be enlarged and led to reduction of adsorption sites; consequently, As in the HFO becomes more easily leachable and tends to be released (Majzlan et al., 2007). Therefore, gossan should also be considered as a source of As contamination in the long term.

### 3.6 Conclusions and recommendations

According to mineralogical and geochemical characteristics, the massive sulfide and skarn-sulfide rocks are possibly the main source of AMD. The massive sulfide, skarn-sulfide and gossan rocks appear to be risky waste rocks. They are classified as hazardous wastes which contain high contents of As, Cu, Mn and Zn; however, only the gossan rocks have high leachable potential under AMD. X-ray mapping can be applied to investigate the distribution of toxic elements found in waste rocks, particular gossan in this case. These microanalyses may lead to understanding of the natural relationship between toxic elements and their host minerals; then, prevention of toxic contamination can be planned properly.

After the mine closure, at least four waste dump sites were left in this area (i.e., SFWD, TSWD and OXWD-1 and OXWD-2). The SFWD and TSWD sites should be of concern for sulfide oxidation because they have massive sulfide and skarn-sulfide rocks, which contain high contents of heavy metals. To prevent an oxidizing reaction of the sulfide minerals, dry cover is suggested by Lottermoser (2010), using a store-and-release cover method modified from Williams et al. (1997). Moreover, concrete ponds were constructed to collect overflow rainfall from these dumps. Therefore, pH of the water in the ponds should be routinely monitored. If AMD occurs, the concentration of As, Cu, Mn and Zn in the surface water and groundwater must be monitored more often.

### 3.7 Electronic Supplementary Material A: Petrographic Description

All types of waste rock were investigated under polarizing microscope for petrographic description which is reported herein. Sandstone mainly consists of quartz (~60%) with minor contents of K-feldspar, biotite and rock fragment with an average grain size of about 1 mm in diameter (Figure 3.7a). Siltstone is composed of 70% quartz with fine particle size (< 0.05 mm in diameter) in association mainly with clay minerals. The granodiorite consists of 40–50% quartz, 15–20% plagioclase, 5–10% K-feldspar, 10–15% hornblende and 5% biotite (Figure 3.7b). The skarn rock is mainly composed of 50% pyroxene (diopside), 40% garnet (andradite) and 10% calcite (Figure 3.7c); some garnet grains are replaced by sulfide minerals (pyrrhotite or chalcopyrite). The skarn-sulfide rock mainly consists of pyrrhotite (50%), chalcopyrite (20%), arsenopyrite (10%) and euhedral pyroxene embedding in these sulfide minerals (Figure 3.7d), with minor marcasite intergrowth with pyrite and pyrrhotite and tremolite inclusions. The massive sulfide rock mainly consists of pyrrhotite (80%) and chalcopyrite (20%) (Figure 3.7e). The gossan samples are composed of 30–40% goethite proved by Raman and FTIR patterns (Figure 3.8), and 40–50% quartz with minor pyrrhotite/chalcopyrite inclusions (Figure 3.7f); moreover, gypsum and oxidized silicate minerals are also found in gossan sample (Figure 3.7g). In addition, the gossan is also consisted of oxidized pyroxene (Ox-Px) and amorphous hydrous ferric oxide (HFO) confirmed by FTIR pattern (Figure 3.8b) that was found along pyroxene rim and sometimes in vein (Figure 3.7h). The last rock type, limestone, is mainly composed of calcite with size of about 0.2 to 1 mm in diameter forming triple junction which is indicator of recrystallization.

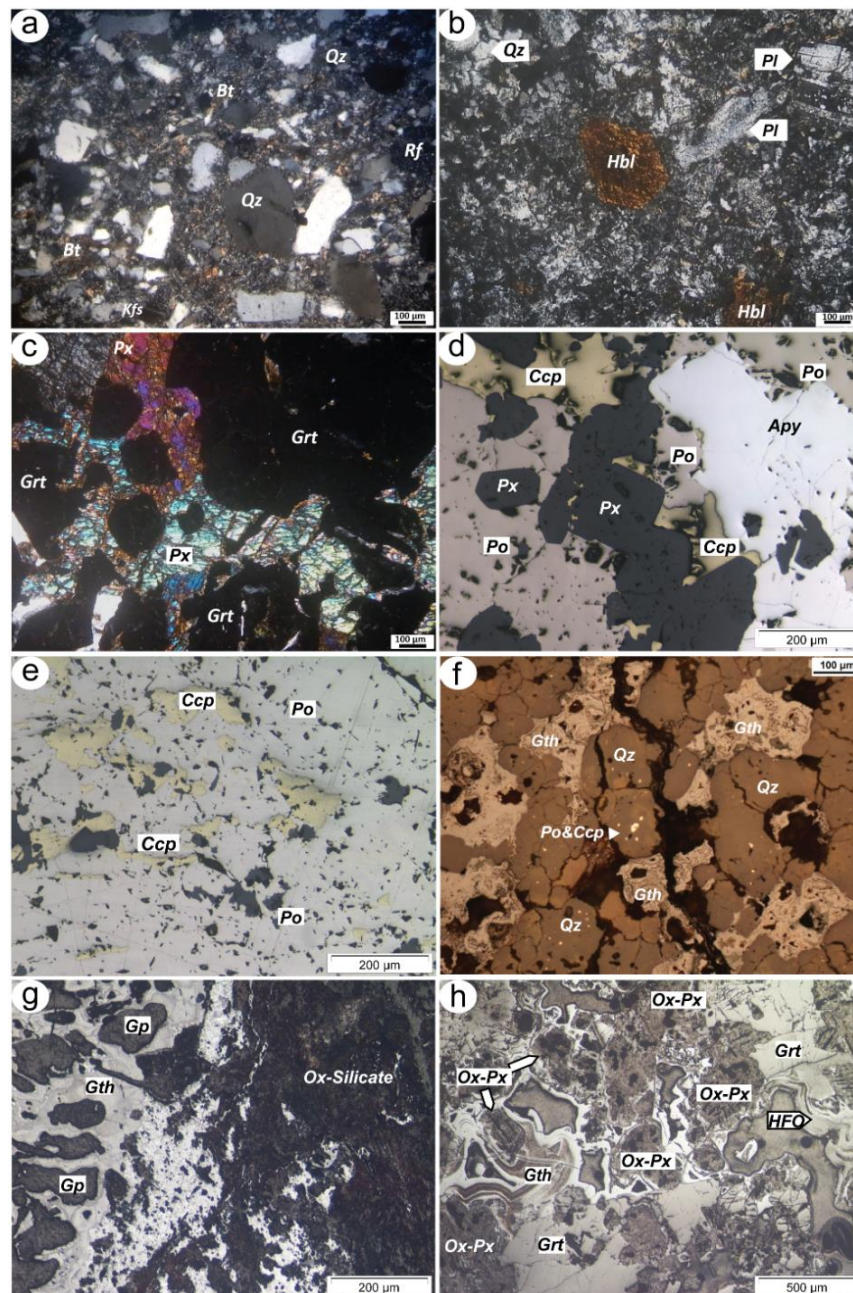


**Figure 3.7** Photomicrographs under transmitted-light of (a) fine-grained sandstone, (b) diorite and (c) garnet-pyroxene skarn rock. Photomicrographs under reflected-light of (d) skarn-sulfide, (e) massive sulfide, (f) gossan showing colloform goethite and sulfide minerals, (g) gossan showing goethite enclosing gypsum and (h) gossan presenting some garnets with relic pyroxene surrounded by goethite or hydrous ferric oxide. Abbreviations are Qz: quartz, Bt: biotite, Rf: rock fragment, Kfs: K-feldspar, Hbl: hornblende, Pl: plagioclase, Px: pyroxene, Grt: garnet, Gth: goethite, Apy: arsenopyrite, Po: pyrrhotite, Ccp: chalcopyrite, Gp: gypsum, Ox-Silicate: oxidized-silicate mineral, Ox-Px: oxidized-pyroxene and HFO: hydrous ferric oxide.

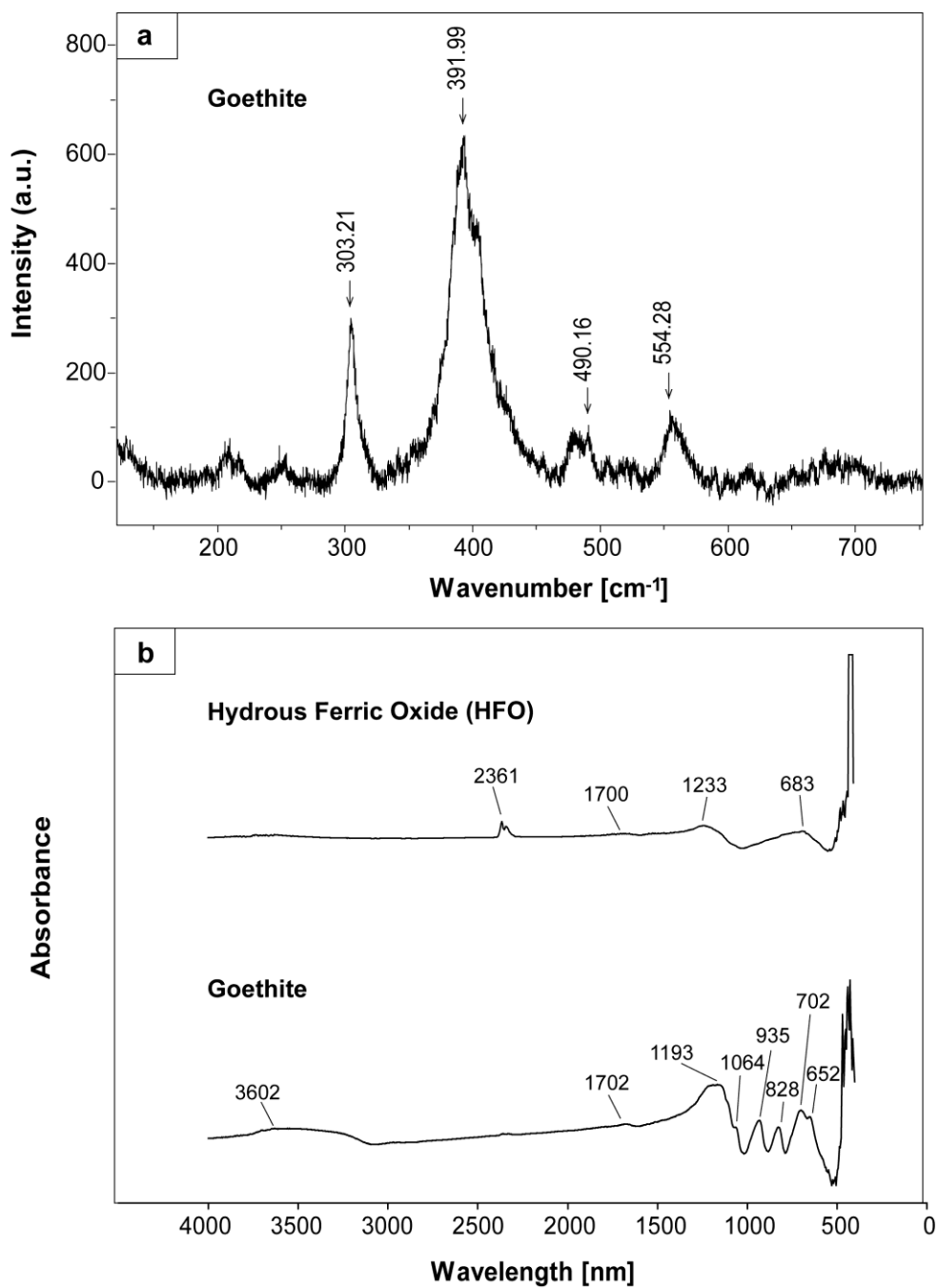


**Figure 3.8** Representative (a) Raman pattern of crystalline goethite and (b) FTIR patterns of hydrous ferric oxide (HFO) (top) and goethite (bottom)



### 3.8 Electronic Supplementary Material B: Whole-rock Geochemistry

The massive sulfide rocks have very high contents of  $\text{FeO}_t$  (37–41 wt.%) and  $\text{SO}_3$  (35–46 wt.%); moreover, they also have high Cu content (2400 to 8200 ppm) but low As content ( $\leq 2$  ppm). Except the sample no. M15 (18600 ppm As) and TK61 (413 ppm As), they were collected from the main pit and the TSWD, respectively. The high As contents in the last sample is clearly caused by occurrence of arsenopyrite.

The skarn-sulfide rocks have moderately high  $\text{FeO}_t$  (25–35 wt.%),  $\text{SO}_3$  (17–28 wt.%) and Cu (1300–2500 ppm) with low As contents ( $\leq 4$  ppm); except sample no. M18 taken from the main pit contains 2474 ppm As because it is composed of arsenopyrite (Figure 3.7d).

Skarn rocks show moderately high CaO content (14–39 wt.%) with 9–25 wt.%  $\text{FeO}_t$ , 3127–4775 ppm Mn, 2–470 ppm As and wide range of Cu (9–7400 ppm). The As and Cu contents in these skarn samples clearly relate to their mineral compositions, arsenopyrite and chalcopyrite in particular.

In addition, some toxic elements are found in sandstone/siltstone consisting of 6–1071 ppm As, 0.2–0.9 ppm Cd, 13–35 ppm Co, 53–86 ppm Cr, 11–241 ppm Cu, 2–12 ppm Hg, 96–560 ppm Mn, 19–40 ppm Ni, 1–19 ppm Pb and 32–380 ppm Zn.

Diorite is composed of 55–61 wt.%  $\text{SiO}_2$ , 15–18 wt.%  $\text{Al}_2\text{O}_3$ , 2–25 ppm As, 0.2–0.7 ppm Cd, 24–29 ppm Co, 17–90 ppm Cr, 0.4–13 ppm Hg, 560–890 ppm Mn, 9–30 ppm Ni, 5–20 ppm Pb and 61–300 ppm Zn.

**Table 3.6** Major and minor oxide contents (wt.%) of waste rocks from the studied gold mine in northeastern Thailand, analyzed from glass beads and some pressed powders using XRF.

Rock type	Sample location	Sample no.	SiO <sub>2</sub>	Al <sub>2</sub> O <sub>3</sub>	CaO	FeO <sub>t</sub>	K <sub>2</sub> O	MgO	MnO	Na <sub>2</sub> O	P <sub>2</sub> O <sub>5</sub>	TiO <sub>2</sub>	SO <sub>3</sub>	LOI
Sandstone/ siltstone	OXWD	TK16	58.75	13.06	4.85	11.14	2.02	3.24	0.06	0.48	2.07	0.61	LD	2.83
	OXWD	TK19	63.62	14.75	2.22	7.31	2.55	2.10	0.06	1.17	0.15	0.73	LD	4.21
	TSWD	TK27	63.48	12.67	8.66	6.38	2.66	1.97	0.08	1.71	0.10	0.60	LD	1.18
	TSWD	TK29	66.77	16.13	4.23	2.42	2.90	1.49	0.03	3.16	0.14	0.79	LD	1.15
	Main Pit	M6	64.67	15.14	10.13	4.20	0.51	1.78	0.02	0.87	0.10	0.71	LD	1.47
	Main Pit	M27	61.72	14.87	5.89	4.98	2.99	2.66	0.10	3.15	0.11	0.60	LD	2.34
	Main Pit	M28	60.19	16.80	6.33	6.74	2.62	2.33	0.04	1.47	0.14	0.66	LD	1.94
	Main Pit	M39	66.29	15.64	3.86	3.36	1.95	2.00	0.02	3.04	0.14	0.74	LD	2.23
Diorite	OXWD	TK8	56.81	16.80	6.91	8.04	2.08	3.34	0.08	2.86	0.14	0.92	LD	1.82
	OXWD	TK9	58.96	16.59	7.01	7.47	1.51	2.82	0.11	2.76	0.14	0.80	LD	1.55
	OXWD	TK11	60.94	15.16	5.80	6.04	2.40	2.90	0.10	2.83	0.19	0.71	LD	2.53
	TSWD	TK25	60.13	15.03	5.77	6.07	2.60	3.06	0.10	2.77	0.18	0.70	LD	2.85
	TSWD	TK26	60.05	15.21	5.84	6.07	2.50	3.02	0.10	2.89	0.18	0.71	LD	2.71
	Main Pit	M1	59.20	15.31	6.69	6.62	2.18	3.25	0.11	2.32	0.17	0.72	LD	2.70
	Main Pit	M2	59.72	15.41	5.90	6.44	2.42	3.29	0.10	2.56	0.17	0.72	LD	2.56
	Main Pit	M25	55.07	17.75	6.21	8.62	1.29	4.11	0.11	1.87	0.22	0.87	LD	2.87
Limestone	OXWD	TK6*	0.59	LD	54.20	1.32	LD	2.65	LD	0.31	LD	LD	LD	-
	OXWD	TK7*	1.86	0.86	53.70	0.45	LD	2.14	LD	LD	LD	LD	LD	-
	TSWD	TK53*	1.40	0.68	56.40	0.42	LD	1.70	LD	LD	LD	LD	LD	-
Gossan	OXWD	TK20	47.93	5.07	15.87	22.31	0.06	4.72	0.66	LD	0.13	0.12	0.29	1.11
	OXWD	TK21	35.34	1.75	8.94	35.22	0.03	0.30	0.06	LD	LD	0.07	13.18	6.10
	OXWD	TK22	38.60	3.05	12.82	25.06	0.03	2.67	0.32	LD	0.17	0.14	1.80	3.61
	TSWD	TK23	26.31	0.72	0.32	48.48	LD	0.04	0.02	LD	0.46	0.02	1.34	9.25
Massive sulfide	SFWD	TK31*	3.51	0.35	4.29	40.18	LD	0.20	0.04	LD	LD	LD	44.16	7.32
	SFWD	TK32*	4.44	0.31	2.75	39.82	LD	0.22	0.04	LD	LD	LD	45.94	7.03
	SFWD	TK33*	4.94	0.29	2.78	39.51	LD	0.32	0.04	LD	LD	LD	43.74	7.15
	Main Pit	M13*	1.96	0.04	0.93	40.95	LD	0.19	0.04	LD	LD	LD	45.10	9.47
	Main Pit	M14*	2.75	0.04	1.49	36.96	LD	0.26	0.07	LD	LD	LD	34.48	15.19
	Main Pit	M15*	0.15	LD	0.37	37.36	LD	0.13	LD	LD	LD	LD	38.04	17.66

\*: analyzed by pressed powder samples

LD: lower than detection limit

-: not analyzed

**Table 3.6 (cont.)** Major and minor oxide contents (wt.%) of waste rocks from the studied gold mine in northeastern Thailand, analyzed from glass beads and some pressed powders using XRF.

Rock type	Sample location	Sample no.	SiO <sub>2</sub>	Al <sub>2</sub> O <sub>3</sub>	CaO	FeO <sub>t</sub>	K <sub>2</sub> O	MgO	MnO	Na <sub>2</sub> O	P <sub>2</sub> O <sub>5</sub>	TiO <sub>2</sub>	SO <sub>3</sub>	LOI
	SFWD	TK37*	18.05	8.06	4.22	35.06	0.10	1.63	LD	1.97	0.40	0.33	27.46	-
Skarn-sulfide	Main Pit	M18*	10.75	2.44	6.33	31.56	LD	1.07	0.11	LD	0.07	0.09	27.39	13.14
	Main Pit	M36*	18.06	4.68	5.40	24.69	0.07	1.77	0.10	0.99	0.17	0.17	17.33	14.09
	Main Pit	M37*	23.26	6.51	6.87	26.45	0.08	2.50	0.11	1.54	0.24	0.19	22.41	5.97
Skarn	Main Pit	M16*	36.16	6.87	18.87	19.95	LD	7.00	0.65	LD	0.17	0.29	0.37	4.34
	Main Pit	M17*	31.22	9.01	23.55	14.90	0.04	3.51	0.48	LD	0.25	0.83	0.06	5.35
	TSWD	TK64	41.90	4.19	28.31	19.15	LD	3.27	0.54	LD	0.03	0.08	LD	1.49
	SFWD	TK41*	33.43	2.01	28.62	18.19	LD	2.50	0.31	LD	0.16	LD	0.28	-
	SFWD	TK44*	35.21	14.15	14.09	11.18	1.02	1.92	0.44	1.94	0.15	0.58	1.68	-
	SFWD	TK42	39.57	2.52	29.31	24.75	0.01	1.58	0.42	LD	0.04	0.05	LD	0.42

\*: analyzed by pressed powder samples

LD: lower than detection limit

-: not analyzed

**Table 3.7** Trace elements (ppm except Au in ppb) in the waste rocks from the studied gold mine in northeastern Thailand, analyzed by ICP-MS using solution samples and some pressed powder samples analyzed by XRF.

Rock type	Sample location	Sample no.	Ag	As	Au	Cd	Co	Cr	Cu	Hg	Mn	Ni	Pb	Zn
Sandstone/ siltstone	OXWD	TK14	0.3	13	1.1	0.3	29	86	90	8.8	136	29	4	34
	OXWD	TK15	0.2	6	1.9	0.2	35	57	241	11.9	96	22	2	293
	OXWD	TK16	0.2	44	1.5	0.5	28	80	150	2.4	484	40	3	347
	OXWD	TK17	0.3	19	2.1	0.5	21	80	21	7.4	550	21	3	372
	OXWD	TK19	0.3	22	0.9	0.9	13	59	25	2.6	324	19	4	375
	TSWD	TK24	0.3	63	0.9	0.5	28	53	175	2.3	311	31	4	339
	TSWD	TK29	0.4	115	0.9	0.4	28	84	101	5.8	230	27	19	293
	SFWD	TK46	0.2	11	1.5	0.3	16	77	11	2.2	553	25	3	312
	TSWD	TK50	0.2	1017	1.7	0.4	16	66	140	1.9	266	25	1	293
TSWD	TK51	0.5	17	2.0	0.2	14	71	78	1.8	559	32	7	32	
Diorite	OXWD	TK8	0.2	25	1.8	0.2	29	17	50	7.5	559	9	5	62
	OXWD	TK9	0.2	10	1.0	0.2	27	22	28	12.6	887	9	6	61
	OXWD	TK10	0.5	3	1.3	0.3	26	89	19	7.6	771	29	12	66
	OXWD	TK11	0.4	2	0.7	0.7	34	87	32	0.4	732	26	14	313
	TSWD	TK25	0.4	2	1.0	0.2	24	87	30	0.4	790	26	20	298
	TSWD	TK26	0.5	2	1.4	0.4	26	90	30	4.0	813	27	15	70
Limestone	OXWD	TK6	0.2	2	0.4	0.2	3	12	1	1.5	635	4	5	597
	OXWD	TK7	0.1	2	0.2	0.5	3	8	1	1.0	171	3	3	38
	TSWD	TK53	0.2	1	0.5	0.2	2	6	3	0.5	496	5	2	31
Gossan	OXWD	TK20	0.4	334	1.1	0.2	12	73	519	7.1	4137	37	4	99
	OXWD	TK21	0.4	810	1.3	0.1	12	69	1081	8.6	1439	5	4	45
	OXWD	TK22	0.3	541	0.5	0.4	13	65	498	2.4	3457	22	12	353
	TSWD	TK23	4.5	11	8.4	0.4	60	35	7480	9.5	316	26	7	320
Massive sulfide	SFWD	TK31*	<20	<20	<20	<20	<20	170	5349	<20	310	<20	<20	<20
	SFWD	TK32*	<20	<20	<20	<20	<20	209	5565	<20	310	<20	<20	<20
	SFWD	TK33	1.2	2	1.3	0.2	183	14	2835	8.0	264	63	2	43
	SFWD	TK39	1.0	2	1.4	0.2	137	23	4909	2.5	1516	50	5	64
	Main Pit	M13*	<20	<20	<20	<20	<20	<20	4460	<20	310	<20	<20	<20
	Main Pit	M14*	<20	<20	<20	<20	<20	<20	4544	<20	542	<20	<20	<20
	Main Pit	M15*	<20	18611	<20	<20	<20	<20	4068	<20	<20	<20	<20	<20
	TSWD	TK59	1.6	1	1.3	0.2	114	8	3176	1.2	292	58	5	36
	TSWD	TK60	2.5	2	88.7	0.3	39	15	8200	6.6	1478	3	7	54
TSWD	TK61	0.7	413	2.3	0.3	58	5	2430	1.1	247	6	10	37	

\*: pressed powder samples analyzed by XRF

\*\* : Total Threshold Limit Concentration of hazardous waste announced by the Ministry of Industry Thailand (2006)

**Table 3.7 (cont.)** Trace elements (ppm except Au in ppb) in the waste rocks from the studied gold mine in northeastern Thailand, analyzed by ICP-MS using solution samples and some pressed powder samples analyzed by XRF.

Rock type	Sample location	Sample no.	Ag	As	Au	Cd	Co	Cr	Cu	Hg	Mn	Ni	Pb	Zn
	SFWD	TK37	0.8	4	2.8	0.2	81	58	1298	5.5	476	61	5	37
Skarn-sulfide	Main Pit	M18*	<20	2474	<20	<20	<20	<20	2055	<20	852	<20	<20	<20
	Main Pit	M36*	<20	<20	<20	<20	<20	<20	1963	<20	775	<20	<20	<20
	Main Pit	M37*	<20	<20	<20	<20	<20	344	2478	<20	852	<20	<20	<20
Skarn	TSWD	TK63	1.2	474	76.3	0.2	10	31	16	3.5	3407	3	44	52
	TSWD	TK64	1.2	3	3.0	0.4	10	41	972	5.6	4775	8	5	145
	TSWD	TK65	0.6	84	3.4	0.2	9	60	9	7.8	4188	10	3	49
	SFWD	TK40	2.4	5	6.3	0.7	40	9	7374	16.8	3127	16	3	140
	SFWD	TK41	0.3	8	2.0	0.3	20	8	581	8.5	3518	2	3	72
	SFWD	TK44	0.2	2	0.5	0.6	15	87	377	2.9	4481	23	11	119
	SFWD	TK42*	<20	<20	<20	<20	<20	91	1394	<20	3254	<20	<20	63
**TTLc			500	500	-	100	8000	500	2500	20	-	2000	1000	5000

\*: pressed powder samples analyzed by XRF

\*\*.: Total Threshold Limit Concentration of hazardous waste announced by the Ministry of Industry Thailand (2006)

CHAPTER 4  
MINERALOGICAL AND CHEMICAL CHARACTERISTICS OF GOSSAN WASTE ROCKS  
FROM A GOLD MINE IN NORTHEASTERN THAILAND

Thitiphan AssawincharoenkiJ<sup>a,\*</sup>, Christoph Hauenberger<sup>b</sup>, Chakkaphan Sutthirat<sup>a,c</sup>

<sup>a</sup> Department of Geology, Faculty of Science, Chulalongkorn University, Bangkok 10330, Thailand

<sup>b</sup> NAWI Graz Geocenter, Petrology and Geochemistry, University of Graz, Universitätsplatz 2, 8010, Graz, Austria

<sup>c</sup> Research Program of Toxic Substance Management in the Mining Industry, Center of Excellence on Hazardous Substance Management (HSM), and Research Unit of Site Remediation on Metals Management from Industry and Mining (Site Rem), Environmental Research Institute, Chulalongkorn University, Bangkok 10330, Thailand

\* Corresponding author

Applied Environmental Research 39(2) (2017): 1-13

## Abstract

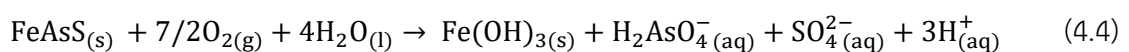
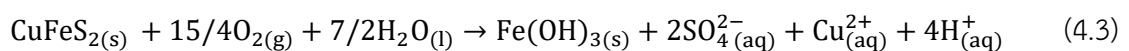
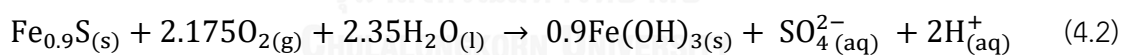
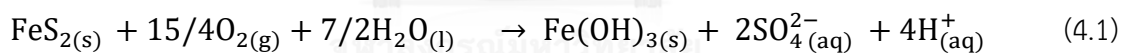
The mineralogical and chemical compositions of various ochre gossans from a gold mine in northeastern Thailand were investigated, including some heavy metals and other toxic elements. Mineralogical characteristics were carried out using X-Ray Diffractometer (XRD) and Scanning Electron Microscope (SEM) whereas chemical compositions were analyzed using Electron Probe Micro-Analyzer (EPMA). These ochre gossans can be classified, initially based on Munsell color, into five types: type-I (pale-yellow color), type-II (brownish-yellow color), type-III (yellowish-brown color), type-IV (dusky-red color) and type-V (red color). The primary silicate minerals (i.e., quartz, garnet, epidote and amphibole) are found in type -I, -II, -III and -IV. They appear to be composed of skarn rock. On the other hand, the secondary minerals (i.e., goethite, jarosite, ankerite, montmorillonite, magnetite, gypsum and secondary quartz) are observed in types-II, -III, -IV and -V. As and Cu are found crucially in types-III, -IV and -V in which both elements can be adsorbed by goethite and/or jarosite. As the result, the gossan rocks in this area are natural adsorbents with high potential to reduce As and Cu contamination into the ecosystem. Therefore, the gossan, a natural attenuation material, is recommended for site remediation because of its low cost and local abundance. Feasibility studies should be conducted to further investigate the potential.

จุฬาลงกรณ์มหาวิทยาลัย  
CHULALONGKORN UNIVERSITY

**Keywords:** gossan, adsorption, toxic element, Thailand

#### 4.1 Introduction

Gossan rocks are commonly associated with massive sulfide ore deposits which have undergone erosion and oxidation processes during uplifting and exposure to the surface (Lottermoser, 2010; Romero et al., 2006; Smuda et al., 2007; Valente et al., 2013; Velasco et al., 2013). Consequently, gossans usually exhibit a mushroom-like morphology (Assawincharoenkij et al., 2017; Velasco et al., 2013). In general, the massive sulfides mainly contain pyrite ( $\text{FeS}_2$ ), pyrrhotite ( $\text{Fe}_{1-x}\text{S}$ ), chalcopyrite ( $\text{CuFeS}_2$ ) and arsenopyrite ( $\text{FeAsS}$ ) (Álvarez-Valero et al., 2008; Ashley et al., 2004; Carrillo-Chávez et al., 2014; Ferreira da Silva et al., 2015; Hunt et al., 2016; Koski et al., 2008; Rodmanee, 2000). Equations 4.1-4.4 present the oxidation reactions of (4.1) pyrite, (4.2) pyrrhotite, (4.3) chalcopyrite and (4.4) arsenopyrite when they react with oxygen and water (Lottermoser, 2010). The resulting secondary minerals generated include as Fe-oxyhydroxide (goethite:  $\alpha\text{-FeOOH}$ ), hydrous ferric oxide (HFO), oxides (hematite:  $\text{Fe}_2\text{O}_3$ , magnetite:  $\text{Fe}_3\text{O}_4$ ), and oxy-sulfates (schwertmannite:  $\text{Fe}_8\text{O}_8(\text{OH})_6(\text{SO}_4) \cdot n\text{H}_2\text{O}$ , jarosite:  $\text{KFe}_3(\text{SO}_4)_2(\text{OH})_6$ ) (Anawar, 2015; Atapour and Aftabi, 2007; Campbell and Nordstrom, 2014; Lindsay et al., 2015; Lottermoser, 2010; Lottermoser, 2011), which are mineral compositions of the gossan rocks (Assawincharoenkij et al., *in prep.*; Atapour and Aftabi, 2007; Romero et al., 2006; Valente et al., 2013; Velasco et al., 2013; West et al., 2009).



The gossan rocks can adsorb toxic elements (including As, Cu, Cd, Fe, Hg, Mn, Pb and Zn) (Assawincharoenkij et al., *in prep.*; Atapour and Aftabi, 2007; Romero et al., 2006; Velasco et al., 2013) that are possibly released during oxidizing process of the sulfide mining. On the other hand, these toxic elements are naturally attenuated by schwertmannite, K-jarosite and goethite via adsorption and co-precipitation (Webster et al., 1998). Therefore, gossan rocks may be useful as attenuation material for site remediation (Majzlan et al., 2007).



In Thailand, gold mining activities have raised numerous environmental and health concerns among local communities. The study area is a gold mine in Loei province, northeastern Thailand. Geologically, this area comprises sandstone, siltstone, limestone, granodiorite, skarn, massive sulfide/skarn-sulfide and gossan (Assawincharoenkij et al., *in prep.*; ERIC, 2012; Rodmanee, 2000). The gossan rocks have potential to carry heavy metals/metalloids such as arsenic (up to 810 mg kg<sup>-1</sup>), copper (up to 7,500 mg kg<sup>-1</sup>), lead (4–12 mg kg<sup>-1</sup>) and zinc (45–350 mg kg<sup>-1</sup>) (Assawincharoenkij et al., *in prep.*). They may be classified as ore-bearing or ore-barren gossan rocks (Assawincharoenkij et al., 2017; Khon Kaen University Report, 2009; Rodmanee, 2000). The aim of this study was to find out characteristics of various ocher materials including their mineralogical and chemical compositions as well as toxic elements, and also to determine the potential of ocher materials as a natural adsorbent for further study.

#### 4.2 Materials and methods

Gossan samples were collected from the waste rock dump site located in a gold mine in the northeastern Thailand (Figure 4.1). These samples were then classified, initially based on Munsell (2010) soil's color. Each sample may have different color zones which were selected for laboratory analysis, as shown in Figure 4.2.

The mineral composition of the samples (types I–V) was determined using a Bruker AXS D8 X-Ray Diffractometer (XRD) based at the NAWI Graz Geocenter, Petrology and Geochemistry, University of Graz, Austria. The operational conditions were set at 40 kV and 40 mA. Micromorphology and texture of the samples were determined by a Scanning Electron Microscope (SEM) (JEOL model LSM-6480LV) at the Faculty of Science, Chulalongkorn University. The operating accelerating voltage was set at 15 kV for capturing images of the samples.



**Figure 4.1** Photographs of mining activities in the study area such as (a) gold processing plant, (b) mining pit showing location of dumped waste rocks of ore-barren gossan in (c) and (d) the dump sites.

The number of powder samples collected from the gossans was lower than 0.5 g, and thus insufficient for normal analyses by X-Ray Fluorescence (XRF) spectrometry, which requires a powder sample of at least 1 g. Therefore, the chemical compositions of these samples were analyzed using a JEOL JXA-8800 Electron Probe Micro-Analyzer (EPMA) at the Department of Geology, Chulalongkorn University. Each sample was ground ( $\leq 1 \mu\text{m}$ ) using an agate mortar to homogenize the small amount of sample. These powdered samples were then sprinkled on a carbon tape and then were carbon coated before EPMA analysis. A probe current of 25 nA with a beam spot size of  $5 \mu\text{m}$  were set up with an accelerating voltage of 15 kV for analysis. The detection limit of all elements was 0.05%.

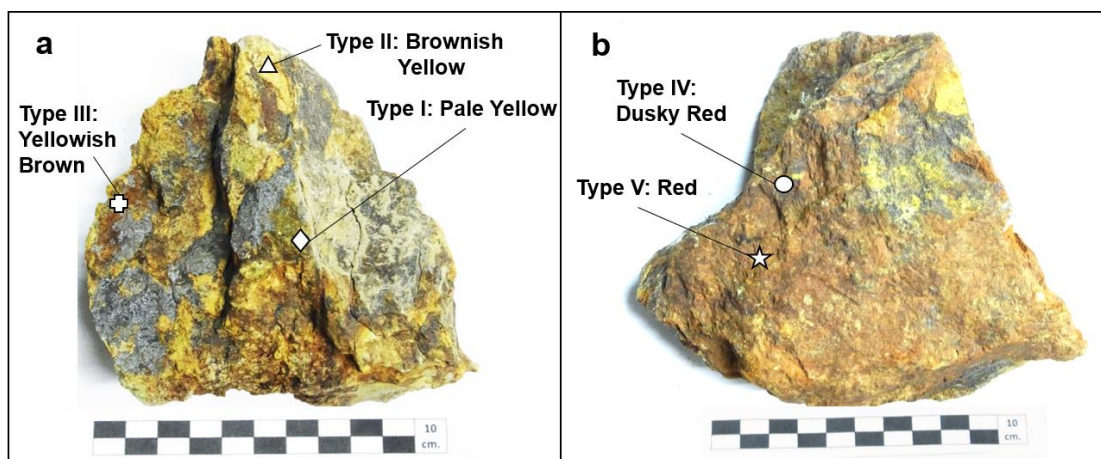


**Figure 4.2** Photographs of gossan rock samples and selected areas for investigation. (a) sample-1 includes type-I: pale yellow, type-II: brownish yellow, and type-III: yellowish brown. (b) sample-2 includes type-IV: dusky red and type-V: red.

## 4.3 Results

### 4.3.1 Mineral texture and assemblage

The ore-barren gossans, dumped as waste rock, were investigated because they contained high levels of toxic elements. These gossans present slightly variable ochre colors ranging from yellow to dark red. These colors are related to the mineral compositions and original rock type. The samples, representatively shown in Figure 4.2, are classified as type-I (pale yellow color: 5Y 8/4), type-II (brownish yellow color: 10YR 6/8), type-III (yellowish brown color: 10YR 5/8), type-IV (dusky red color: 10R 3/4) and type-V (red color: 10R 4/6). The color codes were allocated following the Munsell (2010) soil color standard.

Micromorphology of types-I and -II present many mineral crystals with an average grain size of 2 to 10  $\mu\text{m}$  (Figures 4.3a, b); this was clearly confirmed by XRD patterns (Figures 4.4a, b). They significantly show lath-shaped crystals of primary quartz (Figures 4.3a, b). On the other hand, types-III, -IV and -V were generally of flaky texture, containing very fine-grained materials of goethite and secondary quartz, with grain size smaller than 1  $\mu\text{m}$  (Figures 4.3c-e). In addition, different mineral assemblages are also identified using XRD (see Figure 4.4). Color and mineral assemblage of these sample types are summarized in Table 4.1. Abbreviations of mineral names were suggested by Whitney and Evans (2010).

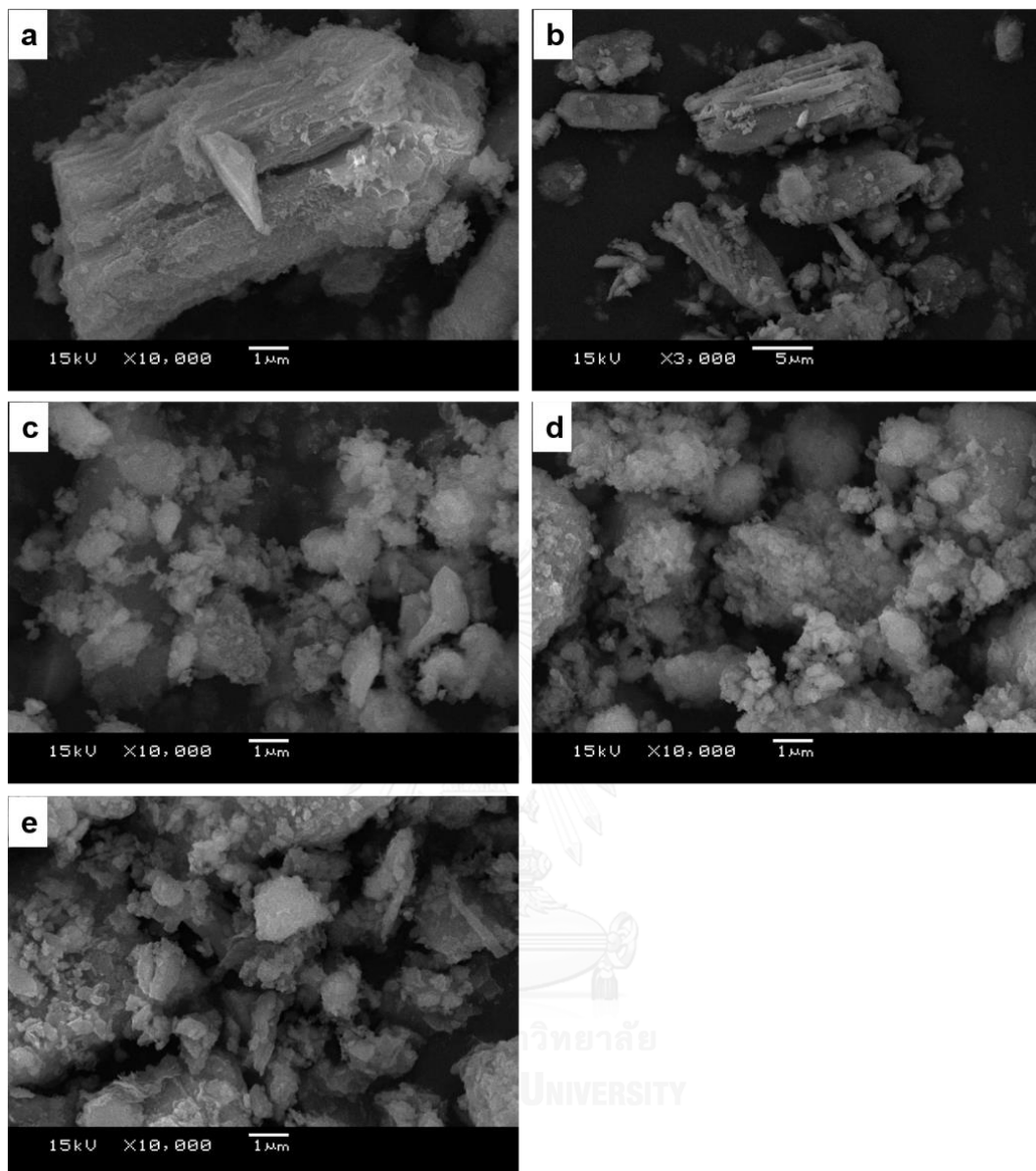


**Figure 4.3** Back Scattering Electron (BSE) images taken from SEM showing micromorphology of: (a) type-I and (b) type-II showing lath-shaped crystals of primary quartz; (c) type-III, (d) type-IV and (e) type-V showing flaky-shaped microcrystalline of goethite and secondary quartz (microcrystalline quartz).

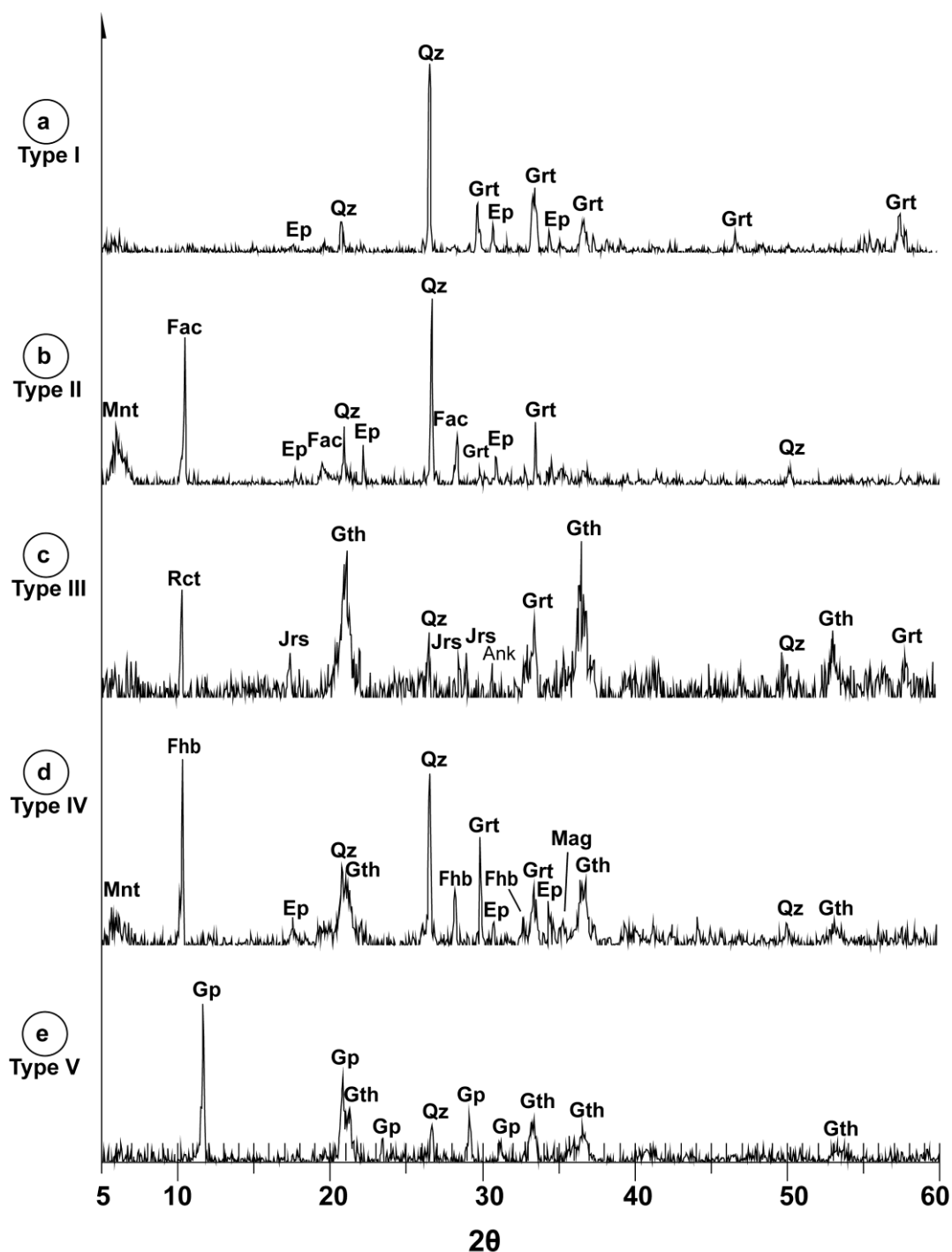


**Figure 4.4** XRD patterns of the samples (a) type-I, (b) type-II, (c) type-III, (d) type-IV and (e) type-V collected selectively from the gossan rocks. Abbreviations of mineral were suggested by Whitney and Evans (2010) i.e., Qz (quartz), Ep (epidote), Grt (garnet), Amp (amphibole), Mnt (montmorillonite), Gth (goethite), Jrs (jarosite), Ank (ankerite), Mag (magnetite) and Gp (gypsum).

**Table 4.1** Mineral assemblages and their ideal chemical formula.

Sample	Color Munsell*	Mineral assemblage (abbreviation)	Ideal chemical formula
Type-I	Pale Yellow 5Y 8/4	Quartz (Qz)	SiO <sub>2</sub>
		Garnet (Grt)	(Ca <sub>1.92</sub> Fe <sub>1.08</sub> )Fe <sub>2</sub> (SiO <sub>4</sub> ) <sub>3</sub>
		Epidote (Ep)	Ca <sub>2</sub> (Al <sub>2</sub> Fe)(SiO <sub>4</sub> )(Si <sub>2</sub> O <sub>7</sub> )O(OH)
Type-II	Brownish Yellow 10YR 6/8	Quartz (Qz)	SiO <sub>2</sub>
		Garnet (Grt)	(Ca <sub>1.92</sub> Fe <sub>1.08</sub> )Fe <sub>2</sub> (SiO <sub>4</sub> ) <sub>3</sub>
		Epidote (Ep)	Ca <sub>2</sub> (Al <sub>2</sub> Fe)(SiO <sub>4</sub> )(Si <sub>2</sub> O <sub>7</sub> )O(OH)
		Amphibole (Amp)	Ca <sub>2</sub> (Mg, Fe, Al) <sub>5</sub> (Al, Si) <sub>8</sub> O <sub>22</sub> (OH) <sub>2</sub>
		Montmorillonite (Mnt)	Na <sub>0.3</sub> (Al,Mg) <sub>2</sub> Si <sub>4</sub> O <sub>10</sub> (OH) <sub>2</sub> ·4H <sub>2</sub> O
Type-III	Yellowish Brown 10YR 5/8	Quartz (Qz)	SiO <sub>2</sub>
		Garnet (Grt)	(Ca <sub>1.56</sub> Fe <sub>1.44</sub> )Fe <sub>2</sub> (SiO <sub>4</sub> ) <sub>3</sub>
		Goethite (Gth)	FeOOH
		Amphibole (Amp)	Ca <sub>2</sub> (Mg, Fe, Al) <sub>5</sub> (Al, Si) <sub>8</sub> O <sub>22</sub> (OH) <sub>2</sub>
		Jarosite (Jrs)	KFe <sub>3</sub> (SO <sub>4</sub> ) <sub>2</sub> (OH) <sub>6</sub>
		Ankerite (Ank)	Ca <sub>1.01</sub> Mg <sub>0.45</sub> Fe <sub>0.54</sub> (CO <sub>3</sub> ) <sub>2</sub>
Type-IV	Dusky Red 10R 3/4	Quartz (Qz)	SiO <sub>2</sub>
		Garnet (Grt)	(Ca <sub>1.56</sub> Fe <sub>1.44</sub> )Fe <sub>2</sub> (SiO <sub>4</sub> ) <sub>3</sub>
		Epidote (Ep)	Ca <sub>2</sub> (Al <sub>2</sub> Fe)(SiO <sub>4</sub> )(Si <sub>2</sub> O <sub>7</sub> )O(OH)
		Amphibole (Amp)	Ca <sub>2</sub> (Mg, Fe, Al) <sub>5</sub> (Al, Si) <sub>8</sub> O <sub>22</sub> (OH) <sub>2</sub>
		Goethite (Gth)	FeOOH
		Magnetite (Mag)	Fe <sub>3</sub> O <sub>4</sub>
		Montmorillonite (Mnt)	Na <sub>0.3</sub> (Al,Mg) <sub>2</sub> Si <sub>4</sub> O <sub>10</sub> (OH) <sub>2</sub> ·4H <sub>2</sub> O
Type-V	Red 10R 4/6	Quartz (Qz)	SiO <sub>2</sub>
		Gypsum (Gp)	CaSO <sub>4</sub> ·2H <sub>2</sub> O
		Goethite (Gth)	FeOOH

\* Munsell standard color code (Munsell, 2010)

#### 4.3.2 Chemical composition

Table 4.2 presents qualitative EPMA chemical analyses of the gossan samples. Each sample was analyzed randomly for twenty points. Although this procedure is

unconventional for whole-rock analyses, multiple points of analyses with big beam spot (5  $\mu\text{m}$ ) can be statistically representative in a qualitative analysis. This procedure was therefore designed for this study, for which only small amounts of sample were available.

Type-I sample contains 11.28–24.35% Si, 2.11–10.45% Al, 5.32–15.37% Fe, 0.05–1.34% Mg, 0.32–18.83% Ca,  $\leq 0.3\%$  Mn,  $\leq 0.06\%$  As, 0.05–0.36% Cu and  $\leq 0.14\%$  S.

Sample type-II is composed of 10.36–17.72% Si, 1.27–4.05% Al, 16.91–28.01% Fe, 0.47–1.82% Mg, 0.96–2.03% Ca,  $\leq 0.26\%$  Mn,  $\leq 0.08\%$  Na,  $\leq 0.11\%$  As, 0.23–0.60% Cu and  $\leq 0.08\%$  S.

Type-III consists of 3.23–11.99% Si, 2.01–5.75% Al, 27.36–40.71% Fe, 0.06–0.31% Mg, 0.20–1.26% Ca, 0.09–2.30% Mn,  $\leq 0.06\%$  Na,  $\leq 0.21\%$  As, 0.4–0.85% Cu and 0.15–1.75% S.

Type-IV comprised 4.57–8.73% Si,  $\leq 2.26\%$  Al, 18.53–21.58% Fe,  $\leq 0.35\%$  Mg, 0.08–1.13% Ca, 0.26–4.30% Mn,  $\leq 0.05\%$  As, 0.50–0.80% Cu and  $\leq 0.43\%$  S.

Type-V sample is mainly comprised of 2.19–17.07% Si, 0.32–1.42% Al, 1.30–16.88% Fe,  $\leq 0.27\%$  Mg, 0.49–9.37% Ca,  $\leq 0.07\%$  Mn,  $\leq 0.05\%$  Na, 0.36–0.57% Cu and 0.35–7.50% S.

Some crucial elements such as Fe, Al, Ca, Mn, S, As and Cu were normalized by Si content and plotted in variation diagrams. Plots of Fe/Si versus other elemental ratios (i.e., Al/Si, Ca/Si, Mn/Si, S/Si, As/Si and Cu/Si) are shown in Figure 4.5.

**Table 4.2** Statistics of EPMA analyses of major and minor elements (Si, Al, Fe, Mg, Ca, Mn and Na), with some crucial trace elements (As, Cu and S) of all types selected from gossan samples, all concentrations in percent weight (%).

	No.	Si	Al	Fe	Mg	Ca	Mn	Na	As	Cu	S
Type-I (n=20)	Min.	11.28	2.11	5.32	0.05	0.32	<0.05	<0.05	<0.05	0.05	<0.05
	Max.	24.35	10.45	15.37	1.34	18.83	0.30	<0.05	0.06	0.36	0.14
	Av.	15.57	5.77	10.35	0.33	6.55	0.12	-	0.02	0.19	0.05
	sd	5.42	3.05	3.40	0.34	6.39	0.09	-	0.03	0.08	0.05
Type-II (n=20)	Min.	10.36	1.27	16.91	0.47	0.96	<0.05	<0.05	<0.05	0.23	<0.05
	Max.	17.72	4.05	28.01	1.82	2.03	0.26	0.08	0.11	0.60	0.08
	Av.	14.47	2.56	23.12	0.92	1.50	0.09	0.05	0.04	0.35	0.03
	sd	2.40	0.87	3.63	0.42	0.39	0.07	0.02	0.03	0.11	0.02
Type-III (n=20)	Min.	3.23	2.01	27.36	0.06	0.20	0.09	<0.05	<0.05	0.40	0.15
	Max.	11.99	5.75	40.71	0.31	1.26	2.30	0.06	0.21	0.85	1.75
	Av.	5.95	2.88	31.46	0.13	0.65	0.72	0.02	0.09	0.58	0.46
	sd	3.15	1.59	6.03	0.07	0.35	0.76	0.02	0.06	0.16	0.44
Type-IV (n=20)	Min.	4.57	<0.05	18.53	<0.05	0.08	0.26	<0.05	<0.05	0.50	0.08
	Max.	8.73	2.26	21.58	0.35	1.13	4.30	<0.05	0.05	0.80	0.43
	Av.	3.34	0.62	10.69	0.11	0.39	1.66	-	0.01	0.49	0.13
	sd	3.11	0.59	7.33	0.10	0.36	1.39	-	0.02	0.19	0.17
Type-V (n=20)	Min.	2.19	0.32	1.30	0.05	0.49	<0.05	<0.05	<0.05	0.36	0.35
	Max.	17.07	1.42	16.88	0.27	9.37	0.07	0.05	<0.05	0.57	7.50
	Av.	7.40	0.67	11.83	0.13	3.30	0.03	0.01	-	0.42	2.62
	sd	4.88	0.36	5.31	0.08	2.41	0.02	0.02	-	0.10	1.96

In general, all types show similar ratios of Al/Si and Mg/Si ranging commonly between 0.06–0.85 and 0.01–0.15, respectively (Figures 4.5a, b). Type-I shows clearly high Ca/Si against low Fe/Si (Figure 4.5c); moreover, it also presents low content of S/Si, As/Si and Cu/Si (see Figures 4.5d-f). Type-II reveals Ca/Si and As/Si ratios similar to the other types but its Fe/Si, S/Si and Cu/Si ratios are lower than the others except Type I. Type-III is obviously high in Fe/Si and As/Si ratios (Figure 4.5e) medium ratios of



S/Si and Cu/Si (Figures 4.5d, f). Type-V yields the highest S/Si ratio (Figure 4.5d). Type-III shows clearly positive correlation between Fe/Si and As/Si ( $R^2=0.6905$ ). Moreover, all types appear to have positive correlation between Fe/Si and Cu/Si ( $R^2=0.8608$  for Type-III,  $R^2=0.5542$  for Type-IV). According to R-squared value, Fe-ratio has significant relationship with As and Cu. This chemistry results would reflect mineral assemblage and alteration processes of the gossan types, which will be discussed further below.

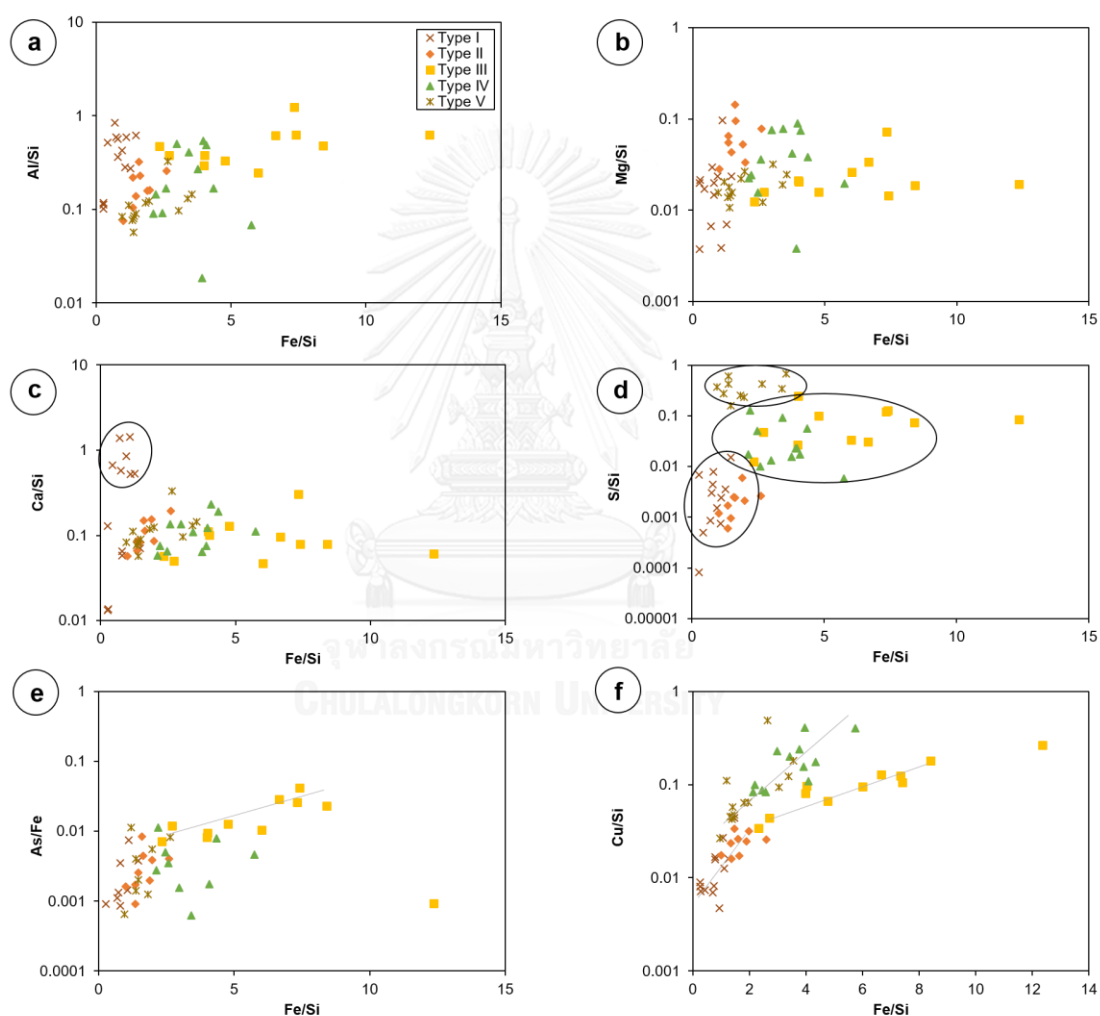


**Figure 4.5** Plots of Fe/Si versus other elemental ratios (Al, Mg, Ca, S, As and Cu against Si)

## 4.4 Discussions

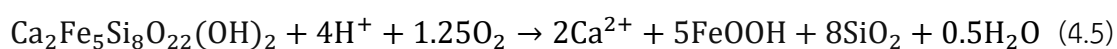
### 4.4.1 Characteristics

In regard to mineral assemblages and chemical compositions (e.g., Si, Al, Ca, Mg, Fe and S), all gossan types contain Si as a major element that is compatible to mineral assemblage including quartz ( $\text{SiO}_2$ ) and some other silicate minerals including garnet  $[(\text{Ca,Fe})_3\text{Fe}_2(\text{SiO}_4)_3]$ , epidote  $[\text{Ca}_2(\text{Al}_2\text{Fe})(\text{SiO}_4)(\text{Si}_2\text{O}_7)\text{O}(\text{OH})]$ , amphibole  $[\text{Ca}_2(\text{Mg,Fe,Al})_5(\text{Al,Si})_8\text{O}_{22}(\text{OH})_2]$  and montmorillonite  $[\text{Na}(\text{Al,Mg})_2\text{Si}_4\text{O}_{10}(\text{OH})_2 \cdot 4\text{H}_2\text{O}]$ . Apart from Si, these silicate minerals also contain Al, Ca, Mg and Fe. In addition, Fe is also found associated with the main component of goethite ( $\text{FeOOH}$ ), magnetite ( $\text{Fe}_3\text{O}_4$ ) and jarosite ( $\text{KFe}_3(\text{SO}_4)_2(\text{OH})_6$ ). Sulfur (S) apparently relates to gypsum ( $\text{CaSO}_4 \cdot 2\text{H}_2\text{O}$ ) and jarosite.

Therefore, type-III with the highest iron contents (27–41% Fe) relate clearly to the high amounts of goethite and jarosite present in XRD peak pattern (Figure 4.4c). Type-V with the highest range of S content (0.35–7.5%) is well fit with the gypsum mainly presented in the XRD peak pattern (Figure 4.4e).

In general, the XRD analyses also indicate that types-I, -II, -III and -IV consist mainly of primary silicate minerals (i.e., quartz, garnet epidote and amphibole) which appear to be the initial composition of skarn rock. On the other hand, secondary minerals, altered/weathered products (i.e., goethite, jarosite, ankerite, montmorillonite and magnetite), are observed in types-II, -III and -IV. In addition, type-V contain secondary minerals of gypsum, goethite and secondary quartz. Moreover, types-III, -IV and -V that can be easily released under acid conditions could affect the environment to a greater extent than types-I and -II.

For goethite ( $\text{FeOOH}$ ), it may be an oxidation product of sulfide minerals (see Eqs. 4.1–4.4) and/or amphibole (see Eq. 4.5) modified from Velbel (1989), or jarosite (see Eq. 4.6) (Grishin et al., 1988; Parbhakar-Fox and Lottermoser, 2015).

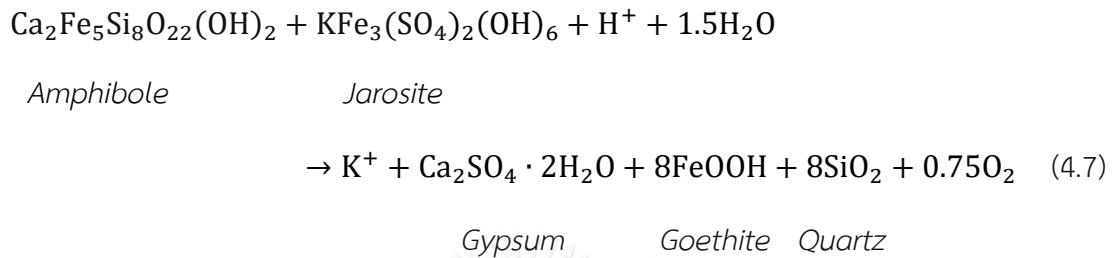


*Amphibole*

*Goethite Quartz*



Type-V consists of quartz, goethite and gypsum which may have weathered from oxidation reaction of amphibole and jarosite (Eq. 4.7).



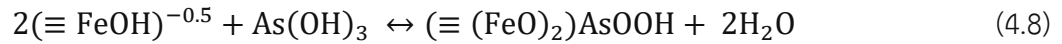
According to equations (4.5) and (4.7), quartz ( $\text{SiO}_2$ ) can be produced by amphibole oxidation. Therefore, quartz found in all gossan types can be both primary and secondary minerals which should be confirmed by its micromorphology. Micro-crystalline quartz is mainly present in types-III, -IV and V (Figures 4.3c–e) which indicate secondary product; on the other hand, gossan types-I and II are composed of primary lath-shaped quartz (Figures 4.3a, b). These indicate that gossan types-III, -IV and -V may have undertaken more/longer oxidation/ alteration processes than types-I and II.

#### 4.4.2 Sorption-desorption of toxic element

Based on chemical analyses, type-III has the highest content of Fe, As and Cu. It also shows a positive correlation between Fe and As, Cu (Figures 4.5e, f); these toxic elements are possibly adsorbed by or co-precipitated with goethite and jarosite (Peacock and Sherman, 2004; Velasco et al., 2013). Moreover, types-IV and -V appear to be a source of Cu. The results also indicate a positive trend between Fe and Cu in relation to goethite occurrences because  $\text{Fe}^{3+}$  in the goethite structure can be substituted by Cu, as suggested by Gerth (1990) and Carbone et al. (2012).

Adsorption of arsenic and copper onto goethite can be described as a process of surface complexation ( $\equiv\text{SOMOH}$ ; S=surface, O=oxygen, M=metal and OH=hydroxyl). Surface complexation of arsenic adsorption onto goethite surface is shown in equation (4.8) arsenite ( $\text{As}^{3+}$ ) and equation (4.9) for arsenate ( $\text{As}^{5+}$ ) as suggested by Kersten and

Vlasova (2009) and Zhang et al. (2007), respectively. In addition, Cu adsorption on goethite is presented in equation (4.10) as suggested by Peacock and Sherman (2004).



Type-II is a remarkable sample because it consists of As ( $\leq 0.11\%$ ) and Cu ( $0.35 \pm 0.11\%$ ) although it does not consist of goethite or jarosite. In this case, arsenic and copper are possibly adsorbed by montmorillonite (a clay mineral) occurring in this gossan type; this assumption is supported by the study of Lottermoser (2010).

Moreover, Assawincharoenkij et al. (*in prep.*) also suggested that As and Cu may be adsorbed by hydrous ferric oxide (HFO: poor crystalline), usually found as oxidized product along the edges of ferro-silicate minerals, which provide an essential assemblage in type-II. This HFO may transform further to goethite (Cornell and Schwertmann, 2003).

In addition, particle size highly influences adsorption of toxic elements because the smaller particles have a greater reactive surface area, and thus a higher surface adsorption capacity (Hua et al., 2012). Therefore, types-III, -IV, and -V, composed of very fine particles  $< 1 \mu\text{m}$ , should have higher adsorption potential than types-I and -II (average grain size  $> 5 \mu\text{m}$ ).

As a result, gossan waste rocks (unwanted rocks) have potential utility as a natural adsorbent material. They consist mainly of goethite ( $\text{FeOOH}$ ), magnetite ( $\text{Fe}_3\text{O}_4$ ) and jarosite ( $\text{KFe}_3(\text{SO}_4)_2(\text{OH})_6$ ) that are recognized as significant natural adsorbents (Asta et al., 2009; Hua et al., 2012). This is supported by prior research into the potential of natural lateritic soil for arsenic adsorption (Maiti et al., 2007; Tongkhan et al., 2016). The natural lateritic soils were characterized and potential arsenic adsorbents identified such as goethite, hematite, aluminium hydroxide and kaolinite. Moreover, the natural lateritic soils adsorb the high arsenic content under a wide pH range (from 4 to 9.8) as shown by Maiti et al. (2007).

Figure 4.6 presents Eh-pH diagram, reported by Majzlan et al. (2007), of Fe-oxyhydroxide minerals (i.e., schwertmannite  $(\text{Fe}_8\text{O}_8(\text{OH})_6(\text{SO}_4)\cdot n\text{H}_2\text{O})$ , ferrihydrite  $(\text{Fe}_5\text{HO}_8\cdot 4\text{H}_2\text{O})$  and green rust  $(\text{Fe}^{\text{II}}-\text{Fe}^{\text{III}}(\text{OH}))$ ); these minerals can adsorb arsenate ( $\text{As}^{5+}$ ) under oxidizing conditions with  $\text{pH} > 2$ . However, the gossan rocks are unstable under acidic aqueous conditions ( $\text{pH} \leq 2$ ); Fe-oxyhydroxide can be dissolved, releasing toxic elements into solution (Romero et al., 2006). Collected field data of runoff and groundwater should be taken place before experimental design. The crucial information include pH, Eh and toxic elements in these water samples. Subsequently, these gossan waste rocks with proper procedure may be used for site remediation around the gold mine.

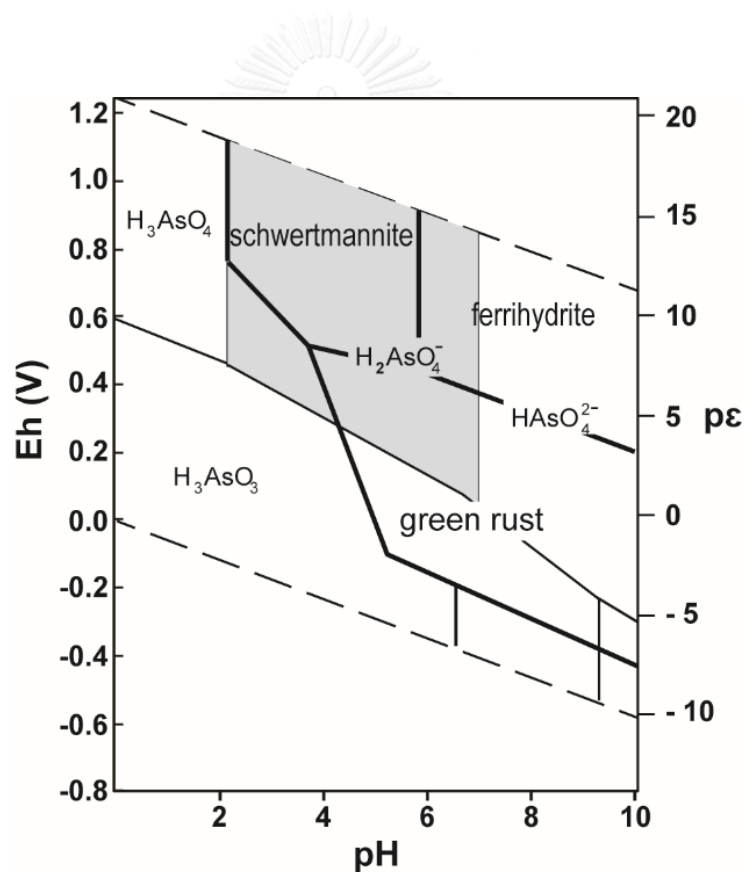


**Figure 4.6** Eh-pH diagram for the systems  $\text{Fe}_2\text{O}_3\text{-SO}_3\text{-H}_2\text{O}$  suggested by Majzlan et al. (2004) showing consistency of Fe-oxyhydroxide minerals (i.e., schwertmannite  $(\text{Fe}_8\text{O}_8(\text{OH})_6(\text{SO}_4)\cdot n\text{H}_2\text{O})$ , ferrihydrite  $(\text{Fe}_5\text{HO}_8\cdot 4\text{H}_2\text{O})$  and green rust  $(\text{Fe}^{\text{II}}-\text{Fe}^{\text{III}}(\text{OH}))$  and the speciation of arsenic in the aqueous phase suggested by Majzlan et al. (2007).

#### 4.5 Conclusion

Gossan waste rocks of various other colors were characterized. These different other gossans show a relationship between mineral assemblages and chemical composition, including some toxic elements. They can be grouped into five types: type-I, pale-yellow color; type-II, brownish-yellow color; type-III, yellowish-brown color; type-IV, dusky-red color; type-V, red color. Moreover, the gossan rocks including types-III, -IV and -V have a high adsorption capacity and comprised absorbent minerals (goethite, jarosite and montmorillonite), offering potential utility as a natural adsorbent to reduce pollutants (i.e., As and Cu) from the ecosystem. As this rock type (gossan) is abundant around this mining site, it can be recommended for low-cost site remediation.



## CHAPTER 5 CONCLUSION AND RECOMMENDATION

### 5.1 Conclusion

The main aims of this research are: 1. to characterize mineral composition, mineral chemistry and bulk geochemistry of mine tailings in relation to acid mine drainage (AMD) potential and source of metal contamination; and 2. to investigate petrography and whole-rock geochemistry of waste rocks in relation to AMD generation and metal releasing. Therefore, the conclusion of this study has been separated into three parts as following below.

#### **Part I: Mineralogy and geochemistry of tailings from a gold mine in northeastern Thailand**

Mine tailings are divided into the upper gray tailings (from top to 6–7 m depth) and the lower ochre tailings (between depths at 7–17 m). The upper gray tailings mainly contain sulfide minerals (i.e., pyrrhotite, pyrite and chalcopyrite) and some silicate minerals (i.e., quartz, andradite and diopside). The lower ochre tailings mainly contain goethite, quartz, muscovite, calcite, hematite with minor pyrrhotite. Based on acid base accounting (ABA) and mineral assemblage, the upper gray tailings are defined as potential acid forming (PAF) whereas the lower ochre tailings are non-acid forming (NAF). Therefore, the upper tailings have potential to generate AMD. Geochemistry, toxic elements are crucially found in the upper gray tailings including 39–268 mg/kg As, 222–425 mg/kg Co, 226–1,111 mg/kg Cu and 1,421–3,524 mg/kg Mn. Moreover, the lower ochre tailings are composed of very high contents of As (238–2,870 mg/kg), Cu (750–2,608 mg/kg) and Pb (10–1,506 mg/kg) which they exceed the Total Threshold Limit Concentration (TTLIC). Consequently, the lower ochre tailings must be declared as “hazardous waste”.

## **Part II: Mineralogical and geochemical characterization of waste-rocks from a gold mine in northeastern Thailand: Application for environmental impact protection**

Waste rocks, collected from three dump sites and also directly from open pit, are characterized by sandstone, siltstone, skarn, skarn sulfide, massive sulfide, diorite, limestone/marble and gossan. Based on mineral composition, the massive sulfide and skarn-sulfide rocks that consist mainly of pyrrhotite, pyrite, arsenopyrite and chalcopyrite are AMD potential. Arsenic and copper which are found in the massive sulfide and skarn-sulfide rocks are clearly related to arsenopyrite and chalcopyrite, respectively; moreover, these elements are found in the gossan rocks (541–810 mg/kg As, 498–7,480 mg/kg Cu) which are related to two main assemblages including goethite ( $\leq 0.17$  wt% As,  $\leq 0.58$  wt.% Cu) and hydrous ferric oxide (HFO) ( $\leq 1.37$  wt% As,  $\leq 0.60$  wt.% Cu). Consequently, the massive sulfide and skarn-sulfide rocks are main potential sources of AMD and toxic elements whereas the gossan rocks are highly potential source of toxic elements.

## **Part III: Mineralogical and chemical characteristics of gossan waste rocks from a gold mine in northeastern Thailand**

According to various shades of ochre colors in gossan waste rocks, these color shades clearly relate to mineral assemblages and chemical composition including some toxic elements. They can be grouped into five types, pale-yellow type-I, brownish-yellow type-II, yellowish-brown type-III, dusky-red type-IV and red type-V. Type-I contains mostly primary silicate minerals (e.g., quartz, garnet and epidote) whereas type-II, type-III, type-IV and type-V are composed of primary silicates (e.g., quartz, garnet, epidote and amphibole) and secondary minerals (e.g., goethite, montmorillonite, jarosite, and gypsum). In addition, types-III, -IV and -V have high adsorption capacity and consist of absorbent minerals (e.g., goethite, jarosite and montmorillonite). Therefore, they can be potentially used as a natural adsorbent to reduce pollutants, particularly As and Cu in the surrounding local area. However, more studies should be considered for gossan prior to recommendation for low-cost site remediation.



## 5.2 Recommendation

(1) Since 2016, the Thung Kham Gold mine has been officially closed by the government but mine pit and waste dumping sites are not restored. This issue should be considered, seriously, because massive sulfide and skarn-sulfide rocks found in the mine area may have been reacted by the atmosphere leading to the environmental impact. Therefore, the mine closer plan is recommended to be designed and proceeded soon.

(2) As the result of acid forming potential (AFP), the upper gray tailings (upper part) are potential source of AMD generation; therefore, the tailing storage should be covered by compacted clay (at least 50 cm thick) to prevent oxidation reaction, and followed by a gravel layer (30 cm thick) to facilitate the drainage during rainy season. The top soil layer (1–2 m) must be covered before plantation. Alternative choices to prevent metal releasing, the upper gray tailings and the lower ochre tailings should be dumped into separated storages. Because the lower ochre tailings have high concentration of toxic elements.

(3) The gossan rock may be source of toxic elements, although it can be used as a natural absorbent. Therefore, more experiments should be carried out prior to removals of arsenic and other toxic elements in the surrounding area. Effects on adsorbent dose, adsorbent particle size, operating pH, contact time, initial arsenic/arsenate concentration, etc., should be taken into account for experimental arsenic removal.

## REFERENCES

- Akcil, A., and Koldas, S., 2006, Acid Mine Drainage (AMD): causes, treatment and case studies: *Journal of Cleaner Production*, v. 14, no. 12-13, p. 1139-1145.
- Álvarez-Valero, A. M., Pérez-López, R., Matos, J., Capitán, M. A., Nieto, J. M., Sáez, R., Delgado, J., and Caraballo, M., 2008, Potential environmental impact at São Domingos mining district (Iberian Pyrite Belt, SW Iberian Peninsula): Evidence from a chemical and mineralogical characterization: *Environmental Geology*, v. 55, no. 8, p. 1797-1809.
- Anawar, H. M., 2015, Sustainable rehabilitation of mining waste and acid mine drainage using geochemistry, mine type, mineralogy, texture, ore extraction and climate knowledge: *Journal of Environmental Management*, v. 158, p. 111-121.
- Ashley, P. M., Lottermoser, B. G., Collins, A. J., and Grant, C. D., 2004, Environmental geochemistry of the derelict Webbs Consols mine, New South Wales, Australia: *Environmental Geology*, v. 46, no. 5, p. 591-604.
- Assawincharoenkij, T., Hauzenberger, C., Ettinger, K., and Sutthirat, C., *in prep.*, Mineralogical and geochemical characterization of waste-rocks from a gold mine in Northeastern Thailand: Potential source of toxic elements: *Environmental Science and Pollution Research*
- Assawincharoenkij, T., Hauzenberger, C., and Sutthirat, C., 2017, Mineralogy and geochemistry of tailings from a gold mine in northeastern Thailand: Human and Ecological Risk Assessment: *An International Journal*, v. 23, no. 2, p. 364-387.
- Asta, M. P., Cama, J., Martínez, M., and Giménez, J., 2009, Arsenic removal by goethite and jarosite in acidic conditions and its environmental implications: *Journal of Hazardous Materials*, v. 171, no. 1-3, p. 965-972.
- Atapour, H., and Aftabi, A., 2007, The geochemistry of gossans associated with Sarcheshmeh porphyry copper deposit, Rafsanjan, Kerman, Iran: Implications for exploration and the environment: *Journal of Geochemical Exploration*, v. 93, no. 1, p. 47-65.

- Basu, A., and Schreiber, M. E., 2013, Arsenic release from arsenopyrite weathering: Insights from sequential extraction and microscopic studies: *Journal of Hazardous Materials*, v. 262, p. 896-904.
- Belzile, N., Chen, Y.-W., Cai, M.-F., and Li, Y., 2004, A review on pyrrhotite oxidation: *Journal of Geochemical Exploration*, v. 84, no. 2, p. 65-76.
- Boonsrang, A., Chotpantarat, S., and Sutthirat, C., Evaluation of release of potentially heavy metals from gold mine tailings using synthetic precipitation leaching procedure (SPLP): A case study of gold mine, Thailand, *in Proceedings the 2<sup>nd</sup> International Conference on Engineering and Applied Science (2013 ICEAS)*, Tokyo, Japan, 15-17 March, 2013.
- Botz, M., 1999, Overview of cyanide treatment methods. Available from: <http://www.infomine.com/library/publications/docs/Botz1999.pdf>.
- Bowen, H. J. M., 1979, *Environmental chemistry of the elements*, London; New York, Academic Press.
- Campbell, K. M., and Nordstrom, D. K., 2014, Arsenic Speciation and Sorption in Natural Environments *in* *Bowell, R. J., Alpers, C. N., Jamieson, H. E., Nordstrom, D. K., and Majzlan, J., eds., Reviews in Mineralogy and Geochemistry, Volume 79: Chantilly, VA, Mineralogical Society of America*, p. 185-216.
- Carbone, C., Dinelli, E., Marescotti, P., Gasparotto, G., and Lucchetti, G., 2013, The role of AMD secondary minerals in controlling environmental pollution: Indications from bulk leaching tests: *Journal of Geochemical Exploration*, v. 132, p. 188-200.
- Carbone, C., Marescotti, P., Lucchetti, G., Martinelli, A., Basso, R., and Cauzid, J., 2012, Migration of selected elements of environmental concern from unaltered pyrite-rich mineralizations to Fe-rich alteration crusts: *Journal of Geochemical Exploration*, v. 114, p. 109-117.
- Carrillo-Chávez, A., Salas-Megchún, E., Levresse, G., Muñoz-Torres, C., Pérez-Arvizu, O., and Gerke, T., 2014, Geochemistry and mineralogy of mine-waste material from a "skarn-type" deposit in central Mexico: Modeling geochemical controls of metals in the surface environment: *Journal of Geochemical Exploration*, v. 144, no. PA, p. 28-36.

- Changul, C., Sutthirat, C., Padmanahban, G., and Tongcumpou, C., 2009a, Assessing the acidic potential of waste rock in the Akara gold mine, Thailand: *Environmental Earth Sciences*, v. 60, no. 5, p. 1065-1071.
- Changul, C., Sutthirat, C., Padmanahban, G., and Tongcumpou, C., 2009b, Chemical characteristics and acid drainage assessment of mine tailings from Akara Gold mine in Thailand: *Environmental Earth Sciences*, v. 60, no. 8, p. 1583-1595.
- Charuseiam, Y., 2012, Acid mine drainage generation potential of waste rocks using weathering cell test in Gold mine, Thailand. Master Thesis: Chulalongkorn University, 210 p.
- Charuseiam, Y., Chotpantararat, S., and Sutthirat, C., The release potential of heavy metals from waste rocks from transition zone using weathering cell test in Gold Mine, Thailand, *in Proceedings the 2<sup>nd</sup> International Conference on Engineering and Applied Science (2013 ICEAS)*, Tokyo, Japan, 15-17 March, 2013.
- Chirijā, P., and Rimstidt, J. D., 2014, Pyrrhotite dissolution in acidic media: *Applied Geochemistry*, v. 41, p. 1-10.
- Chonglakmani, C., 1984, Geological Map of Udon Thani-Wang Wiang, Quadrangle, scale 1:250000: Department of Mineral Resources.
- Choprapawon, C., and Rodcline, A., 1997, Chronic arsenic poisoning in Ronpibool Nakhon Sri Thammarat, the Southern Province of Thailand, *in* Abernathy, C. O., Calderon, R. L., and Chappell, W. R., eds., *Arsenic: Exposure and Health Effects*: Dordrecht, Springer Netherlands, p. 69-77.
- Chotipong, A., Sutthirat, C., and Kallapavit, A., 2014a, Survey of distribution and sources of heavy metals contamination in Phu Thap Fah Gold Deposit, Khao Luang, Wang Sapung, Loei Province: Part 1 Pollutants in soils: *Environmental Journal*, v. 1, p. 72-80 (in Thai).
- , 2014b, Survey of distribution and sources of heavy metals contamination in Phu Thap Fah Gold Deposit, Khao Luang, Wang Sapung, Loei Province: Part 2 Pollutants in sediments: *Environmental Journal*, v. 3, p. 41-52 (in Thai).
- , 2015, Survey of distribution and sources of heavy metals contamination in Phu Thap Fah Gold Deposit, Khao Luang, Wang Sapung, Loei Province: Part 3 Pollutants in surface water: *Environmental Journal*, v. 1, p. 24-37 (in Thai).

- , 2016, Survey of distribution and sources of heavy metals contamination in Phu Thap Fah Gold Deposit, Khao Luang, Wang Sapung, Loei Province: Part 4 Pollutants in groundwater: *Environmental Journal*, v. 1, p. 76-86 (in Thai).
- Cidu, R., Dadea, C., Desogus, P., Fanfani, L., Manca, P. P., and Orrù, G., 2012, Assessment of environmental hazards at abandoned mining sites: A case study in Sardinia, Italy: *Applied Geochemistry*, v. 27, no. 9, p. 1795-1806.
- Corkhill, C. L., and Vaughan, D. J., 2009, Arsenopyrite oxidation – A review: *Applied Geochemistry*, v. 24, no. 12, p. 2342-2361.
- Cornell, R. M., and Schwertmann, U., 2003, The iron oxides: structure, properties, reactions, occurrences and uses, Weinheim, Wiley-VCH Verlag GmbH & Co. KGaA.
- Craw, D., Falconer, D., and Youngson, J. H., 2003, Environmental arsenopyrite stability and dissolution: theory, experiment, and field observations: *Chemical Geology*, v. 199, no. 1-2, p. 71-82.
- Crow, M. J., and Zaw, K., 2011, Metalliferous minerals, in Ridd, M. F., Barber, A. J., and Crow, M. J., eds., *The geology of Thailand*: London, The Geological Society, p. 459-492.
- Da Pelo, S., Musu, E., Cidu, R., Frau, F., and Lattanzi, P., 2009, Release of toxic elements from rocks and mine wastes at the Furtei gold mine (Sardinia, Italy): *Journal of Geochemical Exploration*, v. 100, no. 2-3, p. 142-152.
- Das, K. K., Das, S. N., and Dhundasi, S. A., 2008, Nickel, its adverse health effects & oxidative stress: *The Indian Journal of Medical Research*, v. 128, no. 4, p. 412-425.
- Department of Primary Industries and Mines's Report, 2012, Water quality in Thung Kham mine area: implication for incident of the tailing dam collapse (in Thai) Bangkok, Thailand, Department of Primary Industries and Mines, 7 p.
- EGI, 2005, Chatree Gold Mine: geochemical characterisation and review of site classification programme and quality control testing for site NAG test results, An unpublished document prepared for AKARA mining limited. Document No. 4205/680.

- EPA, 2004, Laboratory sample preparation. April 18. Available from: <https://www.epa.gov/sites/production/files/2015-05/documents/402-b-04-001b-12-final.pdf>
- ERIC, 2012, The final report: Survey of distribution and sources of heavy metals contamination in Phu Thap Fah Gold Mine Deposit, Khao Luang, Wang Sapung, Loei Province, Bangkok, Thailand (in Thai), Environmental Research Institute, Chulalongkorn University.
- Evangelou, V. P., and Zhang, Y. L., 1995, A review: Pyrite oxidation mechanisms and acid mine drainage prevention: *Critical Reviews in Environmental Science and Technology*, v. 25, no. 2, p. 141-199.
- Ferguson, K. D., and Erickson, P. M., 1988, Pre-Mine Prediction of Acid Mine Drainage, *in* Salomons, W., and Förstner, U., eds., *Environmental Management of Solid Waste: Dredged Material and Mine Tailings*: Berlin, Heidelberg, Springer Berlin Heidelberg, p. 24-43.
- Ferreira da Silva, E., Durães, N., Reis, P., Patinha, C., Matos, J., and Costa, M. R., 2015, An integrative assessment of environmental degradation of Caveira abandoned mine area (Southern Portugal): *Journal of Geochemical Exploration*, v. 159, p. 33-47.
- García, C., Ballester, A., González, F., and Blázquez, M. L., 2005, Pyrite behaviour in a tailings pond: *Hydrometallurgy*, v. 76, no. 1-2, p. 25-36.
- Gerth, J., 1990, Unit-cell dimensions of pure and trace metal-associated goethites: *Geochimica et Cosmochimica Acta*, v. 54, no. 2, p. 363-371.
- Grishin, S. I., Bigham, J. M., and Tuovinen, O. H., 1988, Characterization of Jarosite Formed upon Bacterial Oxidation of Ferrous Sulfate in a Packed-Bed Reactor: *Applied and Environmental Microbiology*, v. 54, no. 12, p. 3101-3106.
- Heikkinen, P. M., and Räsänen, M. L., 2008, Mineralogical and geochemical alteration of Hitura sulphide mine tailings with emphasis on nickel mobility and retention: *Journal of Geochemical Exploration*, v. 97, no. 1, p. 1-20.
- Holmström, H., Salmon, U. J., Carlsson, E., Petrov, P., and Öhlander, B., 2001, Geochemical investigations of sulfide-bearing tailings at Kristineberg, northern

- Sweden, a few years after remediation: *Science of The Total Environment*, v. 273, no. 1–3, p. 111-133.
- Hua, M., Zhang, S., Pan, B., Zhang, W., Lv, L., and Zhang, Q., 2012, Heavy metal removal from water/wastewater by nanosized metal oxides: a review: *Journal of Hazardous Materials*, v. 211-212, p. 317-331.
- Huagul, W., 2007, The surveillance quality in Hoi Rivers. Master Thesis: Loei Rajabhat University.
- Hudson-Edwards, K. A., Jamieson, H. E., and Lottermoser, B. G., 2011, Mine wastes: past, present, future: *Elements*, v. 7, no. 6, p. 375-380.
- Hunt, J., Lottermoser, B. G., Parbhakar-Fox, A., Van Veen, E., and Goemann, K., 2016, Precious metals in gossanous waste rocks from the Iberian Pyrite Belt: *Minerals Engineering*, v. 87, p. 45-53.
- Hutchison, I. P. G., and Ellison, R. D., 1992, *Mine waste management*, London Lewis.
- Jackson, L. M., and Parbhakar-Fox, A., 2016, Mineralogical and geochemical characterization of the Old Tailings Dam, Australia: Evaluating the effectiveness of a water cover for long-term AMD control: *Applied Geochemistry*, v. 68, p. 64-78.
- Jambor, J. L., Martin, A. J., and Gerits, J., 2009, The post-depositional accumulation of metal-rich cyanide phases in submerged tailings deposits: *Applied Geochemistry*, v. 24, no. 12, p. 2256-2265.
- Jamieson, H. E., 2011, *Geochemistry and Mineralogy of Solid Mine Waste: Essential Knowledge for Predicting Environmental Impact*: *Elements*, v. 7, no. 6, p. 381-386.
- Janzen, M. P., Nicholson, R. V., and Scharer, J. M., 2000, Pyrrhotite reaction kinetics: reaction rates for oxidation by oxygen, ferric iron, and for nonoxidative dissolution: *Geochimica et Cosmochimica Acta*, v. 64, no. 9, p. 1511-1522.
- Kasprzak, K. S., Sunderman Jr, F. W., and Salnikow, K., 2003, Nickel carcinogenesis: Mutation Research/Fundamental and Molecular Mechanisms of Mutagenesis, v. 533, no. 1–2, p. 67-97.
- Kerr, P. F., 1959, *Optical mineralogy*, New York, McGraw-Hill.

- Kersten, M., and Vlasova, N., 2009, Arsenite adsorption on goethite at elevated temperatures: *Applied Geochemistry*, v. 24, no. 1, p. 32-43.
- Khamthat, S., 2007, Determination of heavy metals in ground water in the communities surrounding the Gold mine, Khao Luang Sub-district, Wang Saphung District, Loei Province. Master Thesis: Loei Rajabhat University.
- Khodadad, A., Teimoury, P., Abdolahi, M., and Samiee, A., 2008, Detoxification of Cyanide in a Gold Processing Plant Tailings Water Using Calcium and Sodium Hypochlorite: *Mine Water and the Environment*, v. 27, no. 1, p. 52-55.
- Khon Kaen University Report, 2009, Final report of Environmental Impact Assessment (EIA), Khon Kaen Province, Thailand (in Thai), Khon Kaen University.
- Kim, J. Y., Kim, K. W., Ahn, J. S., Ko, I., and Lee, C. H., 2005, Investigation and risk assessment modeling of As and other heavy metals contamination around five abandoned metal mines in Korea: *Environmental Geochemistry and Health*, v. 27, no. 2, p. 193-203.
- Klongsamran, C., Chotipong, A., and Sutthirat, C., The impact of pH on the leaching of heavy metal from waste rock at Phutabpha gold mine, *in Proceedings the 52<sup>th</sup> Academic conference*, Kasetsart University, Bangkok, Thailand, 4-7 February, 2014, p. 111.
- Koski, R. A., Munk, L., Foster, A. L., Shanks Iii, W. C., and Stillings, L. L., 2008, Sulfide oxidation and distribution of metals near abandoned copper mines in coastal environments, Prince William Sound, Alaska, USA: *Applied Geochemistry*, v. 23, no. 2, p. 227-254.
- Lapakko, K., 2002, Metal Mine Rock and Waste Characterization Tools: An Overview, p. 30.
- Lawrence, R. W., Jaffe, S., and Broughton, L. M., 1988, In-House Development of the Net Acid Production Test Method, Canada, Coastech Research, v. .
- Lengke, M. F., Davis, A., and Bucknam, C., 2010, Improving Management of Potentially Acid Generating Waste Rock: *Mine Water and the Environment*, v. 29, no. 1, p. 29-44.
- Lindsay, M. B. J., Condon, P. D., Jambor, J. L., Lear, K. G., Blowes, D. W., and Ptacek, C. J., 2009, Mineralogical, geochemical, and microbial investigation of a sulfide-



- rich tailings deposit characterized by neutral drainage: *Applied Geochemistry*, v. 24, no. 12, p. 2212-2221.
- Lindsay, M. B. J., Moncur, M. C., Bain, J. G., Jambor, J. L., Ptacek, C. J., and Blowes, D. W., 2015, Geochemical and mineralogical aspects of sulfide mine tailings: *Applied Geochemistry*, v. 57, p. 157-177.
- Lottermoser, B. G., 2010, *Mine Wastes*, Springer-Verlag Berlin Heidelberg, Characterization, Treatment and Environmental Impacts, 400 p.
- Lottermoser, B. G., 2011, Mine wastes: acidic to circumneutral: *Elements*, v. 7, no. 6, p. 393-398.
- Maiti, A., Dasgupta, S., Basu, J., and De, S., 2007, Adsorption of arsenite using natural laterite as adsorbent: *Separation and Purification Technology*, v. 55, no. 3, p. 350-359.
- Majzlan, J., Lalinská, B., Chovan, M., Jurkovič, L. u., Milovská, S., and Göttlicher, J., 2007, The formation, structure, and ageing of As-rich hydrous ferric oxide at the abandoned Sb deposit Pezinok (Slovakia): *Geochimica et Cosmochimica Acta*, v. 71, no. 17, p. 4206-4220.
- Majzlan, J., Navrotsky, A., and Schwertmann, U., 2004, Thermodynamics of iron oxides: Part III. Enthalpies of formation and stability of ferrihydrite ( $\sim\text{Fe}(\text{OH})_3$ ), schwertmannite ( $\sim\text{FeO}(\text{OH})_{3/4}(\text{SO}_4)_{1/8}$ ), and  $\epsilon\text{-Fe}_2\text{O}_3$ : *Geochimica et Cosmochimica Acta*, v. 68, no. 5, p. 1049-1059.
- Marescotti, P., Azzali, E., Servida, D., Carbone, C., Grieco, G., De Capitani, L., and Lucchetti, G., 2009, Mineralogical and geochemical spatial analyses of a waste-rock dump at the Libiola Fe–Cu sulphide mine (Eastern Liguria, Italy): *Environmental Earth Sciences*, v. 61, no. 1, p. 187-199.
- Marescotti, P., Carbone, C., De Capitani, L., Grieco, G., Lucchetti, G., and Servida, D., 2008, Mineralogical and geochemical characterisation of open-air tailing and waste-rock dumps from the Libiola Fe-Cu sulphide mine (Eastern Liguria, Italy): *Environmental Geology*, v. 53, no. 8, p. 1613-1626.
- Marshall, D., Anglin, C. D., and Mumin, H., 2004, *Ore Mineral Atlas*, Canada, Mineral Deposits Division, Geological Association of Canada.

- Miller, R. O., and Kissel, D. E., 2010, Comparison of soil pH methods on soils of North America: Soil Science Society of America Journal, no. 74 p. 310-316.
- Miller, S., Robertson, A., and Donahue, T., Advances in Acid Drainage Prediction using the Net Acid Generation (NAG) Test, *in* Proceedings the 4<sup>th</sup> International Conference on Acid Rock Drainage, Vancouver, British Columbia, 1997, p. 533-549.
- Miller, S., Rusdinar, Y., Smart, R., Andrina, J., and Richards, D., Design and construction of limestone blended waste rock dumps - lessons learned from a 10-year study at Grasberg, *in* Proceedings the 7<sup>th</sup> International Conference on Acid Rock Drainage (ICARD), St. Louis, Missouri, 2006, The American Society of Mining and Reclamation (ASMR).
- Ministry of Industry Thailand, 2006, Notification of Ministry of Industry, Subject : Waste Disposal. December 20, 2015. Available from: <http://www2.diw.go.th/PIC/download/waste/waste11.pdf>.
- Mohan, D., and Pittman, C. U., Jr., 2007, Arsenic removal from water/wastewater using adsorbents--A critical review: Journal of Hazardous Materials, v. 142, no. 1-2, p. 1-53.
- Moncur, M. C., Jambor, J. L., Ptacek, C. J., and Blowes, D. W., 2009, Mine drainage from the weathering of sulfide minerals and magnetite: Applied Geochemistry, v. 24, no. 12, p. 2362-2373.
- Moncur, M. C., Ptacek, C. J., Lindsay, M. B. J., Blowes, D. W., and Jambor, J. L., 2015, Long-term mineralogical and geochemical evolution of sulfide mine tailings under a shallow water cover: Applied Geochemistry, v. 57, p. 178-193.
- Munsell, C., 2010, Munsell soil color charts : with genuine Munsell color chips. .
- Murciego, A., Alvarez-Ayuso, E., Pellitero, E., Rodriguez, M. A., Garcia-Sanchez, A., Tamayo, A., Rubio, J., Rubio, F., and Rubin, J., 2011, Study of arsenopyrite weathering products in mine wastes from abandoned tungsten and tin exploitations: Journal of Hazardous Materials, v. 186, no. 1, p. 590-601.
- Murphy, R., and Strongin, D., 2009, Surface reactivity of pyrite and related sulfides: Surface Science Reports, v. 64, no. 1, p. 1-45.

- Nicholson, R. V., and Scharer, J. M., 1993, Laboratory Studies of Pyrrhotite Oxidation Kinetics, *Environmental Geochemistry of Sulfide Oxidation*, Volume 550: Washington, DC, American Chemical Society, p. 14-30.
- Noack, Y., Colin, F., Nahon, D., Delvigne, J., and Michaux, L., 1993, Secondary-mineral formation during natural weathering of pyroxene: review and thermodynamic approach: *American Journal of Science* v. 293, p. 111-134.
- Nonthee, R., 2010, Water quality analysis in the communities surrounding the Gold mine, Khao Luang Sub-district, Wang Saphung District, Loei Province. Master Thesis: Loei Rajabhat University.
- Nordstrom, D. K., and Alpers, C. N., 1999, Negative pH, efflorescent mineralogy, and consequences for environmental restoration at the Iron Mountain Superfund site, California: *Proceedings of the National Academy of Sciences*, v. 96, no. 7, p. 3455-3462.
- Nugraha, C., Shimada, H., Sasaoka, T., Ichinose, M., Matsui, K., and Manege, I., 2009, Geochemistry of waste rock at dumping area: *International Journal of Mining, Reclamation and Environment*, v. 23, no. 2, p. 132-143.
- Paktunc, D., 2013, Mobilization of arsenic from mine tailings through reductive dissolution of goethite influenced by organic cover: *Applied Geochemistry*, v. 36, p. 49-56.
- Parbhakar-Fox, A., Lottermoser, B., and Bradshaw, D., 2013, Evaluating waste rock mineralogy and microtexture during kinetic testing for improved acid rock drainage prediction: *Minerals Engineering*, v. 52, p. 111-124.
- Parbhakar-Fox, A., and Lottermoser, B. G., 2015, A critical review of acid rock drainage prediction methods and practices: *Minerals Engineering*, v. 82, p. 107-124.
- Parbhakar-Fox, A. K., Edraki, M., Hardie, K., Kadletz, O., and Hall, T., 2014, Identification of acid rock drainage sources through mesotextural classification at abandoned mines of Croydon, Australia: Implications for the rehabilitation of waste rock repositories: *Journal of Geochemical Exploration*, v. 137, p. 11-28.
- Parbhakar-Fox, A. K., Edraki, M., Walters, S., and Bradshaw, D., 2011, Development of a textural index for the prediction of acid rock drainage: *Minerals Engineering*, v. 24, no. 12, p. 1277-1287.

- Peacock, C. L., and Sherman, D. M., 2004, Copper(II) sorption onto goethite, hematite and lepidocrocite: a surface complexation model based on ab initio molecular geometries and EXAFS spectroscopy: *Geochimica et Cosmochimica Acta*, v. 68, no. 12, p. 2623-2637.
- Rancourt, D. G., Fortin, D., Pichler, T., Thibault, P.-J., Lamarche, G., Morris, R. V., and Mercier, P. H. J., 2001, Mineralogy of a natural As-rich hydrous ferric oxide coprecipitate formed by mixing of hydrothermal fluid and seawater: Implications regarding surface complexation and color banding in ferrihydrite deposits: *American Mineralogist*, v. 86, no. 7-8, p. 834-851.
- Rodmanee, T., 2000, Genetic model of Phu Thap Fha gold deposit, Ban Huai Phuk Amphoe Wang Saphung, Changwat Loei. Master Thesis: Chiang Mai University.
- Romero, A., González, I., and Galán, E., 2006, Estimation of potential pollution of waste mining dumps at Peña del Hierro (Pyrite Belt, SW Spain) as a base for future mitigation actions: *Applied Geochemistry*, v. 21, no. 7, p. 1093-1108.
- Rosler, H. J., and Lange, H., 1972, *Geochemical Table*, Amsterdam, Netherlands, Elsevier.
- Satoh, H., Ishiyama, D., Mizuta, T., and Ishikawa, Y., 1999, Rare earth element analysis of rock and thermal water samples by Inductively Coupled Plasma Mass Spectrometry (ICP-MS): Scientific and technical reports of Faculty of Engineering and Resource Science, Akita University, v. 20, p. 1-8.
- Simate, G. S., and Ndlovu, S., 2014, Acid mine drainage: Challenges and opportunities: *Journal of Environmental Chemical Engineering*, v. 2, no. 3, p. 1785-1803.
- Singer, P. C., and Stumm, W., 1970, Acidic Mine Drainage: The Rate-Determining Step: *Science*, v. 167, p. 1121-1123.
- Singh, R., Gautam, N., Mishra, A., and Gupta, R., 2011, Heavy metals and living systems: An overview: *Indian Journal of Pharmacology*, v. 43, no. 3, p. 246-253.
- Smedley, P. L., and Kinniburgh, D. G., 2002, A review of the source, behaviour and distribution of arsenic in natural waters: *Applied Geochemistry*, v. 17, no. 5, p. 517-568.

- Smith, L. J. D., Bailey, B. L., Blowes, D. W., Jambor, J. L., Smith, L., and Segó, D. C., 2013, The Diavik waste rock project: Initial geochemical response from a low sulfide waste rock pile: *Applied Geochemistry*, v. 36, p. 210-221.
- Smuda, J., Dold, B., Friese, K., Morgenstern, P., and Glaesser, W., 2007, Mineralogical and geochemical study of element mobility at the sulfide-rich Excelsior waste rock dump from the polymetallic Zn–Pb–(Ag–Bi–Cu) deposit, Cerro de Pasco, Peru: *Journal of Geochemical Exploration*, v. 92, no. 2-3, p. 97-110.
- Sobek, A. A., Schuller, W. A., Freeman, J. R., and Smith, R. M., 1978, Field and laboratory methods applicable to overburden and mine soils, United States Environmental Protection Agency EPA 600/2-78-054, 203 p.
- Sracek, O., Choquette, M., Gélinas, P., Lefebvre, R., and Nicholson, R. V., 2004, Geochemical characterization of acid mine drainage from a waste rock pile, Mine Doyon, Québec, Canada: *Journal of Contaminant Hydrology*, v. 69, no. 1–2, p. 45-71.
- Sracek, O., Gélinas, P., Lefebvre, R., and Nicholson, R. V., 2006, Comparison of methods for the estimation of pyrite oxidation rate in a waste rock pile at Mine Doyon site, Quebec, Canada: *Journal of Geochemical Exploration*, v. 91, no. 1-3, p. 99-109.
- Stumm, W., and Morgan, J. J., 1981, *Aquatic chemistry: An introduction emphasizing chemical equilibria in natural waters*, New York, Wiley
- , 1996, *Aquatic Chemistry Chemical Equilibria and Rates in Natural Waters*, New York, John Wiley & Sons Inc.
- Sutthirat, C., 2011, Geochemical application for environmental monitoring and metal mining management, *in* Ekundayo, E. O., ed., *Environmental Monitoring: Croatia*, InTech, p. 91-108.
- Sutthirat, C., and Changul, C., 2012, Geochemical Characteristics of Waste Rocks from the Akara Gold Mine, Phichit Province, Thailand: *Arabian Journal for Science and Engineering*, v. 38, no. 1, p. 135-147.
- Thai Meteorological Department, 2012, Areage temperature and rainfall amount 30 years of Loei Province. March 3, 2016. Available from: [http://www.tmd.go.th/province\\_weather\\_stat.php?StationNumber=48353](http://www.tmd.go.th/province_weather_stat.php?StationNumber=48353).

- Thornton, I., 1995, Metals in the global environment : facts and misconceptions, Ottawa, International Council on Metals and the Environment.
- Tongkhan, W., Tantemsaya, N., and Thathong, V., Adsorption of arsenic on laterite soil from gold mining area, *in* Proceedings the 40<sup>th</sup> National Graduate Research Conference "Higher Education Harmonization", Prince of Songkla University, Songkla, Thailand, 2016, Graduate School, Prince of Songkla University, p. 431-438.
- Transbordernews, 2014, Deep divisions in fight over mine. February 10, 2017. Available from: <http://transbordernews.in.th/home/?p=4609>
- Tuisakda, N., 2008, Analysis of cyanide in rain water and heavy metals in groundwater in the communities surrounding the Gold mine, Khao Luang Subdistrict, Wang Saphung District, Loei Province. Master Thesis: Loei Rajabhat University.
- Turekian, K. K., and Wedepohl, K. H., 1961, Distribution of the elements in some major units of the Earth's Crust: Bulletin Geological Society America, v. 72, no. 2, p. 175-192.
- Valente, T., Grande, J. A., de la Torre, M. L., Santisteban, M., and Cerón, J. C., 2013, Mineralogy and environmental relevance of AMD-precipitates from the Tharsis mines, Iberian Pyrite Belt (SW, Spain): Applied Geochemistry, v. 39, p. 11-25.
- Valente, T. M., and Leal Gomes, C., 2009, Occurrence, properties and pollution potential of environmental minerals in acid mine drainage: The Science of the Total Environment, v. 407, no. 3, p. 1135-1152.
- Velasco, F., Herrero, J. M., Suárez, S., Yusta, I., Alvaro, A., and Tornos, F., 2013, Supergene features and evolution of gossans capping massive sulphide deposits in the Iberian Pyrite Belt: Ore Geology Reviews, v. 53, p. 181-203.
- Velbel, M. A., 1989, Weathering of hornblende to ferruginous products by a dissolution-precipitation mechanism; petrography and stoichiometry: Clays and Clay Minerals, v. 37, no. 6, p. 515.
- Webster, J. G., Swedlund, P. J., and Webster, K. S., 1998, Trace metal adsorption onto an acid mine drainage iron(III) oxy hydroxy sulfate: Environmental Science & Technology, v. 32, no. 10, p. 1361-1368.

- West, L., McGown, D. J., Onstott, T. C., Morris, R. V., SuchECKI, P., and Pratt, L. M., 2009, High Lake gossan deposit: An Arctic analogue for ancient Martian surficial processes?: *Planetary and Space Science*, v. 57, no. 11, p. 1302-1311.
- Whitney, D. L., and Evans, B. W., 2010, Abbreviations for names of rock-forming minerals: *American Mineralogist*, v. 95, no. 1, p. 185-187.
- Wilkie, J. A., and Hering, J. G., 1996, Adsorption of arsenic onto hydrous ferric oxide: effects of adsorbate/adsorbent ratios and co-occurring solutes: *Colloids and Surfaces A: Physicochemical and Engineering Aspects*, v. 107, p. 97-110.
- Williams, D. J., Wilson, G. W., and Currey, N. A., A cover system for a potentially acid forming waste rock dump in a dry climate, *in Proceedings the 4<sup>th</sup> International Conference on Tailings and mine waste '97*, Rotterdam, Fort Collins, Colorado, 13-17 January, 1997, Balkema, p. 231–236.
- Wolfe, A. L., Liu, R., Stewart, B. W., Capo, R. C., and Dzombak, D. A., 2007, A method for generating uniform size-segregated pyrite particle fractions: *Geochemical Transactions*, v. 8, p. 9-9.
- Yadav, S. K., 2010, Heavy metals toxicity in plants: An overview on the role of glutathione and phytochelatins in heavy metal stress tolerance of plants: *South African Journal of Botany*, v. 76, no. 2, p. 167-179.
- Zhang, J. S., Stanforth, R., and Pehkonen, S. O., 2007, Proton-arsenic adsorption ratios and zeta potential measurements: implications for protonation of hydroxyls on the goethite surface: *Journal of Colloid and Interface Science*, v. 315, no. 1, p. 13-20.

## VITA

Miss Thitiphon Assawincharoenkij was born in Samut Songkhram, central part of Thailand, on November 27, 1984. After her completing the high school from Sattahasamut School, Samut Songkhram in 2003, she entered Chulalongkorn University. She acquired the B.Sc. degree (2nd class honor) in Geology, Faculty of Science, Chulalongkorn University in 2007 and then she continued the M.Sc. program in Geology at Department of Geology, Faculty of Science, Chulalongkorn University. The research work has been focused on volcanic rocks and tectonic setting. During she was the master student, she received a scholarship from Deutscher Akademischer Austausch Dienst (DAAD) for 2 weeks to study visits on mining, environmental geology, and hydrogeology at the University of Muenster and vicinity, Germany in 2007; moreover, she was an exchanged student at Graduate School of Life and Environmental Sciences, University of Tsukuba, Japan, which funded by Japan Student Service Organization (JASSO) for 1 year.

In 2011, she graduated the Master of Science program in Geology and then she applied for the Doctoral program at Department of Geology, Faculty of Science, Chulalongkorn University. She received the scholarship form the Division of Earth and Planetary Sciences at the Graduate School of Science, Kyoto University to attend the 7th KAGI21 International Spring School, and received the scholarship from JASSO again to attend the Short-Stay Program Sustainable Resource Development at Akita University in 2013 and 2014, respectively. In 2015, she received the ASEA-Uninet/Ernst Mach Grant (Ernst Mach weltweit TSOA) scholarship (Technology Grants) to be a sandwich PhD student at University of Graz, Institute of Earth Sciences, Mineralogy and Petrology, Graz, Austria for 6 months.

She had received the Science Achievement Scholarship of Thailand (SAST) from Commission on Higher Education, Ministry of Education Thailand for her Bachelor, Master and Doctoral Programs since 2003.